25

A FINITE ELEMENT MODEL OF SKIN DEFORMATION

CONTENTS

I. Introduction

A. The modeling of wound closure -- an historical overview 5

B. Aims and objectives 6

II. Biomechanics of skin and soft tissue

A. Biomechanics of biological solids 7

B. Experimental investigations -- a review 11

C. Theoretical investigations -- a review 18

III. A finite element model of skin deformation

A. The finite element method 27

B. Design of the model 33

IV. The experimental model

A. The animal model 40

B. Design of the skin extensometer 41

C. Experimental measurements of the viscoelastic properties of skin in the piglet 43

D. Measurement and standardization of the deformation field 46

E. Determination of a practical range of stress and strain for clinical wound closure 48

F. Measurement and prediction of the major variables for the mathematical model 50

V. Modeling of skin deformation

A. Linear deformation of a rectangular skin island 53

B. Modeling of wound closures 55

VI. Discussion 56

VII. Summary 60

VIII. References

IX. Appendices

A. The finite element model

B. Software developed to control the skin extensometer

C. Software developed to measure skin deformation

ABSTRACT

Skin flap design has traditionally been based on geometric models which ignore the elastic properties of skin and its subcutaneous attachments. This study reviews the theoretical and experimental mechanics of skin and soft tissues, and proposes a mathematical model of skin deformation based on the finite element method. Finite element technic facilitates the modeling of complex structures by analyzing them as an aggregate of smaller elements. An animal model is developed to study the deformation and mechanical properties of skin, including its viscoelastic properties (hysteresis, creep, and stress relaxation). A new skin extensometer, constructed with digital stepper motors and controlled with a microcomputer, is described to measure these properties for both skin and its subcutaneous attachments. Deformation grids are quantitated from photographs with a digitalizing tablet, and computer software is introduced to standardize and analyze them. The mathematical model is used to simulate wound closures such as the ellipse and rectangular advancement flap. In addition, a series of mathematical experiments are performed to simulate deformation of a strip of skin; the relationships between the various elastic constants are investigated, and a comparison of these simulations with actual deformation is presented. Limitations of the model and areas for future investigation are discussed.

I. Introduction

A. The modeling of wound closure -- an historical overview

Complex wound closures were performed in India as early as 300 BC.[1] Since that time, the major advance in the science of wound closure has been the progressive understanding of the skin tension lines.[2] These lines were described by Dupuytren in 1834, when he noted that a round puncture wound in a suicide victim assumed a fusiform shape.[3] His observations were elaborated upon by Langer in 1861, who made systematic observations on the skin of cadavers by inserting an awl into the skin and diagramming the resultant major axis of the ellipsis.[4] Kocher in 1892 was the first to advocate that surgical incisions follow Langer's lines.[5] Cox in 1941 performed a more extensive study on unclaimed bodies, photographing the cleavage lines.[6] He noted some differences between his study and that of Langer, and documented that the cleavage lines remained in skin removed from the body. More recently the importance of placing surgical excisions in the relaxed skin tension lines (perpendicular to the lines of maximal extensibility) has been emphasized by Borges.[7]

The application of mathematics to skin flap design really began with Limberg.[8,9] He studied triangular skin flaps with paper models and plane geometry, and published his classic book in 1946. Others have extended the application of plane geometry to describe

skin flap design.[10,11,12] MacGregor's description of the theoretical basis for the Z-plasty in 1957 is an excellent example of this approach. All of these mathematical descriptions, however, utilize plane geometry, and none allow for the elasticity of the skin or skin attachments.

I. B. Aims and objectives

Current models of wound closure are based almost completely on plane geometry or paper models. Surgeons are well aware of the complex elastic properties of skin and subcutaneous tissue and use them effectively, but they have no realistic technic with which to model wound closures. The aims and objectives of this study are threefold:

1. To review the relevant literature, both experimental and theoretical, on the biomechanics of skin and soft tissue.

2. To develop a preliminary mathematical model, based on the finite element method, that could eventually be used as a practical technic to study and design wound closures.

3. To design and standardize an animal model to estimate the elastic constants necessary for the mathematical model, and to correlate skin deformation in the animal with the mathematical model.

II. Biomechanics of skin and soft tissue

A. Biomechanics of biological solids

A quantitative analysis of the mechanical properties of skin and soft tissue requires application of engineering principles.[13] These mechanical properties are defined in terms of the deformation produced by a given force over time. Force is standardized as force per unit area or stress and can be related either to the original cross-sectional area or to the deformed cross-sectional area. Stress placed on a physical material acts in a specific direction, and therefore is defined as a stress vector. The standardized notation for stress vectors acting on a small cube is seen in Figure 1. The stresses perpendicular to the surface are normal stresses; the other stresses are shearing stresses.

When a solid is deformed, the change in length is defined in terms of strain. For the simplest case, a rod of original length L_0 is stretched to a new length of L (Figure 2). Various dimensionless ratios can then be used to represent this change in length:

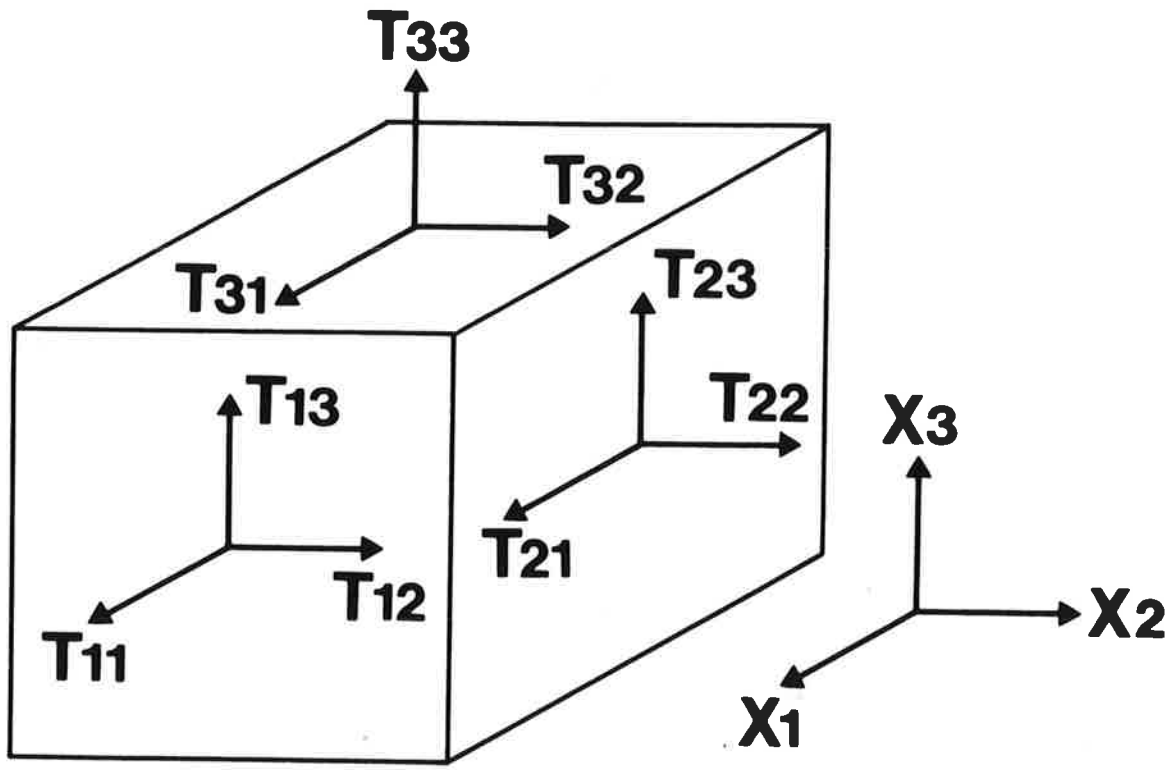

Figure 1. Orientation of standardized stress vectors acting on a small cube.

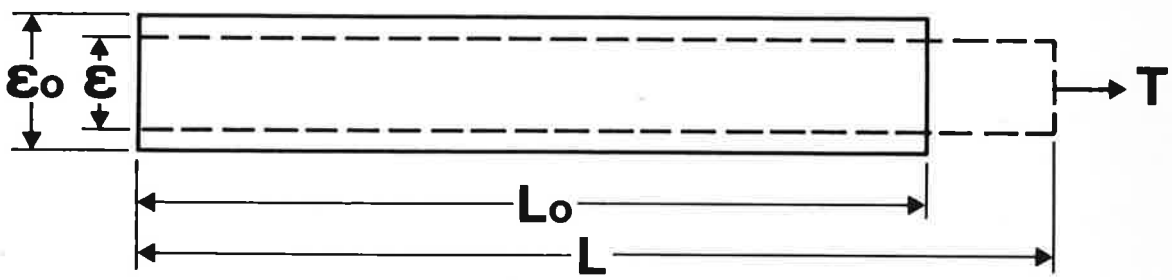

Figure 2. Elongation of a simple rod of length L_0 to length L by a force T. The width changes from w_0 to w. The stretch ratio and strain measures are defined in terms of these quantities.

1. The stretch ratio or $\lambda = \dfrac{L}{L_0}$

2. Strain measures

$$\varepsilon = \frac{L - L_0}{L_0} \qquad E = \frac{L - L_0}{L}$$

3. $$e = \frac{L^2 - L_0^2}{2L^2} \qquad \xi = \frac{L^2 - L_0^2}{2L_0^2}$$

These strain measures are all roughly equal for very small deformations (infinitesimal elongations), but they become different for large deformations (finite elongations). Strain measures represent a vector, defined with the same orientation seen in Figure 1. When analyzing deformation of a physical material, one is usually not interested in actual motion or displacement of the entire body but in the relative displacements of parts of the body. For this reason the actual strains or x_1, x_2, x_3 displacements are transformed into three strain invariants which measure only relative deformation.

Hooke's law applies to many engineering materials subject to small strains (infinitesimal strains) and for uniaxial deformation can be written $\sigma = Ee$, where σ is stress, E is a constant (Young's modulus), and e is strain. Hooke's law can be exactly applied only to materials with a linear stress-strain relationship and for infinitesimal strains. A Hookean elastic solid is one that follows Hooke's law. When describing a three-dimensional Hookean solid,

multiple elastic constants are required. The equations can be greatly simplified, however, for an isotropic instead of an anisotropic material. Isotropic materials have the same elastic properties in all directions (equal stress produces equal displacement in any direction), whereas with anisotropic materials elastic properties have a directional variation. Hooke's law can be further simplified for a simple two-dimensional (versus a three-dimensional) problem. A two-dimensional description of an isotropic Hookean solid requires only two elastic constants: E or Young's modulus, which is the slope of the stress-strain curve; and ν or Poisson's ratio, which is the ratio of the contraction of the surface in one dimension when one elongates it in the other (both expressed in terms of strain).[14] Just as elastic bodies can be idealized as Hookean elastic solids, liquids can be idealized as Newtonian fluids. For an elastic body, the stress and strain are related by unique single-valued function, and this relationship is not changed with variation in strain rates or with repeated strain.

Liquids are traditionally modeled according to the theory of hydrodynamics which states that perfectly viscous liquids obey Newton's law:

$$\sigma = \eta \frac{d\varepsilon}{dt}$$

where η is viscosity, ε is strain, and t is time. With Newton's law, stress is directly proportional to the rate of strain but independent of the strain itself.

Many biologic materials combine the characteristics of elastic solids and viscous liquids and therefore are termed viscoelastic. Some common properties of viscoelastic materials are hysteresis, stress relaxation, and creep. Hysteresis implies that stress-strain relationships in cyclic loading and unloading are different. If soft tissue is stretched and then allowed to return to its original length, the stress-strain curve with loading will not superimpose on the unloading curve. Stress relaxation describes the decreasing stress seen when a constant strain is placed on a viscoelastic material. Creep refers to the increasing strain or length of a material over time when placed at a constant stress. Most biologic solids are viscoelastic.

Various mechanical models of viscoelastic behavior have been described. Based on Hooke's law and Newton's law, these models are a combination of a linear spring with a Young's modulus E and a dashpot with a viscosity η. The elastic spring produces a deformation directly proportional to the load; the dashpot produces a velocity proportional to the load. The dashpot can be likened to a shock absorber. These two basic components are then combined in various ways to describe the viscoelastic material. The two simplest combinations are the Maxwell and Voight models seen in Figure 3. An excellent theoretical discussion of these models is presented by Jamison.[15]

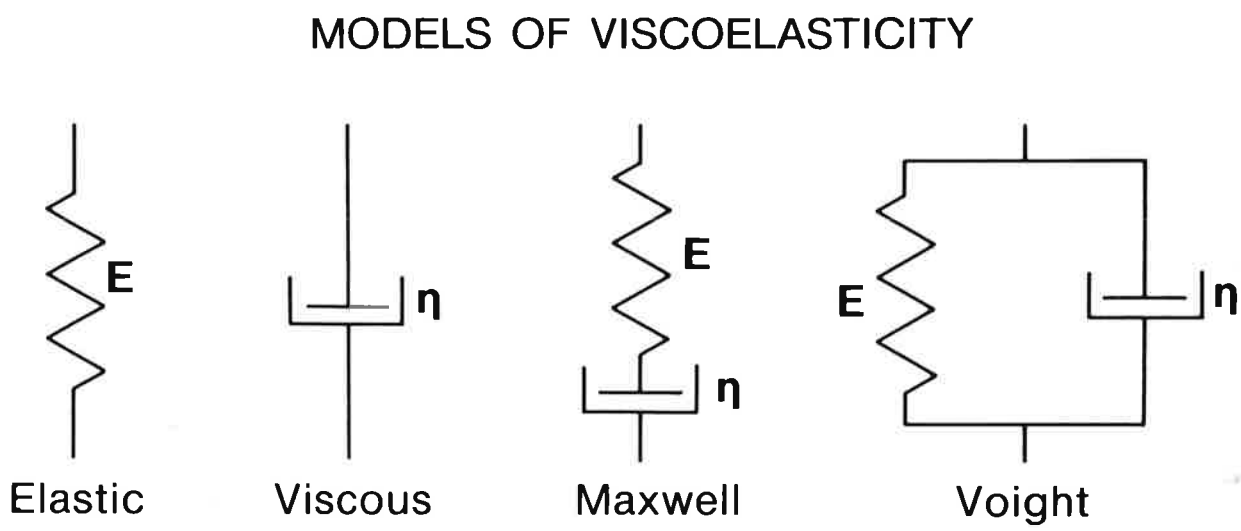

Figure 3. Models for viscoelastic behavior of soft tissue. The Maxwell and Voight are the most common models for viscoelastic behavior. The elastic spring obeys Hooke's law and produces a deformation proportional to the load; the dashpot obeys Newton's law and produces a velocity proportional to the load.

II. B. Experimental investigations -- a review

Skin has been extensively studied both in vitro and in vivo, and in both human and animal models. Skin is a complex organ which is anisotropic, has extremely nonlinear stress-strain properties, and exhibits viscoelastic or time-dependent behavior. The major structural components of the skin which affect mechanical behavior are the elastin fibers, the collagen fibers, and the ground substance. Collagen is the most important structure, representing approximately 72% of the dry weight of dermal tissue,[16] while elastin represents 4%, and the ground substance 20%. Because of its complexity, almost all significant work has been done on isolated skin in vitro. There has been very little sophisticated work done in vivo, and almost no study of the mechanical properties of the subcutaneous attachments to the skin. The problems with deterioration of skin after it is removed from the living animal were noted by Marangoni et al,[17] who developed a quick freeze-low temperature storage technic in an attempt to maintain the skin in the in vivo condition as long as possible. Even with such a technic, however, the skin has lost its blood supply, nerve supply, and attachments to the surrounding skin and subcutaneous tissue; all of which must greatly alter its mechanical properties.

Mechanical properties of collagen have been well studied, both in strained and unstrained states. Histologic studies of collagen fibers by both light and electron microscopy demonstrate a wavy and

somewhat random pattern of the fibers in an unstrained specimen. As a specimen of skin is progressively strained, the fibers become oriented in the direction of the strain.[18,19,20,21] Morgan[22] performed an extensive series of experiments on collagen fibers obtained from ox hide and described stress-strain curves which could be adequately described by the power law: $\sigma = 0.386\ E^{1.23}$ where E = strain, σ = stress in kg/sq mm. Elden provides a sophisticated engineering analysis of collagen fibers including their orientation and hydration status.[23]

Elastin exists in the skin as a composite assembly of small tapering fibers which form a network. These small ropelike filaments are paired structures, about 1.5 nm in width, which are periodically linked longitudinally.[24] Carton et al[25] dissected single elastic fibers free from ligamentum nuchae of the ox and performed stress-strain measurements on these single fibers. The strain-tension curves of these fibers were very consistent and demonstrated an exponential relationship between stress and strain. He was able to fit his tension-strain curves for single elastic fibers to the regression:

$$e = 1.3 - A \exp^{-bt}$$

where e is strain, t is tension in dynes, and A,b are constants. Elastin is the only mammalian protein known to have truly elastic properties. Daly[26] treated skin specimens with the enzyme elastase, which degrades elastin but does not affect collagen. When the elastase treated human cadaver skin was tested,

it was found that the elasticity of the skin had been almost totally lost. Similar results were described by Wood[27] in experiments on ligamentum nuchae. Dick[28] analyzed skin discs from cadavers mechanically and histologically; he concluded the loss of elastin fibers in older individuals resulted in a loss of skin resistance to deformation at low stress. King and Lawton[29] investigated the behavior of elastin-rich tissues in terms of elastomer theory and found good agreement with experimental data. When other structural components such as collagen and ground substance are present, however, the elastomer theory is no longer applicable.

The amorphous matrix or ground substance in which the collagen and elastin fibers are embedded is a third factor which affects the mechanical properties of skin. Harkness and Harkness[30] demonstrated increasing creep (elongation with constant load) of collagenous soft tissue treated with trypsin or chymotrypsin. They attributed this mechanical change to loss of the cementing substance in connective tissue. Minns, Soden, and Jackson performed stress-strain and relaxation studies on human tendon, aorta, and bovine ligamentum nuchae after removing the ground substance with an enzyme or chelating agents.[31] They noted a decrease in stress level, stiffness, stress relaxation, hysteresis, and other time-dependent effects in all three tissues. These changes were explained primarily as a reduction in the viscosity of the interfiber matrix.

The majority of the experimental investigations into the mechanical properties of skin have utilized uniaxial test procedures. With uniaxial testing, a length of skin is deformed in one direction, and the resulting stress-strain relationship determined. A typical stress-strain curve for human skin is seen in Figure 4. The accepted mechanism is that the initial deformation (A in Figure 4) is due to deformation of the delicate elastin network, the second part of the curve (B) is due to a gradual straightening of the randomly oriented collagen fibers, and the final part of the curve (C) results when the majority of the collagen fibers are elongated in the direction of the stress.[32,33,34]

There have been many investigations of the mechanical properties of both animal and human skin, using uniaxial tests in vitro. Many of these early experiments were flawed due to unsophisticated equipment and poor control of such variables as temperature and humidity. Early studies by Wohlisch[35] were performed by recording the displacement of strips of skin when loaded with weights. He recorded both the load elongation properties of the skin as well as some of the viscoelastic properties. Ridge and Wright[36,37,38] developed a skin extensometer which stretched strips of skin 1 cm in length by 0.4 cm in width at a constant rate of 0.2 inches per minute. They characterized the resulting stress-strain curves with the equation

$$e = C + kL^b$$

where e = extension, L = load, and C, b, and k = constants.

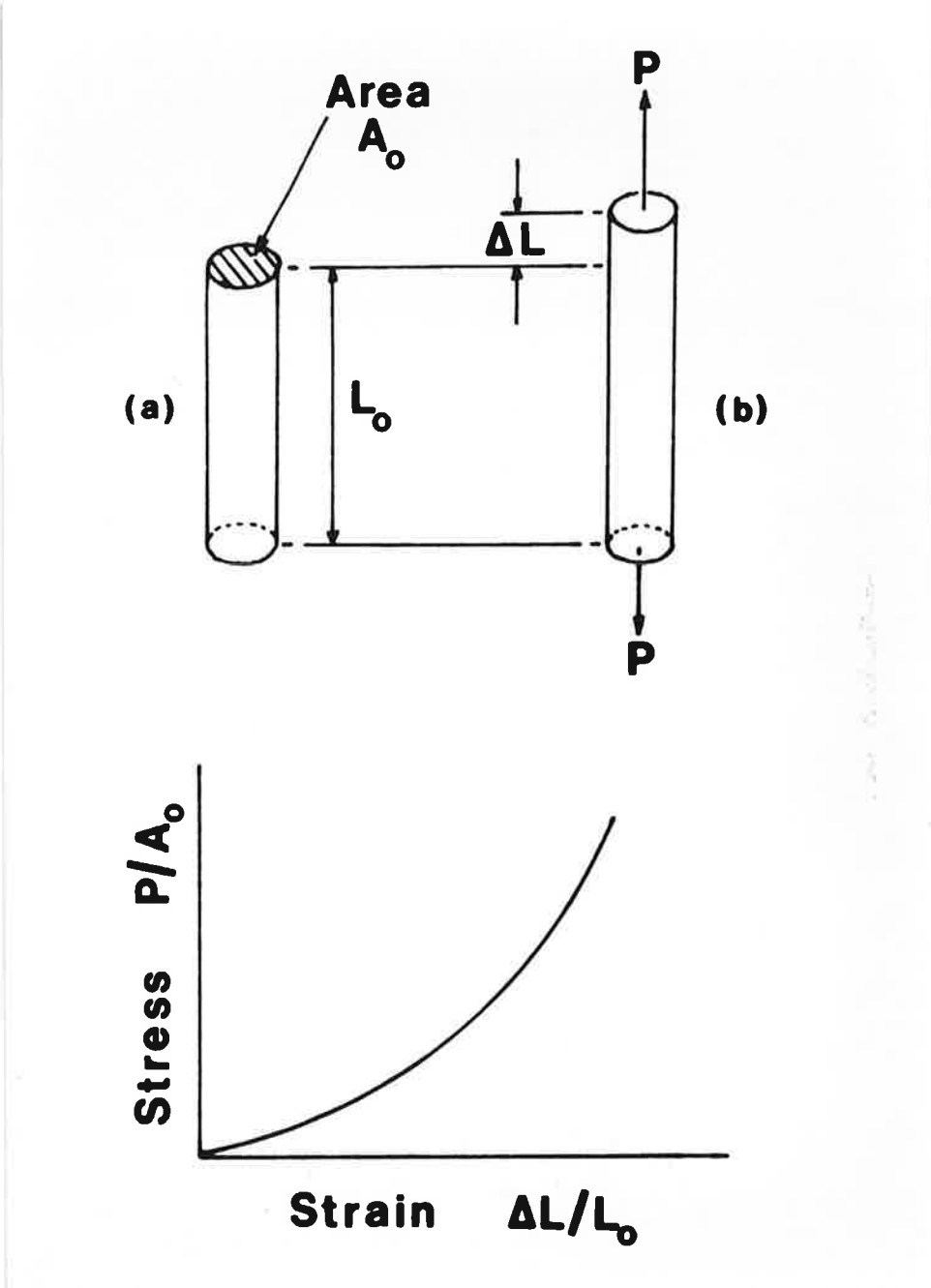

Figure 4. Typical stress-strain curve for soft tissue. (From Daly and Odlund, J Invest Dermatol 73:85, 1979.)

They felt that the constant b reflected a specific property of the collagen fibers, and the constant k represented the condition of the fiber network, which was related to the length and area of the fibers. Kenedi, Gibson, and Daly[31] also performed a series of uniaxial tests on cadaver skin harvested from the anterior abdominal wall using a static testing procedure which allowed five minutes to elapse between each increase in load. Their data revealed fairly typical stress-strain curves. The most significant result from their tests was a large variation in Poisson's ratio. The contraction in width with a given extension varied from 0.2 to more than 1.0.

Daly[40] further refined uniaxial testing. He first appreciated that for consistent results the specimens must be tested in a constant temperature, humidity, and pH, and with a constant strain rate. In addition to measuring stress-strain curves and Poisson's ratio, he performed extensive experiments documenting stress relaxation and creep in human cadaver skin. Ridge and Wright[41] also performed a series of experiments with an extensometer in which they stretched pieces of skin with and against the normal skin tension lines. They were able to show a clear difference in the directional mechanical properties in the skin, which corresponded to Langer's lines.

In addition to these in vitro uniaxial tests, a number of investigators have attempted in vivo uniaxial testing. Gibson,

Stark, and Evans[42] demonstrated with an in vivo skin extensometer, attached to the skin with tabs, that the direction of maximal extensibility is at right angles to Langer's lines. Barbenel, Evans, and Finlay[43] described a rotary device, attached by adhesive to the forearm of a patient, which they utilized to measure the viscoelastic properties of the skin. The most interesting result of their experiments was a surprising independence of their mechanical measurements from the frequency of the displacements. Daly[40] also experimented with both uniaxial tensions and rotary torque motors to perform in vivo experiments. He demonstrated a broad similarity between the mechanical behavior of skin in vivo and in vitro, but the additional variables prevented absolute measurements of mechanical properties in vivo. Ohura[44] has recently refined a similar device and has used it in multiple clinical situations to look at clinical wound healing problems. Wijn et al[45] studied the mechanical properties of human skin in vivo with both the uniaxial strain technics and torsion technics. They found that on a homogenous isotropic medium (a sheet of pararubber) both methods gave very consistent values. However, when they applied both technics to the forearm of a volunteer there was considerable variation between the technics. Thacker et al[46] also described and utilized an in vivo extensometer for uniaxial testing. Alexander and Cook[47] designed a complex device which uses a strain-gauged pretension device to determine the underlying skin tension and a low pressure suction attachment to determine two-dimensional tension-extension action.

Uniaxial experiments cannot exactly define the mechanical properties of a three-dimensional solid. More specifically, the constitutive equations that characterize soft tissues in three dimensions cannot be generalized from one-dimensional data. It is possible to determine three-dimensional mechanical properties from two-dimensional tests for an incompressible solid. Most biomechanists feel that for practical analysis the skin can be treated as an incompressible solid. Lanir and Fung[48] have developed such a two-dimensional experimental system for biaxial testing. It is an optomechanical system in which a rectangular specimen of skin floats in physiologic saline. The specimen is hooked along its edges by many small staples (up to 68 in number). Each hook connects by means of a small thread to a force-distributing platform, where tension can be individually adjusted. Stretching of the specimen can be performed at a variable rate, and true two-dimensional measurements made. They utilized this device to measure the biomechanics of rabbit skin. In their study the deformed skin always returned to its predeformed state so long as no surface dimension had been allowed to decrease below its initial unstressed value. This is obviously different from the uniaxial tests in which the skin essentially always diminishes in lateral diretions and usually does not return to its prestress state. Their experiments clearly documented the anisotropy in various directions. Biaxial tests showed:

1. Stress-strain relations are extremely nonlinear.
2. Hysteresis was present at all strain rates.
3. Stress-strain relationships were minimally dependent on the strain rate.
4. The relaxation curve does not terminate at the origin and returns to it only after a long period of relaxation.

A comparison of uniaxial and biaxial stretch tests on the same specimen shows that for a given stretch ratio in the loading direction, the stress with the uniaxial test is considerably lower than than in the biaxial stress condition. This same experimental setup was utilized by Schneider, Davidson, and Nahum[49] to study the mechanical characteristics of human cadaver skin. They also noted that skin was a viscoelastic material which had distinct anisotropic properties.

II. C. Theoretical work -- a review

An accurate biomechanical description of skin requires a more theoretical approach than the empirical equations presented thus far. The major advocate of this theoretical approach has been Fung.[13] He has pointed out that Young's modulus is a relatively meaningless number on a stress-strain curve unless an exact stress level is specified. He also notes that the customary application of the infinitesimal theory of elasticity, which deals with small strains (such as 0.2%) to a material such as skin which has a 10%

to 40% deformation, leads to inaccuracies. He proposes an exponential stress-strain function which can be applied to uniaxial tests, such as one-dimensional experiments on rabbit mesentery, muscle, and skin.[13,50,51] The following equations were described by Fung in 1967 and 1981 and essentially represent the first derivative of stress vs time as a straight line:

1. $$\frac{dT}{d\lambda} = \alpha(T+\beta)$$

   T is Lagrangian stress, load divided by original cross sectional area

   λ is extension ratio, deformed length divided by original length

   $\alpha + \beta$ are constants

   α is slope of λ vs $dT/d\lambda$

   Integration gives:

2. $$T + B = Ce^{\alpha\lambda}$$

   C is an integration constant.

   To find the integration constant:

3. $$T = (T^* + \beta)e^{\alpha(\lambda-\lambda^*)} - \beta$$

   When $T=T^*$

   $\lambda=\lambda^*$

If λ is referred to the original length then:

$T=o$ when $\lambda=1$ and:

4. $$\beta=\frac{T^{*}e^{-\alpha(\lambda^{*}-1)}}{1-e^{-\alpha(\lambda^{*}-1)}}$$

For Hookean material $dT/d\lambda$ = constant

One of the most common approaches to modeling bodies which can undergo finite deformation is to postulate a strain-energy function. The work of Veronda and Westmann is typical and will be presented as an example of this approach.[52]

In order to deform an elastic body, a certain amount of work is required which is stored in the body as strain energy. Therefore for a homogenous deformation of an elastic isotropic material the following strain-energy function can be defined:

1. $$W=\sum_{i=1}^{3}\int_{\lambda_i=1}^{\lambda_i}\sigma_i d\lambda_i=W(\lambda_i)$$

W is strain energy function per unit volume of undeformed body

σ_i is stress per area undeformed body

λ_i is ratio of principle extension of the deformed body to the initial length of undeformed body

The three strain invariants are:

2. $$I_1 = \lambda_1^2 + \lambda_2^2 + \lambda_3^2$$

3. $$I_2 = \lambda_1^2 \lambda_2^2 + \lambda_2^2 \lambda_3^2 + \lambda_3^2 \lambda_1^2$$

4. $$I_3 = \lambda_1^2 \lambda_2^2 \lambda_3^2$$

5. From = 1:

$$\sigma_i = \frac{\partial W}{\partial \lambda_i}$$

6. Total derivative is:

$$\sigma_i = \frac{\partial W}{\partial I_1} \frac{\partial I_1}{\partial \lambda_i} + \frac{\partial W}{\partial I_2} \frac{\partial I_2}{\partial \lambda_i} + \frac{\partial W}{\partial I_3} \frac{\partial I_3}{\partial \lambda_i}$$

7. Substitute derivatives from 2, 3, 4 into 6:

$$\sigma_i = \frac{2}{\lambda_i} \left[\lambda_i^2 \frac{\partial W}{\partial I_1} + I_2 \frac{\partial W}{\partial I_2} - \frac{I_3}{\lambda_i^2} \frac{\partial W}{\partial I_2} + I_3 \frac{\partial W}{\partial I_3}\right]$$

8. For the uniaxial case with $\sigma_1=\sigma$, $\sigma_2=\sigma_3=0$ and the isotropic case for which

$\lambda_2 = \lambda_3$:

$$\frac{\sigma}{2\left(\lambda_1 - \frac{\lambda_2^2}{\lambda_1}\right)} = \frac{\partial W}{\partial I_1} + \lambda_2^2 \frac{\partial W}{\partial I_2}$$

9. For an incompressible material $I_3 = 1$ and $\lambda_2^2 = \lambda_3^2 = \frac{1}{\lambda_1}$:

$$\frac{\sigma}{2(\lambda_1 - \frac{1}{\lambda_1^2})} = \frac{\partial W}{\partial I_1} + \frac{1}{\lambda_1}\frac{\partial W}{\partial I_2}$$

10. The strain energy function is determined by analysis of experimental data:

$$W = c_1[e^{\beta(I_1-3)}-1]+c_2(I_2-3)+g(I_3)$$

$g(1) = 0$

c_1, c_2, β are constants

11. Considering the material incompressible, and curve fitting the uniaxial experimental data from cat skin, one can determine the appropriate values for c_1, c_2, and β. Using their experimental data and equation 10 yields:

$$W = 0.0134[e^{4.4(I_1-3)} - 1] - 0.0295(I_2 - 3) + g(I_3)$$

Blatz, Chu, and Wayland[53] propose an alternative to the functions of Fung. They present an elastic model for the loading curve that is applicable to large deformations. Fung, also working with finite deformation theory, chose an exponential stress-strain law. Blatz, Chu, and Wayland, however, selected a power-law form of the function which fits very nicely with experimental data. They initially chose to represent the strain energy as an arbitrary logarithmic function of the stretch ratios as follows:

Strain energy function:

$W=\sum f(\text{In } \lambda_i)$

A power law of f is selected:

$f\ (\text{In } \lambda_i)= C\ (\lambda_i \alpha -1)$

Stress stain relationhip for uniaxial tension:

$\sigma\lambda= (2G/\alpha)[\lambda^{\alpha} - (1/\lambda^{\alpha/2})]$

α and G are experimentally determined constants.
σ is load per unit of the undeformed area
λ is stretch ratio - the length of deformed to undeformed length

They compared their power law to experimental data for uniaxial tests on human papillary muscle and frog muscle, and to strip biaxial data on rabbit mesentery. In each of these cases a good correlation was found with experimental data. They also developed an alternate form of biaxial testing based on a fan-shaped segment of the rabbit mesentery and described in terms of radial and circumferential stress.

Multiple other authors, including Crisp,[54] Demiray,[55,56] and Allaire,[56] have described the application of strain energy functions to skin. Crisp reviews and compares these functions, and concludes that any worthwhile function will require an experimental approach over a wide range of deformation states and a basis in finite (versus infinitestimal) mechanics. Demiray[55] in 1972

proposed a strain-energy density function exponential in the strain invariants; Demiray and Vito[56] in 1976 presented a relatively simple form of the strain-energy density based on numerical experimentation:

$$W = \frac{\beta}{2\alpha} (e^{\alpha(I_2-3)} - 1]$$

α and β are material constants

I_2 is a strain invariant

They matched this function to experimental data from the literature for papillary muscle and artery and found a good correlation.

Allaire et al[57] in 1977 proposed a finite deformation model of human skin based on in vivo measurements. They felt that over the physiologic load range the strain-energy function for uniaxial deformation could be expressed as a linear function of the first two strain invariants and a quadratic function of the third. Thus only three independent constants were necessary to specify the strain-energy function; this formulation was much simpler than the similar formulation by Veronda and Westmann[52] for cat skin.

Tong and Fung[58] in 1976 described a pseudostrain potential for skin. Their model was based on experimental data for rabbit skin

collected by Lanir. They observed during their experiments that the stress-strain curves are essentially independent of the strain rate in loading-unloading cycles. They also noted that under repeated loading-unloading cycles the tissue became preconditioned so that a state of homeostasis was achieved. The equations developed by Tong and Fung apply only to the loading process (increasing strain) in a preconditioned specimen. Because of these limitations their strain-energy function does not have a true thermodynamic meaning, and therefore they term their equations pseudostrain potentials:

Pseudostrain potential

$$\rho_o W = f(\alpha,e) + c \exp[F(a,e)]$$

where

$$f(\alpha,e) = \alpha_1 \varepsilon_{11}^2 + \alpha_2 e_{22}^2 + 2\alpha_4 e_{11} e_{22}$$

$$F(a,e) = a_1 e_{11}^2 + a_2 e_{22}^2 + a_3 e_{12}^2 + 2a_4 e_1 e_2 + \gamma_1 e_1^3 + \gamma_2 e_2^3 + \gamma_4 e_1^2 e_2 + \gamma_5 e_1 e_2^2$$

$\alpha_1, \alpha_2 \cdots, a_1, a_2 \cdots, \gamma_1 \cdots \gamma_5$, and c are constants

exp ( ) is the exponential function

W is the strain energy per unit mass

ρ_o is density of material in the initial undeformed state

e_{ij} is the Green strain tensor (referred to undeformed state)

i, j range over 1, 2, 3

Danielson[59,60] in 1973 and 1975 developed the concept of the skin as an elastic membrane. He applied the mathematical theory of thin extensible membranes to skin. The classical tension-field theory requires that the stress along a tension ray be linearly related to the displacement and therefore modifications are required to apply it directly to skin. The concepts developed by Danielson and Atrajan require that the skin undergo large deformation and that the tension rays extend all the way to the outer boundaries. Tension is developed as a ray from the deformed site and is independent of lateral connections. They use a simple exponential stress-strain law and, applying their tension-field theory to the experimental Z-plasty results of Furnas,[61] show a reasonable approximation.

Many investigators have attempted to derive a structural theory for skin and other collagen-containing tissues. These efforts were well summarized by Lanir[62] in 1979, who then presented his structural model for the biaxial stress-strain relations of soft collagenous tissue. His model is based on a network of collagen and elastin, with two variations: 1) tissues with a large number of collagen crosslinks and elastin-induced undulation; and 2) tissues with a low density of collagen crosslinks and collagen undulations which are not related to elastin. He defines both the collagen and elastin fibers as linearly elastic and therefore associated with a single spring constant each. The interaction of the ground substance is ignored. His model describes a biaxial

stress-strain relationship for flat collagenous tissue fairly effectively.

III. A finite element model of skin deformation

A. The finite element method

"The engineer in need of numbers with which his design process can be described is often impatient with a 'properly formulated' problem for which complex equations exist, but for which only comparatively trivial solutions can be achieved by classical mathematics."

This statement by Zienkiewicz[63] describes the historical development of the finite element method. Faced with complex equations for the elastic continuum, which were in many cases insoluble, the engineers developed the finite element method which reduces the continuum to an assembly of discrete elements. The technic divides the domain of the solution into a finite number of simple subdomains, the finite elements. The finite element model was initially developed by engineers in the context of physical elements such as rods and beams, but has evolved into a powerful analytical tool with a solid theoretical basis. The situation of the surgeon studying skin flap design seems analogous to that of Zienkiewicz's engineer. Clinical needs dictate the design of

complex wound closures, but these are currently based on inadequate plane geometric models. The theoretical investigations of soft tissue mechanics, however, have resulted in equations too complex to solve practical problems.

The finite element method, in essence, is a technic to approximate the solution of a continuous function with a series of trial functions (shape functions). Visually one can imagine the one-dimensional line, seen in Figure 5, whose mechanical properties can be described by a continuous function. In the finite element method this line is subdivided by a series of nodes. The properties of the line can then be described by a series of shape functions ("hat" functions) centered at each node. For the more complicated two-dimensional system with triangular elements, the shape function describes the displacement of a point in the triangle as a function of displacement of the node or triangular vertex. Visually, for a two-dimensional problem with one central vertex and surrounding triangles, imagine lifting the node or vertex off the plane of the paper; a "circus tent" would be described. In this case the shape function ("tent" function) describes the properties of a simple two-dimensional structure. The same illustration for multiple vertices would describe a "geodesic dome."

The classic work of Courant[64] in 1943 defined the concept of breaking the elastic continuum into triangular finite elements.

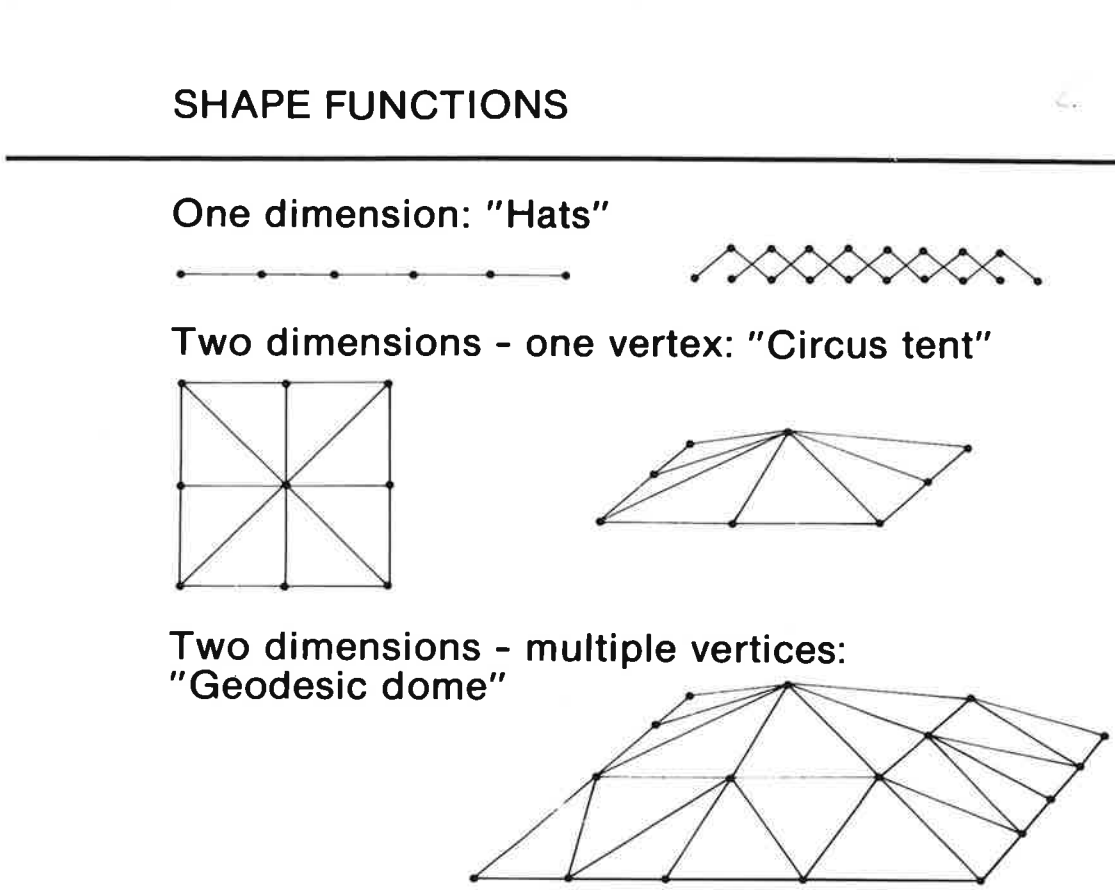

Figure 5. A visual interpretation of the shape functions for one- and two-dimensional structures. One-dimensional shape functions can be interpreted as hat functions. A two-dimensional shape function can be visualized as a tent function.

Initially the technic was limited to structural engineering fields. Excellent descriptions of the mathematical basis for the finite element method are available.[65,66] Zienkiewicz[14] and others have applied the finite element method to nonstructural fields such as fluid mechanics, heat conduction, and biologic problems. Advances in the ability of modern digital computers to handle the large matrices required to solve the finite element formulations were necessary to make the method practical.

The advantages of the finite element method over the older finite differences method are primarily:

1. the ease of arbitrary positioning of nodal points;
2. the potential to improve the result by increasing the number of nodal elements;
3. an improvement in boundary value approximations;
4. the ease with which different shapes and sizes of elements can be adopted.

Although triangles are the simplest shape function for two-dimensional problems, and the tetrahedron for three, other shapes such as rectangular or hexagonal can be utilized. The obvious advantage of the finite element technique to engineers or surgeons is the ability to correlate the shape and density of the elements with the physical shape of the structure.

Orthopedic surgeons have been the primary clinicians interested in the finite element method.[67] Simple stress analysis of bone or prosthetic implants are easily performed with the finite element method, frequently with little change from the software used for engineering analysis. Other areas of medicine for which the finite element method has proved useful include the rheology of blood flow, analysis of lung mechanics, the estimation of mechanical properties of the heart including stress analysis of the valves, and the modeling of cranial injuries. Typical examples of the use of finite elements to model bone and the heart are seen in Figures 6 and 7.

The finite element technic has not previously been applied to the modeling of wound closures or skin deformation. The obvious advantage of the technique is that its empirical nature allows the modeling of very complex geometries or anatomies based on some fairly simple stress-strain relationships.

The major goal was to design a model for skin deformation which, if not totally accurate, was an improvement over the current geometric models, and was simple enough to be potentially useful as either a training device or as a research tool for the design of skin flaps. In other words, this model is an attempt to bridge the gap between the simple models clinicians currently use in the design of skin flaps and wound closures and the elegant but impractical constitutive equations currently advocated by biomechanists to

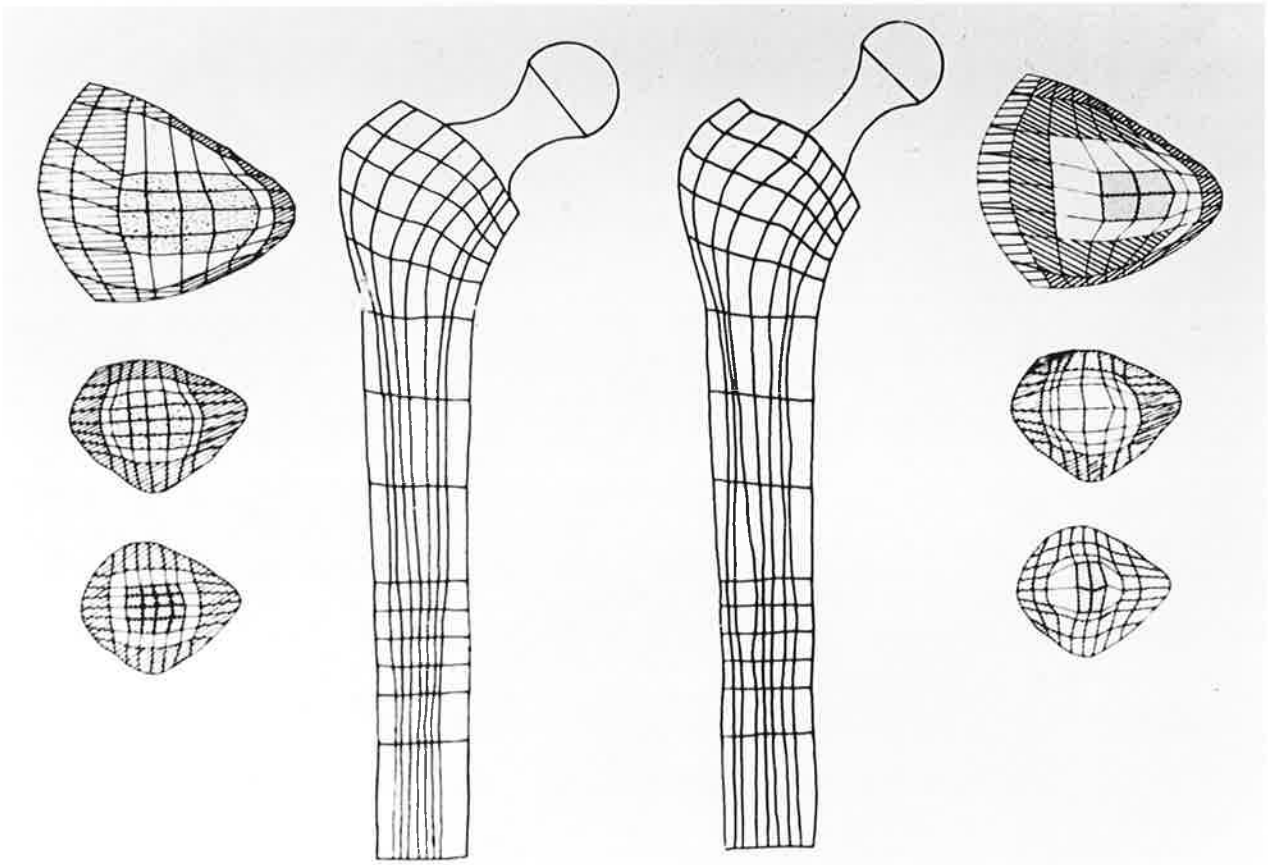

Figure 6. Finite element representation of a natural femur implanted with stem-type prosthesis. (From Gallagher et al, Finite Elements in Biomechanics, p 347, 1982.)

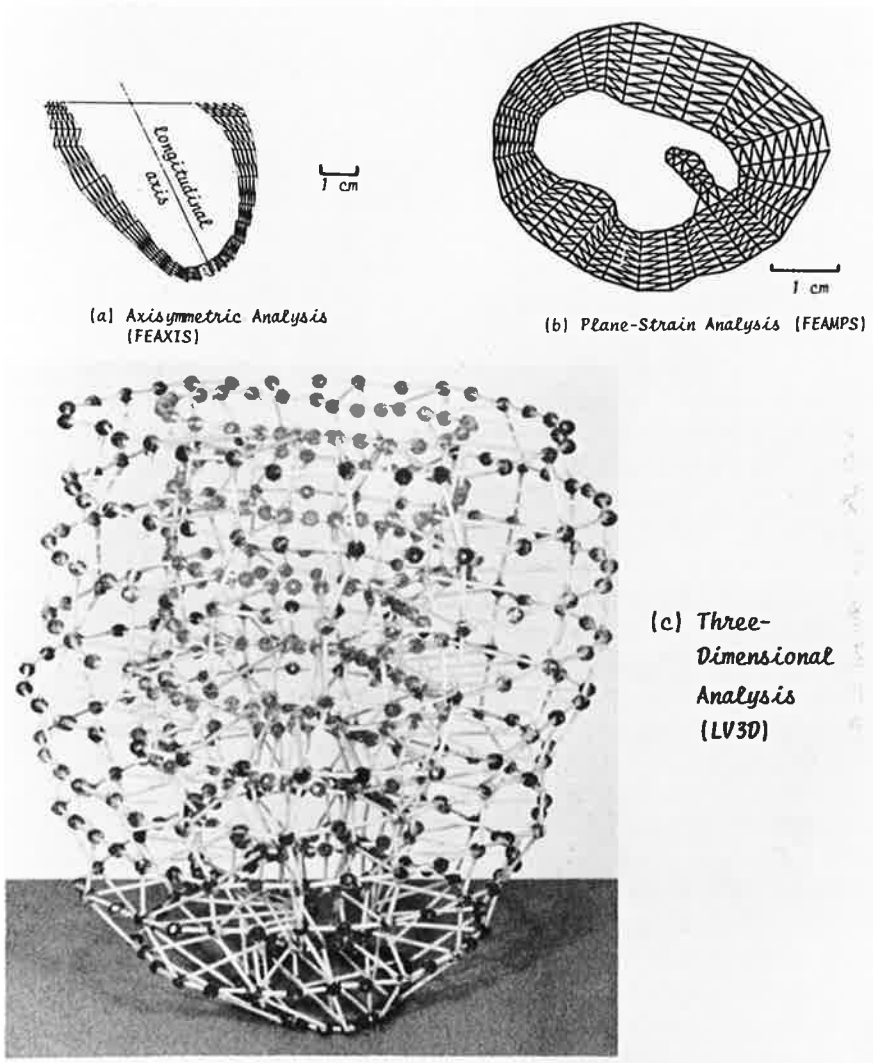

Figure 7. Finite element models of the heart. (From Gallagher et al, Finite Elements in Biomechanics, p 131, 1982.)

describe tissue properties. The following simplications and generalizations were made:

1. It is necessary to model only the strain and stress range that is clinically relevant. The extreme portions of the stress-strain curves are rarely invoked clincally and can be ignored for a practical model. Initially the model is designed with a linear stress-strain relationship; at later stages this could be improved with two or three piecewise linear functions.

2. Loading curves and the deformation state at initial wound closure are modeled. Viscoelastic properties are ignored. In most cases the immediate results of wound closure approximate the final result, and this simplication seems acceptable.

3. For the initial model, the skin is considered isotrophic with zero tension in the resting state. Neither of these assumptions is true, and eventually both variables must be incorporated into the model. There are techniques with the finite element method to include underlying and directional stresses; and these can be incorporated after the initial model has been sufficiently tested.

4. Classical continuum mechanics is utilized to define the basic stress-strain relationships. Theoretically these methods are

applicable only to infinitesimal strains. These methods are fairly accurate, however, to strains in perhaps the 10% to 15% range; they become less accurate with large deformations. Again these limitations were felt necessary to obtain a practical model.

5. Initially the skin was modeled as a simple two-dimensional system, with subcutaneous attachments. It is important to include these attachments as they are one of the major variables in wound closure. Also torsional forces on the skin cannot be well represented without them. A two-dimensional model would be useful for research and teaching in flap design, and perhaps even clinically useful on a flat body surface. It is possible to transfer a two-dimensional model to a shell model (curved two-dimensional model), and this would be the next step in the evolution of the model. A true three-dimensional model would be very complex and probably impractical.

6. The model should be kept simple enough, with one or at most two elastic constants, that these constants can potentially be estimated in vivo with a skin extensometer.

7. The ultimate test of a model is how well it approximates the actual skin deformation seen in a patient or animal. All the various test measurements on isolated skin are done with

elaborate equipment, and the results are dependent upon test technique. The measurement of skin deformation, however, is noninvasive and relatively independent of test technique. How accurately the model predicts the skin deformation field should be the ultimate measure of its accuracy. It is again of note that the current plane geometric or paper models do not allow any material deformation.

III. B. Design of the model

As seen in Figure 8, the skin is idealized as an elastic membrane with nodes at regular intervals. Attached to each node is a small spring representing the subcutaneous attachments. The stress and strain properties of the skin are related by the standard equations of classical elasticity, with the following variables:

1. E or Young's modulus, which represents the slope of the stress-strain curve in the defined range

2. ν or Poisson's ratio; this ratio is 0.5 for an incompresible material

3. k represents the "spring constant" of the subcutaneous attachment; it assumes a linear relationship between nodal displacement and force

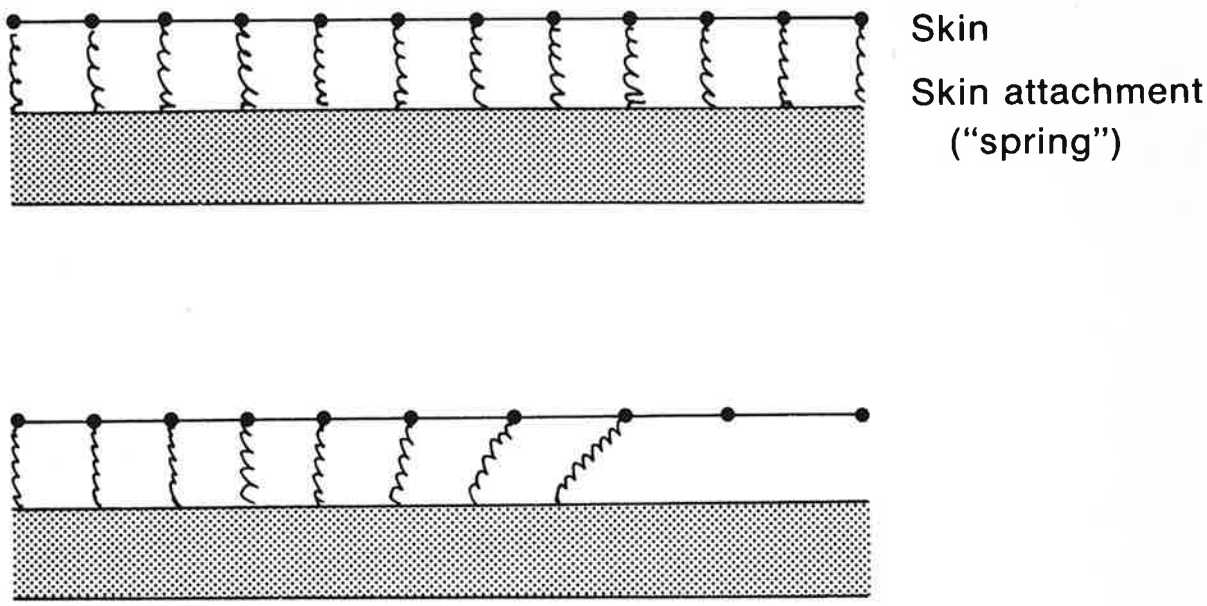

Figure 8. Conceptualization of the finite element model. The skin is visualized as an elastic membrane divided by a series of nodes. The subcutaneous attachments are represented by a small spring attaching each node to a nonmobile underlying structure. In the lower figure, the skin has been undermined and advanced.

The governing equations of the model are described as follows and related to Figure 9:

σ_{11}= Stress along side perpendicular to x_1- axis in x_1 direction

σ_{12}= Stress along side perpendicular to x_1- axis in x_2 direction

σ_{21}= Stress along side perpendicular to x_2- axis in x_1 direction

σ_{22}= Stress along side perpendicular to x_2- axis in x_2 direction

Force equilibrium for a small element of area dxdy leads to the equations:

$$\frac{\partial \sigma_{11}}{\partial x_1} + \frac{\partial \sigma_{21}}{\partial x_2} - ku_1 = 0$$

$$\frac{\partial \sigma_{21}}{\partial x_2} + \frac{\partial \sigma_{22}}{\partial x_1} - ku_2 = 0$$

Where u_1, u_2 are the displacement of the element in the x_1, x_2 directions respectively.

ku_i = force/unit area in the x_i direction $\quad i = 1,2$

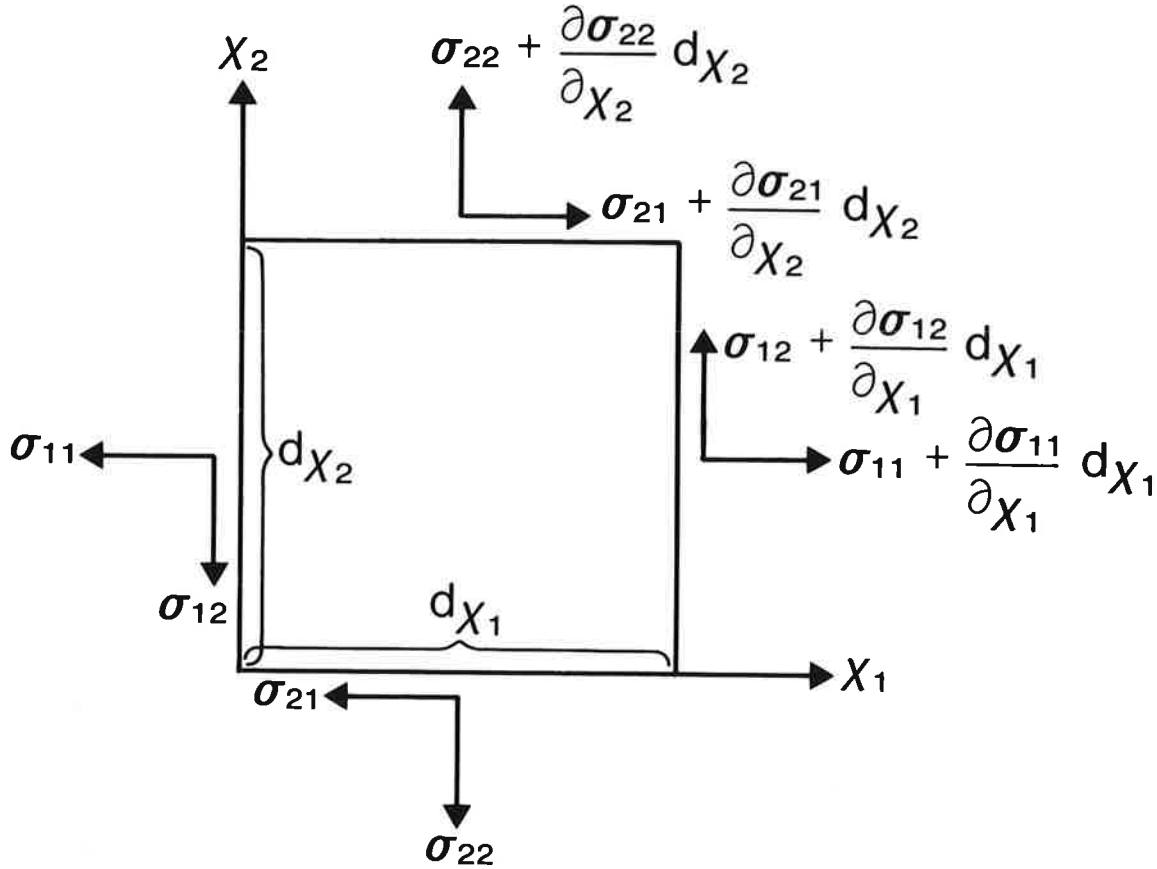

Figure 9. Terminology for the equations that govern the deformation of a small square of skin $dx_1\ dx_2$.

The stresses are related to the displacements by

$$\sigma_{11} = \frac{E}{1-\nu^2}\frac{\partial u_1}{\partial x_1} + \frac{\nu E}{1-\nu^2}\frac{\partial u_2}{\partial x_2}$$

$$\sigma_{22} = \frac{\nu E}{1-\nu^2}\frac{\partial u_1}{\partial x_1} + \frac{E}{1-\nu^2}\frac{\partial u_2}{\partial x_2}$$

$$\sigma_{12} = \sigma_{21} = \frac{E}{2(1-\nu)}\left(\frac{\partial u_1}{\partial x_2} + \frac{\partial u_2}{\partial x_1}\right)$$

E = Young's modulus

ν = Poisson's ratio

Inserting these into the equilibrium equations gives:

$$\frac{E}{1-\nu^2}\left(\frac{\partial^2 u_1}{\partial x_1^2} + \frac{(1-\nu)}{2}\frac{\partial^2 u_1}{\partial x_2^2} + \frac{1+\nu}{2}\frac{\partial^2 u_2}{\partial x_1 \partial x_2}\right) - ku_1 = 0$$

$$\frac{E}{1-\nu^2}\left(\frac{(1-\nu)}{2}\frac{\partial^2 u_2}{\partial x_1^2} + \frac{\partial^2 u_2}{\partial x_2^2} + \frac{1+\nu}{2}\frac{\partial^2 u_1}{\partial x_1 \partial x_2}\right) - ku_2 = 0$$

To solve these equations for u_1, u_2 we will use the finite element method with triangular elements.

Use two-dimensional shape functions as basis functions:

$\Phi^j(x_1 x_2) = a^j x_1 + b^j x_2 + c^j$ with a^j, b^j, c^j chosen

so that $\Phi = 1$ if $(x_1 x_2)$ is the position of vertex j

$\Phi = 0$ if $(x_1 x_2)$ is the position of any other vertex or if $(x_1 x_2)$ is outside the triangles with grid point j as a vertex

a^j, b^j, & c^j will depend on which triangle the point $(x_1 x_2)$ is in.

Try a solution of the form $U_i(x_1 x_2) = \sum_{j=1}^{N} C_i^j \Phi^j(x_1 x_2) \quad i = 1,2$

The method of weighted residuals with Galerkin weighting functions leads to

$$\sum_{j=1}^{N} \begin{bmatrix} \int \left(\alpha\Phi_{,11}^{j}\Phi^{k} + \frac{\alpha\,(1-\upsilon)}{2}\,\Phi_{,22}^{j}\Phi^{k} - k\Phi^{j}\Phi^{k}\right) dx_1 dx_2 & \int \alpha\,\frac{(1+\upsilon)}{2}\,\Phi_{,12}^{j}\Phi^{k} dx_1 dx_2 \\ \int \frac{\alpha(1+\upsilon)}{2}\,\Phi_{,12}^{j}\Phi^{k} dx_1 dx_2 & \int\left(\alpha\,\frac{(1-\upsilon)}{2}\,\Phi_{,11}^{j}\,\Phi^{k} + \alpha\Phi_{,22}^{j}\Phi^{k} - k\Phi^{j}\Phi^{k}\right) dx_1 dx_2 \end{bmatrix} \begin{bmatrix} C_1^j \\ C_2^j \end{bmatrix} = 0$$

for $k = 1,2,\ldots N$ $\qquad \alpha = \dfrac{E}{1-\upsilon^2}$

$$\Phi_{,ij} \equiv \frac{\partial^2\Phi}{\partial x_i \partial x_j}$$

We can write all these equations as $\quad AC = 0$

where

$$A = \begin{bmatrix} A_{11} & A_{12} \cdots\cdots & A_{1N} \\ A_{21} & & \vdots \\ \vdots & & \vdots \\ A_{N1} & & A_{NN} \end{bmatrix}$$

and the A_{kj} are the 2 x 2 matrices above.

$$C = \begin{bmatrix} C_1^1 \\ C_2^1 \\ C_2^1 \\ C_2^2 \\ \vdots \\ C_N^1 \\ C_N^2 \end{bmatrix}$$

The 2nd derivatives of the Φ^j are infinite at the triangle boundaries. To get by this, integrate by parts:

$$\int \Phi,^j_{11}\ \Phi^k\ dx_1dx_2 = \oint_S \Phi^k\ \Phi,^j_1\ \ell_1 ds - \int \Phi,^k_1\ \Phi,^j_1\ dx_1dx_2$$

$$\int \Phi,^j_{22}\ \Phi^k\ dx_1dx_2 = \oint_S \Phi^k\ \Phi,^j_2\ \ell_2 ds - \int \Phi,^k_2\ \Phi,^j_2\ dx_1dx_2$$

$$\int \Phi^k\ \Phi,^j_{12}\ dx_1dx_2 = \oint_S \Phi^k\ \Phi,^j_2\ \ell_1 ds - \int \Phi,^k_1\ \Phi,^j_2\ dx_1dx_2$$

$$\text{or} = \oint_S \Phi^k\ \Phi,^j_1\ \ell_2 ds - \int \Phi,^k_1\ \Phi,^j_2\ dx_1dx_2$$

Where $\ell_1\ \ell_2$ are the direction cosines of the outward normal in the $x_1\ x_2$ direction, respectively.

There are no contributions to the surface integrals if either vertex k or vertex j is an interior vertex.

The initial model was developed on a VAX* and programmed in Fortran 77. The program is listed in Appendix A. The current program uses an Apple IIE† computer with a digitalizing pad to input data and an IBM 9000§ to analyze and perform graphic output.

To model a wound closure, a series of vertices or nodes is first determined with the digitalizing pad. These vertices are numbered in the manner shown in Figure 10A.

After the vertices are stored in a file, a triangle-generating program defines the triangles, making them as simple and as close to equilateral as possible. These triangles are then stored in a file with the format seen in Figure 10B. Various experiments can then be performed on the defined deformation field.

One of the major problems to be solved in the model was how to remove a hole or defect and close it. There is no analogous situation for engineering materials where external stresses deform material, and therefore no available mathematical techniques. For the hole problem, the boundary conditions are set so that the outer boundaries do not move. One then selects which nodes ("suture points") are to be approximated, and solves the matrix for that situation (Figure 10C).

---

* VAX is a registered trademark of Digital Equipment Corporation
† Apple IIE is a registered trademark of Apple Computer Inc
§ IBM 9000 is a registered trademark of International Business Machines Inc

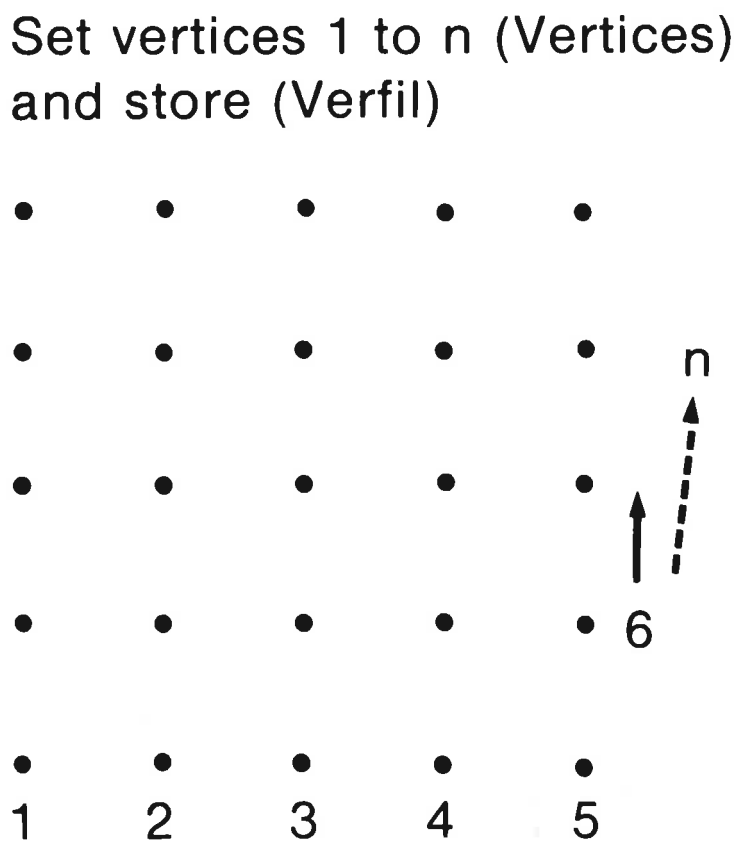

Figure 10A. Vertices are input to the model with a digitalizing tablet and numbered as shown; this data is stored in the file Verfil.

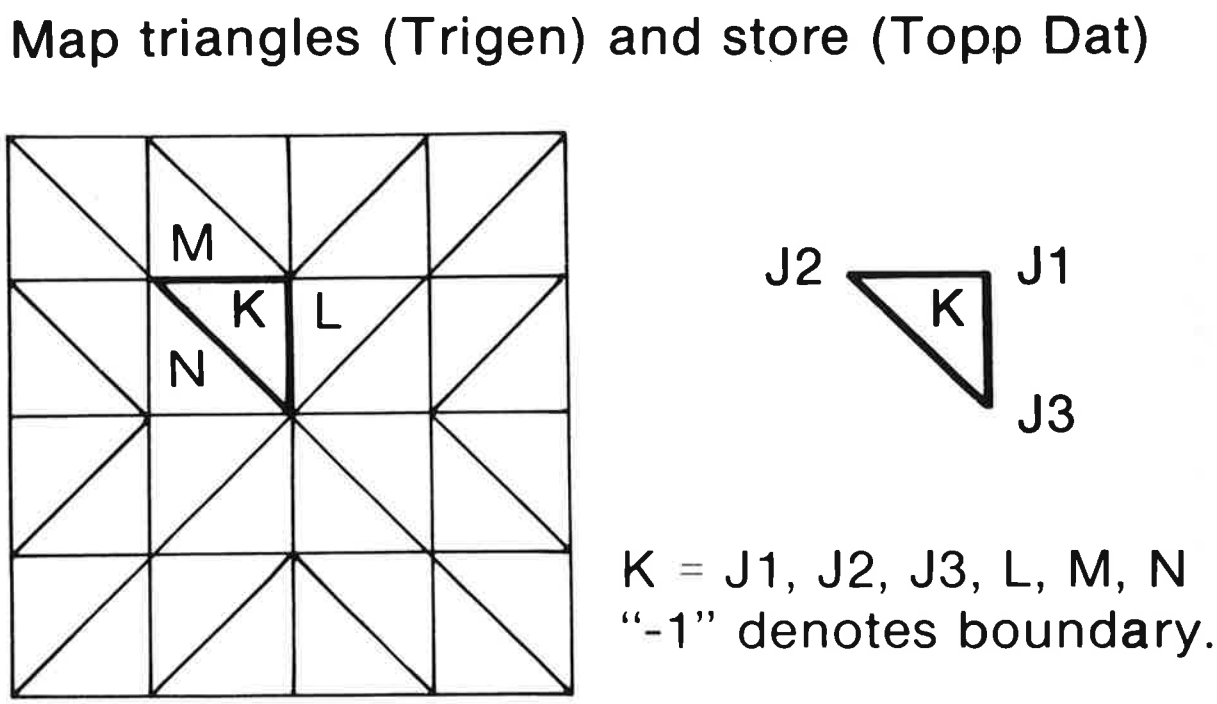

Figure 10B. A triangle-generating program connects the vertices to create the finite element triangles; this data is stored in the file Topp Dat.

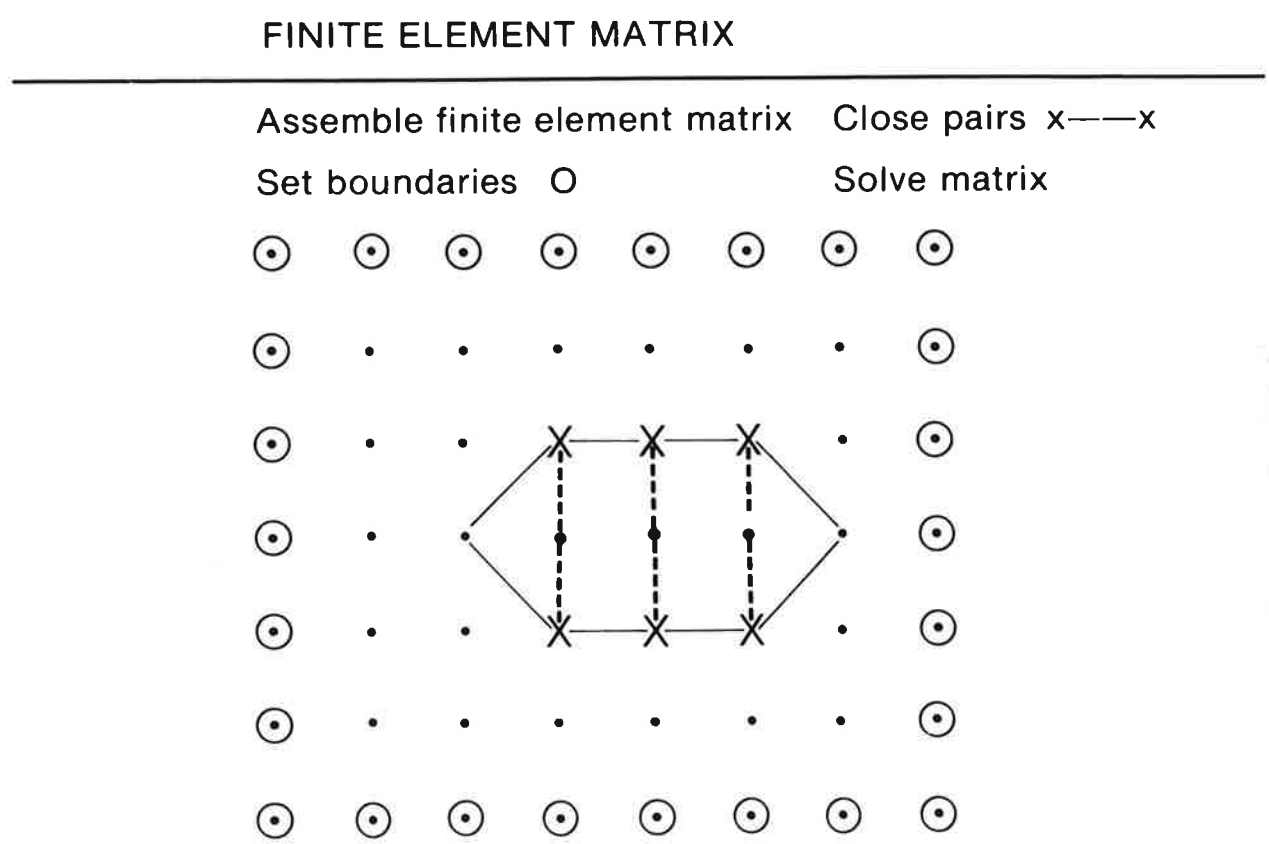

Figure 10C. The matrix of shape functions is assembled, and boundaries are set. The pairs to be approximated are input, and the matrix solved.

The model can also analyze the deformation of a rectangular strip of skin. One end of the strip is fixed, and the other can be displaced to any distance. The edges are allowed to contract based on the skin mechanics. The resulting deformation can be compared to experimental data.

IV. The experimental model

A. The animal model

An animal model is required to approximate the elastic constants, and to determine the experimental deformation fields. Although the biomechanical literature is replete with data on in vitro skin experiments, there is minimal in vivo data and no useful data available on the strength of the subcutaneous attachments. There is also essentially no data available on the measurement and analysis of deformation fields other than extremely small fields tattooed on excised skin.

Experiments have been performed on cadaver skin, rabbits, guinea pigs, dogs, pigs, rats, cats, and others. Human cadaver skin, although useful for some types of experiments, is mechanically different from that in the living human. All of the above animals except the pig have a layer of muscle (panniculus carnosis) between the skin and the underlying muscle. This is the layer which allows

the skin to move easily over the underlying muscle and makes them a poor mechanical model if one wishes to study the attachment of the skin to the subcutaneous tissue. The piglet has neither a developed panniculus carnosis nor a well-developed layer of fat beneath the skin. Piglet skin bears a close resemblance to human skin histologically. A control hematoxylin and eosin stain from a piglet is seen in Figure 11. All of the potential animal models have less elastin than humans, but the elastin content of the piglet dermis is closest to that of man.[68] In addition, the piglet has lower hair density than most of the other animal models. The skin thickness in the piglet is approximately the same as in man. For all of these reasons plus the moderately large working surface the piglet allows, it is probably the best animal model for in vivo skin testing.

IV. B. Design of the skin extensometer

As discussed above (II.B.), several individuals have designed mechanical testing devices to measure skin properties in vivo. These have varied from fairly simple hardware devices with limited flexibility to extremely complex ones with both extensive and expensive hardware features and more flexibility.

A new skin extensometer was designed for this study which is based on the control of digital stepper motors by a microcomputer. Digital stepper motors offer extreme flexibility. When interfaced

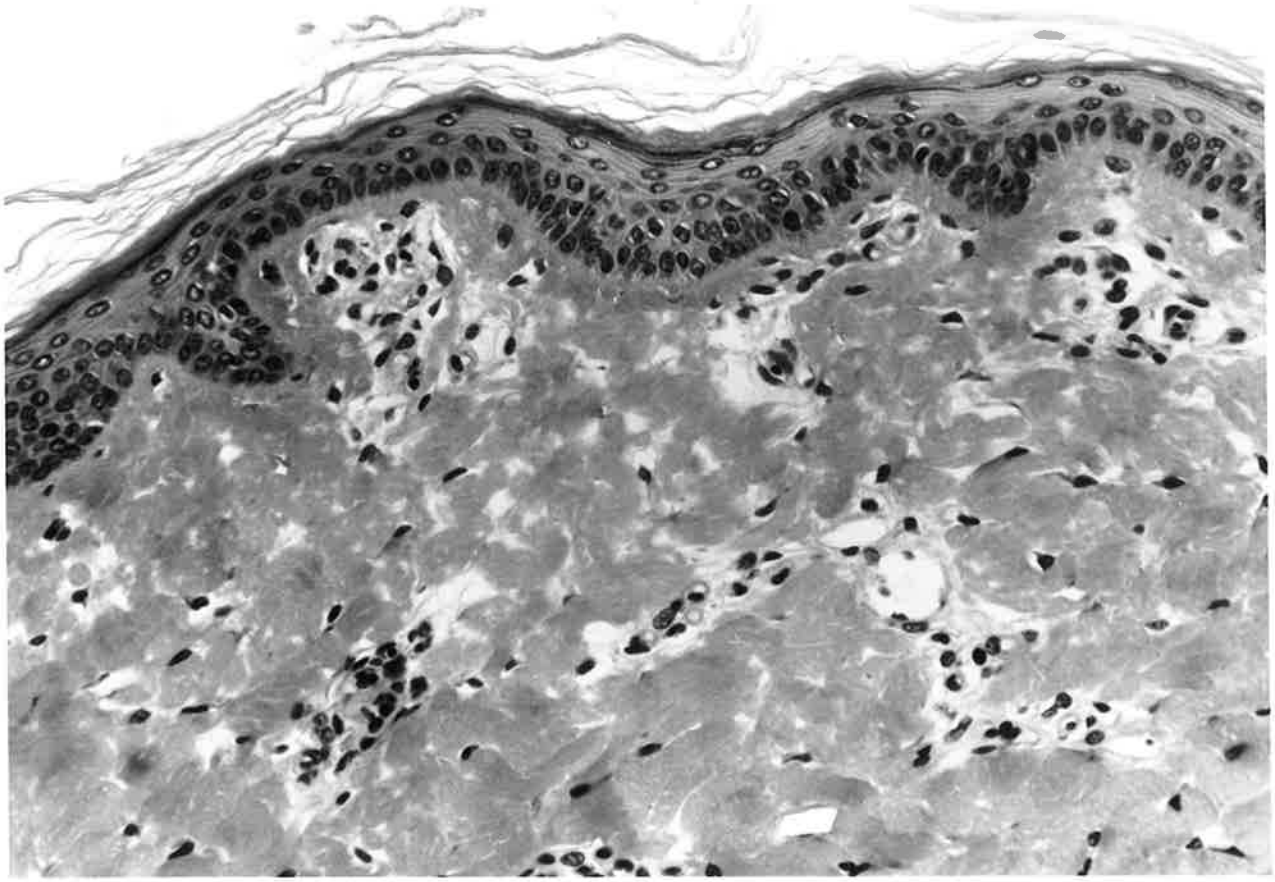

Figure 11. Hemotoxylin and eosin stain of a pig skin control.

with a realtime clock, they can run at a speed of one step per year, or several thousand steps per second. Two strain gauges are connected to the digital stepper motors via a pinion drive. The gauges and stepper motors are built into a mobile mechanical arm which connects to an operating microscope stand. One thus has the mechanical flexibility of the microscope stand in addition to the motion possible with the mechanical apparatus itself. This allows the investigator to place the strain gauges perpendicular to an irregular skin surface easily. The physical arrangement of the strain gauges and the operating microscope stand is seen in Figure 12. The analog output from the strain gauges themselves is fed into an analog digital convertor which then connects to a microcomputer (Apple IIE). The mechanical design of the skin extensometer results in a linear motion for the strain gauges of 0.015 cm/step. The stepper motors are controlled by a timer-driver board* inserted into an Apple IIE microcomputer. The device is relatively accurate and inexpensive; in addition, it offers great flexibility because the motors are programmed with software, not hardware. Software developed to control the motors is listed in Appendix B. One or both strain gauges can be moved at a selected rate and for a given distance or until a maximum stress is reached. In addition, the gauges can be set at a given distance and will monitor stress over time (to measure stress relaxation). They can also be programmed to extend the arms to a given stress and to maintain that stress for a given time (to measure creep).

---

* A6 T/D timer driver board from Rogers Labs Inc., Santa Ana, California

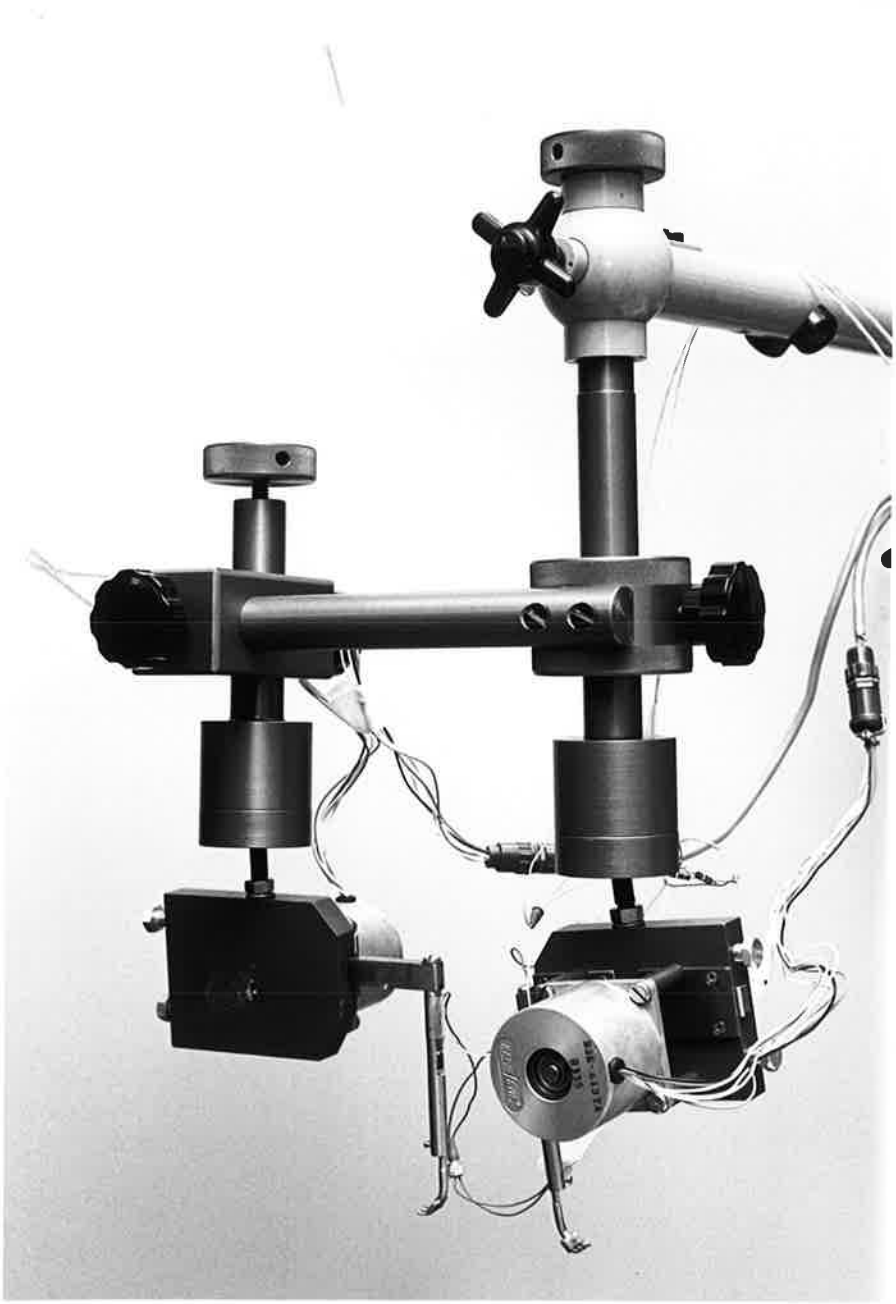

Figure 12. The skin extensometer attaches to an operating microscope stand.

IV. C. Experimental measurements of the viscoelastic properties of skin in the piglet

Because little sophisticated mechanical work has been done in the pig model, a series of descriptive experiments were performed to ensure that the basic biomechanical and viscoelastic properties described in other animals are similar in the piglet. All experiments in this study were performed with interperitoneal pentobarbital sodium and/or intramuscular xylazine sedation, combined with 1.0% xylocaine with 1:100,000 epinephrine as an injectable local anesthetic.

The skin thickness in the piglet seemed to approximate that of the human. To obtain a range of thicknesses, 10 rectangular pieces of skin were excised from five piglets in various places along the side. Each of these was then lightly compressed between two microscope slides, and the thickness read with a micrometer. Skin thickness varied from 1.3 to 1.8 mm, with a mean of 1.6 mm.

The major limitation of this animal model is the marked anisotropy of the skin. The relaxed skin tension lines run in a dorsal to ventral direction. As can be seen in Figure 13, when simple incisions are made on the side of the animal there is a great difference in the wound separation and in the amount of force required to close that separation. In this particular example,

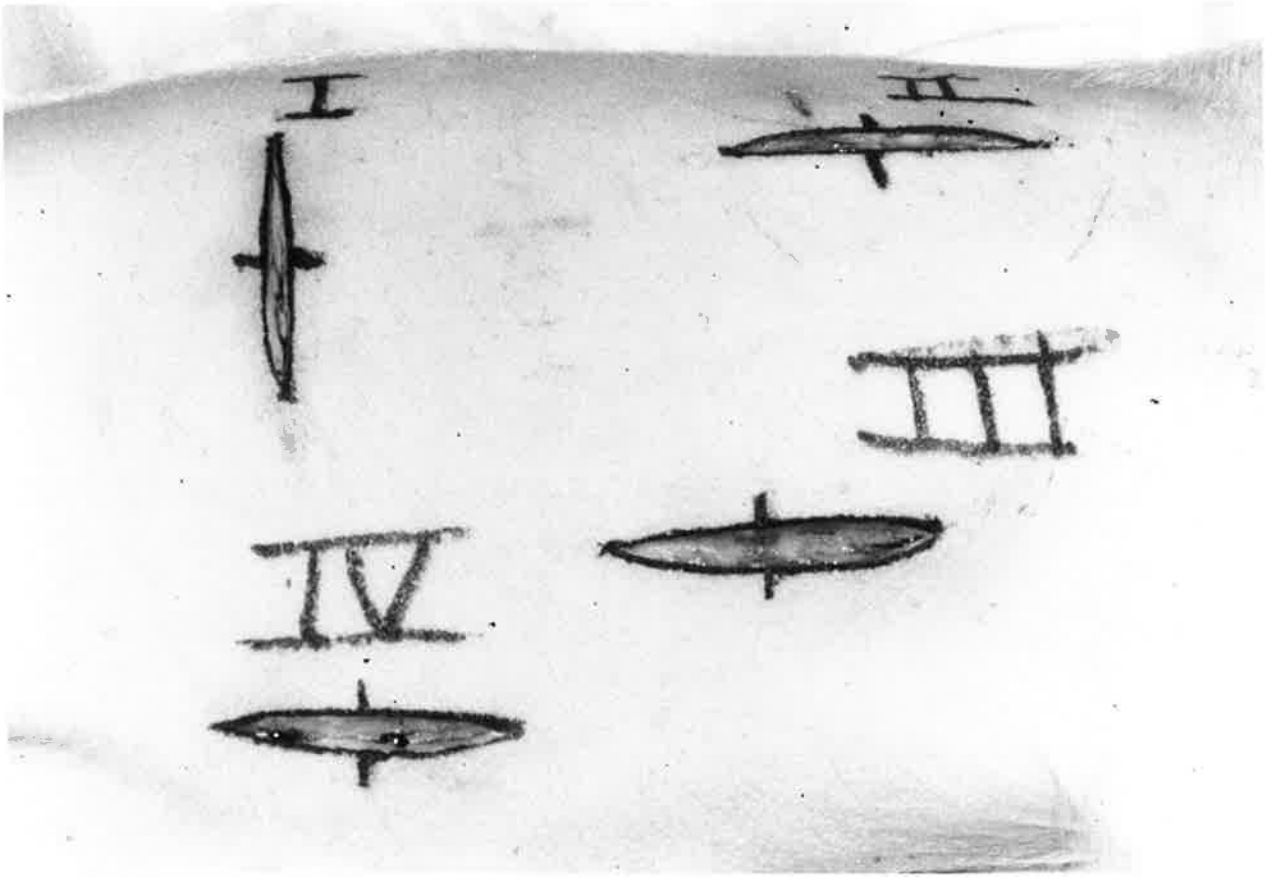

Figure 13. The side of a piglet demonstrating skin anisotropy.

incision number 1 (top left) resulted in a separation which required 14 grams to close; incision 2 required 98 grams; incision 3 required 28 grams; and incision 4 required 7 grams for closure.

This anisotropic property is related to the skin itself as well as to the underlying tissues. A strip of skin 2 cm wide by 6 cm long was removed parallel to incision 1, and a strip of the same length removed parallel to incision 2. A strip biaxial test was then performed on the skin. The skin was clamped along its length with a serrated clamp adhesed with Eastman 910 glue. The skin was then floated in a 37° C bath of Ringer's lactate, and stepwise loading was performed. One minute was allowed at each load level, and loads from 10 grams to 1,000 grams were placed along the 6 x 2 cm strip. The results are seen in Figure 14. The strip excised with its length parallel to the relaxed skin tension lines was much more extensible than the one excised with its length perpendicular to the relaxed skin tension lines. This corresponds to human studies and demonstrates the anisotropic properties inherent in the skin.

Studies of the viscoelastic properties of the skin were then performed. It was of interest to see if the properties of hysteresis, stress relaxation, and creep persist when the skin is tested in vivo. For this series of experiments a length of skin along the piglet's side 7 cm in length and 1 cm in width was incised through skin and subcutaneous tissue. This island of tissue was left pedicled on the subcutaneous tissue. One

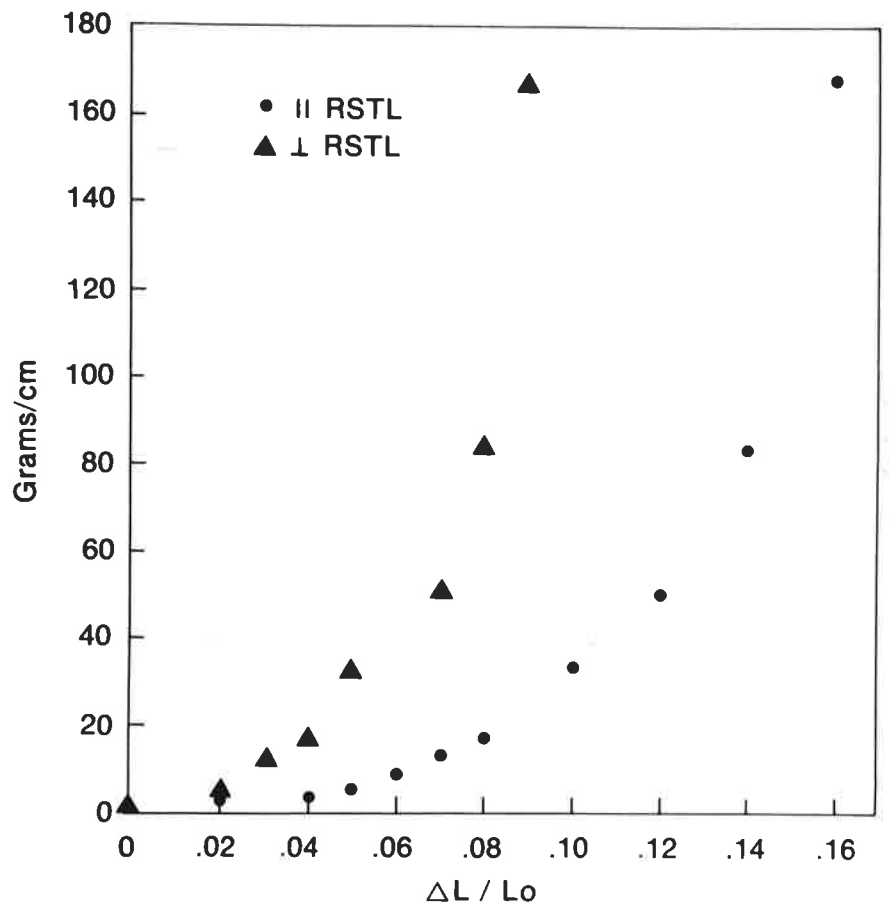

Figure 14. Strip biaxial test with and against relaxed skin tension lines (RSTL), demonstrating intrinsic skin anisotropy.

centimeter tabs attached with double-sided adhesive tape and fixed with Eastman 910 glue were then attached on either end, and the strain gauge arms were attached to these tabs. This gave an effective strip dimension of 5 x 1 cm.

Loading and unloading curves were measured. The adhesive tabs were separated at a rate of 1 mm/sec for a distance of 2.5 cm (50% strain) and then returned at the same rate. A typical result of these experiments is seen in Figure 15, demonstrating a distinct separation between the loading and unloading curves.

Stress relaxation was measured with the same experimental setup. The 5 cm length of skin was extended for a distance of 1 cm, and the tension measured at each second for 100 seconds. Tension showed a decrease over that time from 129 grams to 55 grams as seen in Figure 16.

Creep was measured in a similar fashion by placing a constant tension of 100 grams on a 5.0 cm skin island. There was a gradual lengthening of the skin, with a final strain of about 0.25 reached at 120 seconds, as depicted in Figure 17. The majority of this increasing strain took place over the initial 30 seconds.

Finally, using the same experimental setup, a 5 cm skin island was repeatedly stretched to a strain of 50% at a rate of 1 mm/sec, with 60 seconds between the initiation of the loading process. These

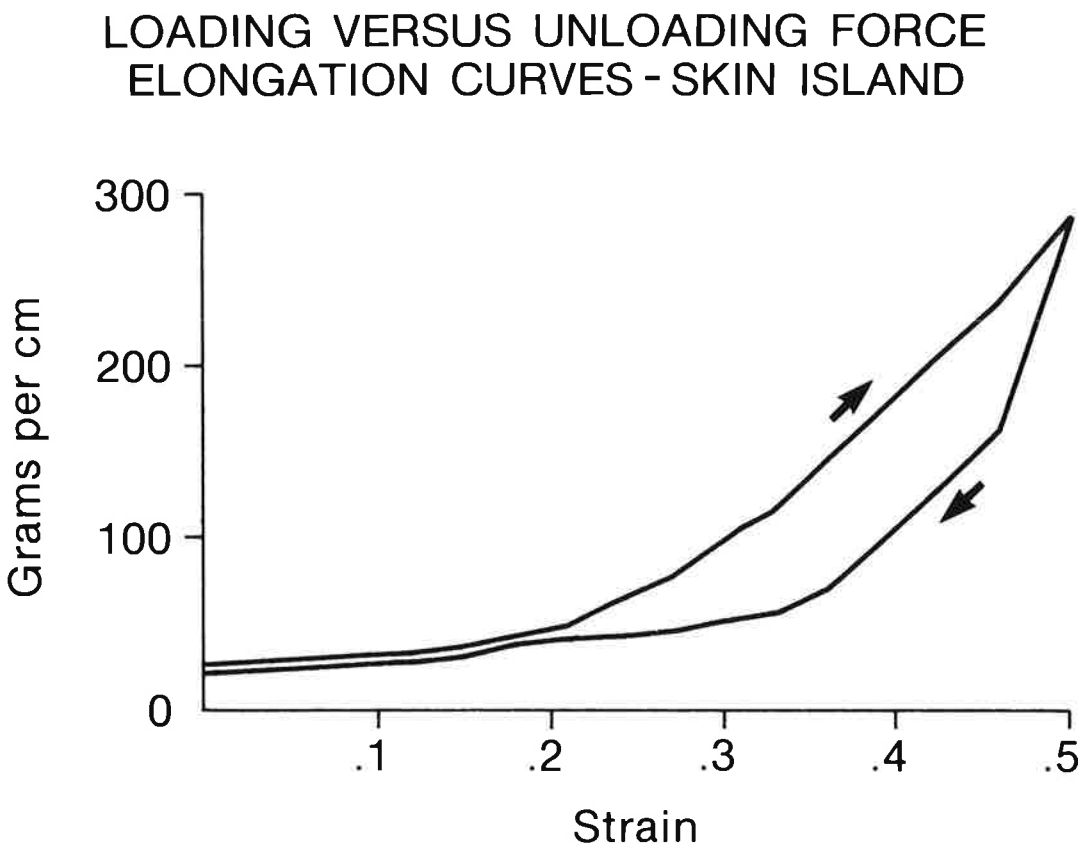

Figure 15. Loading versus unloading curves of a skin island, demonstrating hysteresis with separation of the two curves.

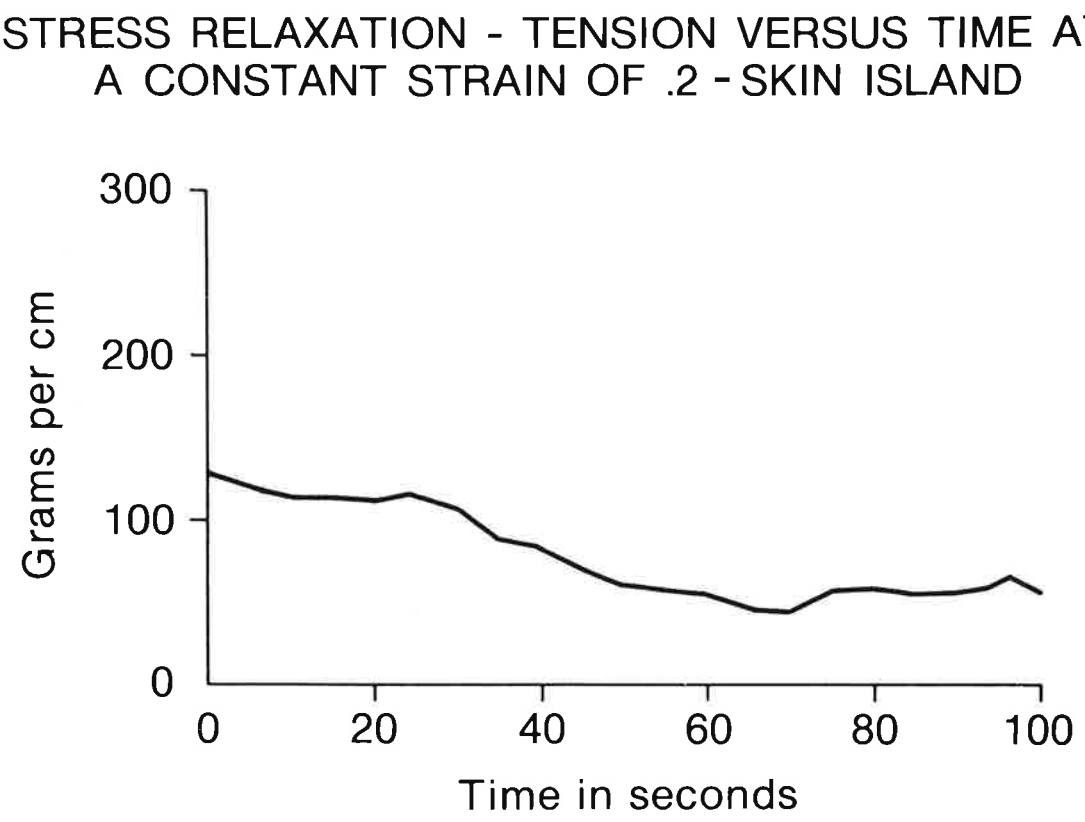

Figure 16. Stress relaxation in the skin island. A 5 cm length of skin was extended 1 cm, and resulting tension monitored for 100 seconds.

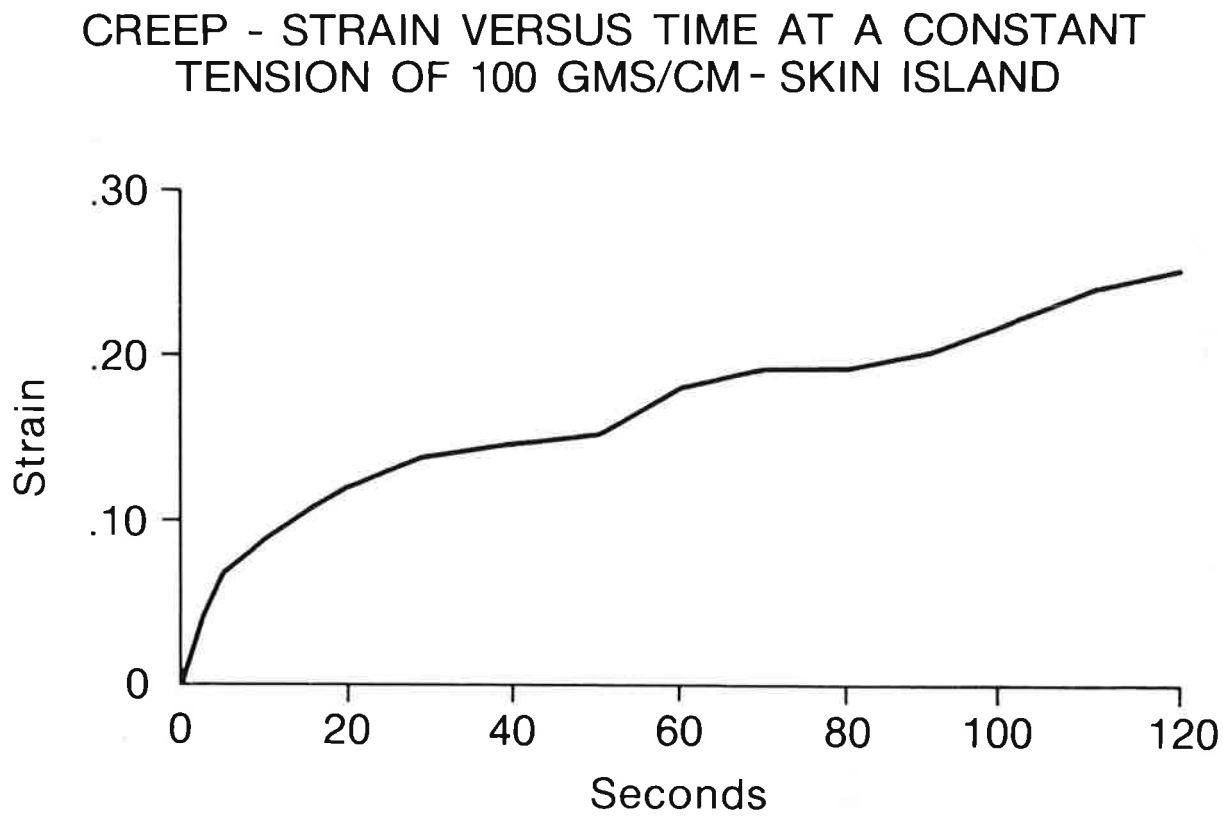

Figure 17. Creep. Strain measured in a 5 cm skin island with a constant tension of 100 grams.

data are depicted in Figure 18, and demonstrate the same hysteresis seen in other animal models: a shift of the curve to the right with repeat loading.

In summary, the skin island on the piglet displays the same viscoelastic properties seen in isolated skin of humans and other animal models.

IV. D. Measurement and standardization of the deformation field

Although there are many ways to measure the mechanical properties of skin, the ultimate result of a wound closure is deformation of the surrounding skin. This deformation field can be measured noninvasively (photographically); one can imagine the skin itself acting as a series of small strain gauges, which if appropriately analyzed will tell how much tension exists in any given area of the skin. Another advantage of analyzing the deformation is that the technique can be applied noninvasively to patients. For the animal experiments in this study, a 1 cm deformation grid was placed on the side of the piglets. A grid as fine as 5 mm could be placed and still be fairly easily read, but this seemed to offer no significant additional advantage. During the course of the experiments on the piglets, a 35 mm camera with a 55 mm macro lens was used with panatomic X film to photograph the skin at various stages of the experiments. The camera was fixed overhead and kept

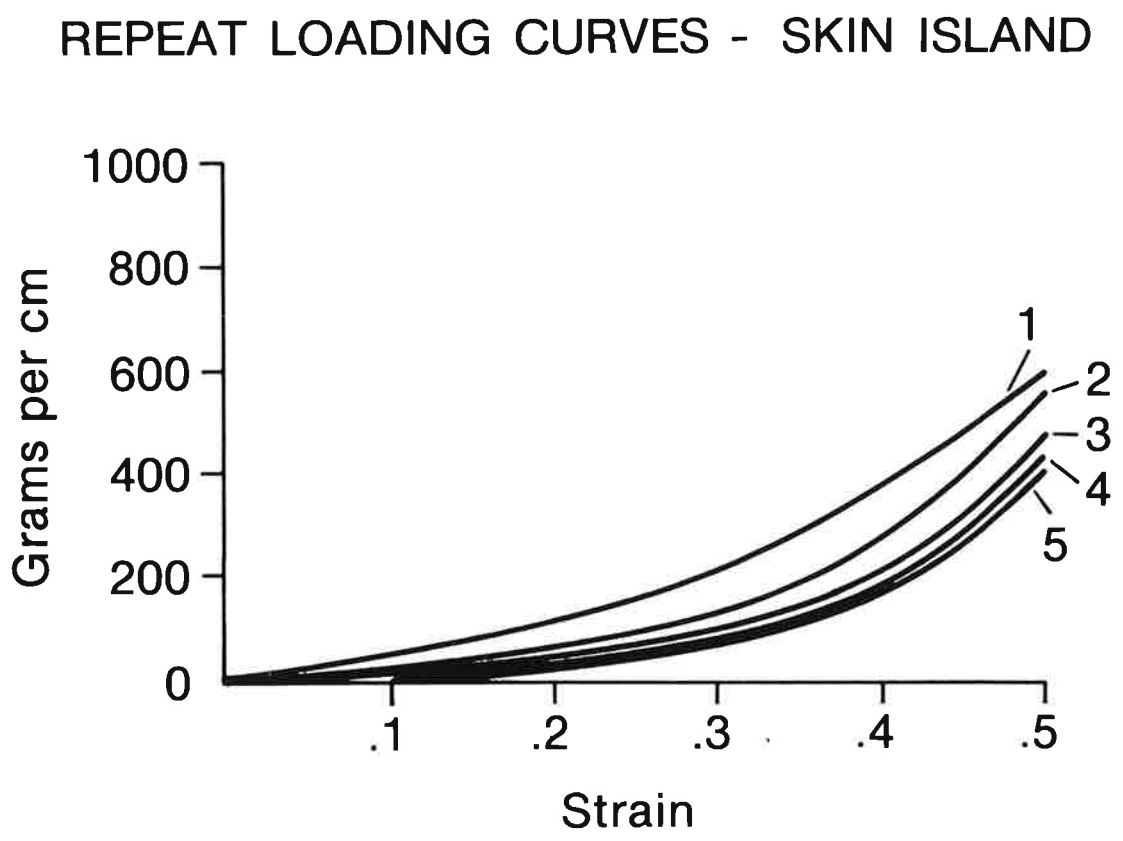

Figure 18. Repeated loading of a 5 cm skin island, demonstrating hysteresis.

in the same position. A typical deformation field for the closure of a fusiform lesion is seen in Figure 19.

A standardized technique was developed to measure skin deformation from black and white photographs. The deformation grid marked on the piglet's side was digitalized using a crosshair cursor to mark each vertex of the grid. A GTCO digitalizing tablet (DIGI-PAD 5)* with a resolution of 0.001 inch was utilized with an RS 232 interface. The pad was connected to an Apple IIE microcomputer. The DIGI-PAD 5 operates on an electromagnetic principle producing absolute coordinate information based upon measuring the time for an electromagnetic wavefront to travel down an axis. The wavefront is generated by switching at a crystal-controlled rate a current in an array of precisely positioned parallel conductive wires in a rigid tablet enclosure. This particular pad is reliable because it requires no magnetization or adjustment to maintain performance, and damages to the tablet surface (scratches, ink, etc.) do not significantly affect tablet precision. The absolute xy coordinates digitalized from the photograph, however, depend upon how the photograph is laid on the digitalizing pad, and therefore absolute coordinates cannot be simply compared from photograph to photograph. Software was therefore developed for the Apple IIE microcomputer to standardized a rectangular grid and allow such comparisons. This software is listed in Appendix C. For any

* GTCO Corporation, Rockville, Maryland

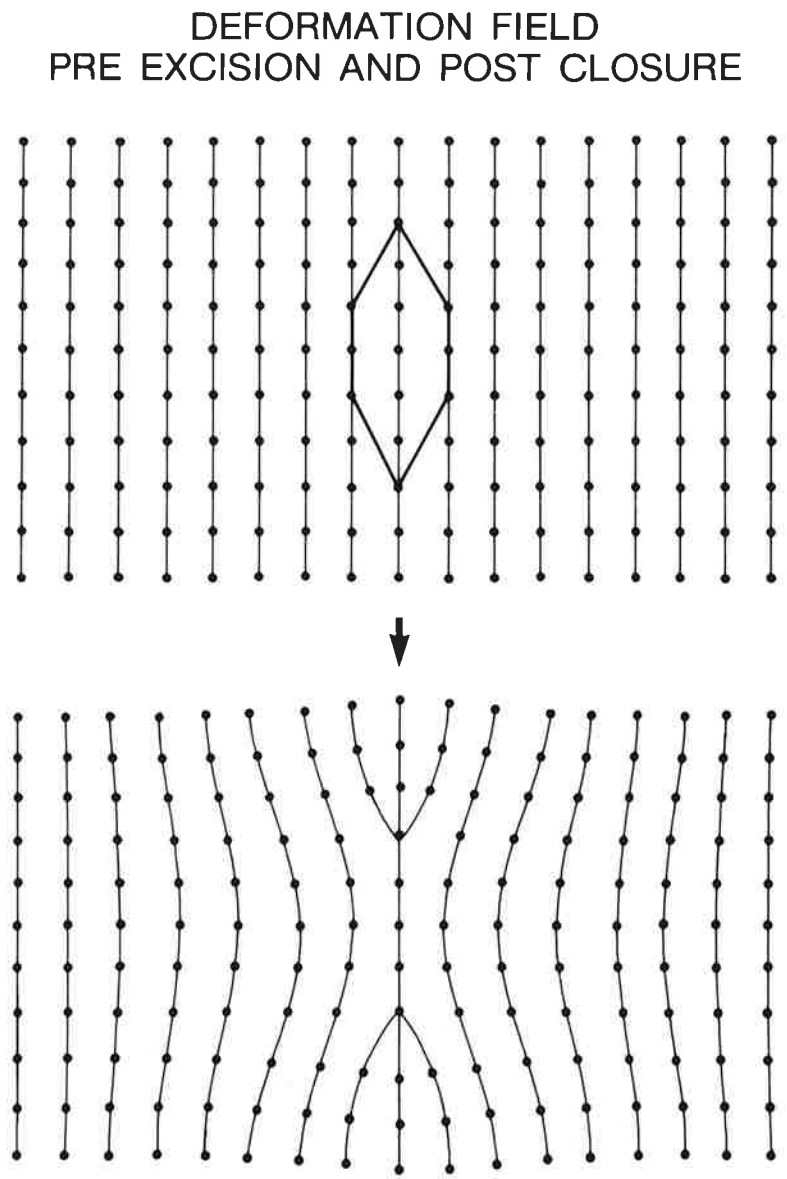

Figure 19. Skin deformation before and after excision of a fusiform lesion; experimental data from the piglet.

rectangular grid, it automatically moves the bottom left corner to 0,0, the top left corner to 0,h (where h = the actual height of the rectangle), and the bottom right corner to 0,d (where d = the actual length of the rectangle). A transformation matrix is then multiplied by the absolute values of each x,y coordinate in the grid to transform them into the standardized format. Once this is done the software will allow comparison of pre- and postoperative photographs to analyze the actual displacement of any given point. It will also allow averaging of the positions of a specific vertex over multiple closures to determine mean deformation fields.

IV. E. Determination of a practical range of stress and strain for clinical wound closure

A series of experiments was then undertaken to determine the practical stress and strain range for clinical wound closure. Three sets of experiments were performed:

1. A 4 cm incision was made parallel to the relaxed skin tension lines. 2 cm of undermining was performed in a subcutaneous layer. Using a 1 cm adhesive tab attached to the midportion of the wound edge, a stepwise loading procedure was performed with the skin extensometer. The skin flap was advanced 1 mm at a time with 30 seconds between advancement cycles. For each millimeter advanced the force was recorded in seconds. The mean of these 10 measurements is graphed as millimeters

advancement versus grams tension in Figure 20. From the graph, closure of a 2 cm defect (1 cm advancement from each side) would result in a tension of about 100 grams.

2. Five 2 x 6 cm fusiform defects were designed and closure performed with 2 cm of undermining. The final closure line with each site numbered is seen in Figure 21. Table I summarizes the tension distribution along the closure sites as well as the mean tension at each site. Again for this fairly typical clinical closure, the mean closing tension/cm is somewhat over 100 gm.

3. In a final set of experiments, a 1 cm grid was placed on the side of the animals and photographed (section IV.D.). A 2 x 6 cm defect was then excised and closed with 2 cm of undermining. The deformation grid was rephotographed. Utilizing a digitalizing pad, the linear deformation over the first 2 cm at the midportion of the closure was measured. Three such experiments were performed and the average strain over this area was 10%.

In summary, although skin is capable of extreme deformation, for a typical wound closure tensions between 100 and 150 grams and strains of 10% to 20% would define a practical range.

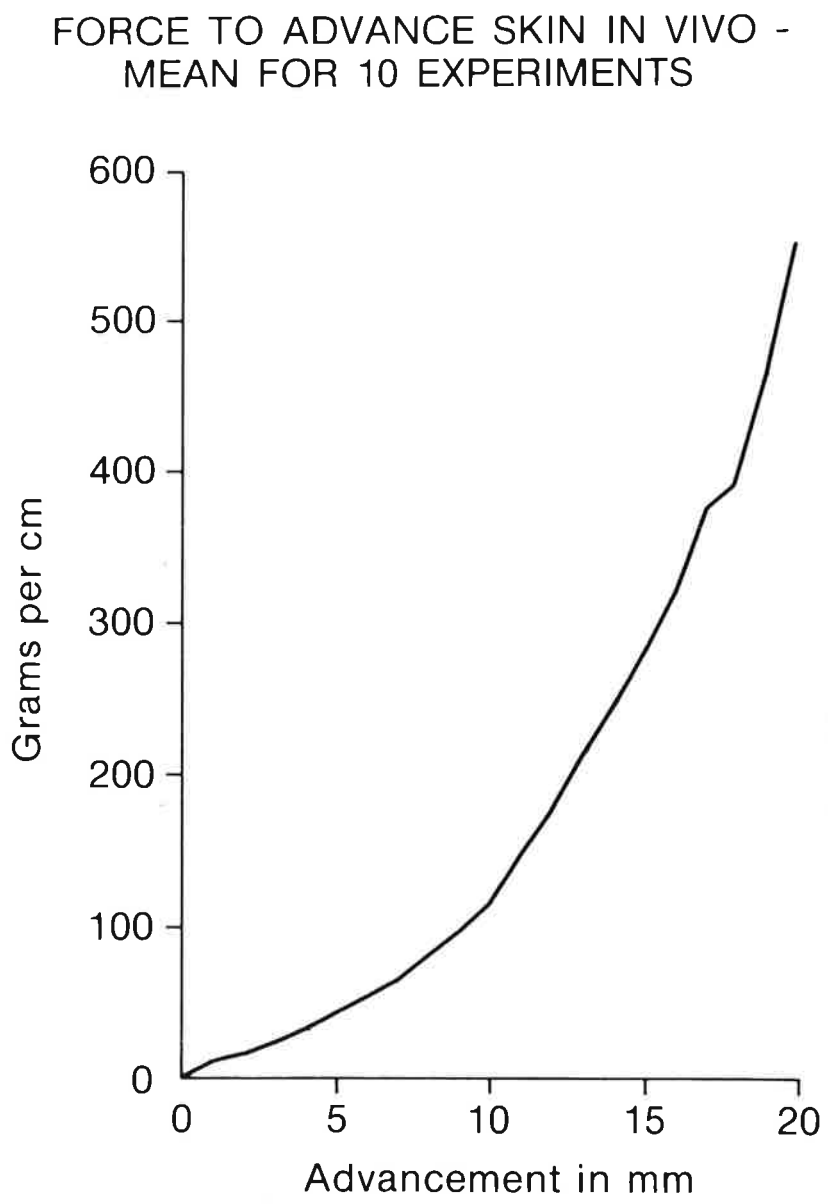

Figure 20. Mean tension versus skin flap advancement for 10 experiments.

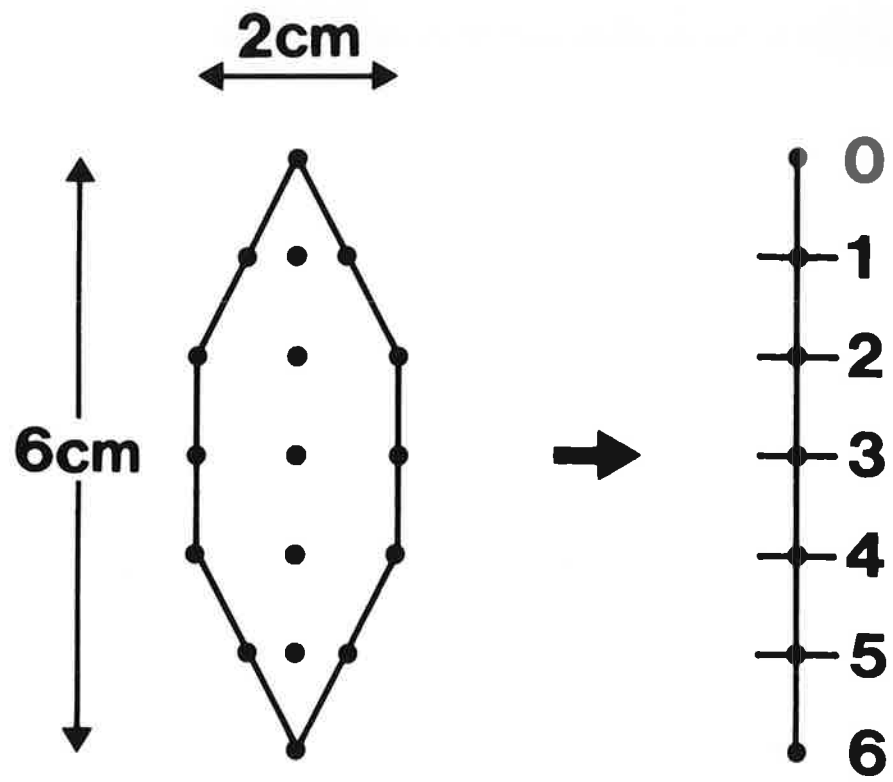

Figure 21. Location of closure sites for a fusiform defect.

TABLE I.

Tension Distribution Along Closure of 2 x 6 cm Fusiform Defect

	Tension at Each Site Along Closure (Grams)				
Pig	1	2	3	4	5
1	126	168	127	112	70
2	113	125	113	59	71
3	140	120	119	119	70
4	134	175	127	134	140
5	140	98	84	91	77
Mean	131	137	114	103	86
Tension Distribution by Site	23%	24%	20%	18%	15%

IV. F. Measurement and prediction of the major variables for the mathematical model

A series of experiments was then undertaken to determine the elastic constants E (Young's modulus), k (spring constant), and ν (Poisson's ratio) in the animal model over a practical range of stress and strain. In addition, an attempt was made to predict wound closing tensions and the range of these elastic constants with an in vivo measurement system. For the first set of experiments, a 7 cm length of skin, 1 cm in width, was outlined on the side of the piglet, running in an anterior to posterior direction. Tabs were attached to the end 1 cm of each strip and then connected to the strain gauge arms of the skin extensometer. The arms were separated at a rate of 1 mm/sec for a distance of 2.5 cm (50% strain) and then returned to their original position at the same rate. The skin was excised along the boundaries, creating a skin island. The adhesive tabs were left in the same position and the skin island deformed in the same manner as the intact skin. The skin was then excised totally, and the same experiment repeated on the isolated skin, with the skin floating on a 37° bath of Ringer's lactate. Approximately three minutes were allowed between the successive measurements on intact skin, the skin island, and isolated skin. A total of five sets of experiments were performed on three piglets. The resulting curves of strain versus force are depicted in Figures 22 to 26. Although there is variation from experiment to experiment, the general shape of the curves is

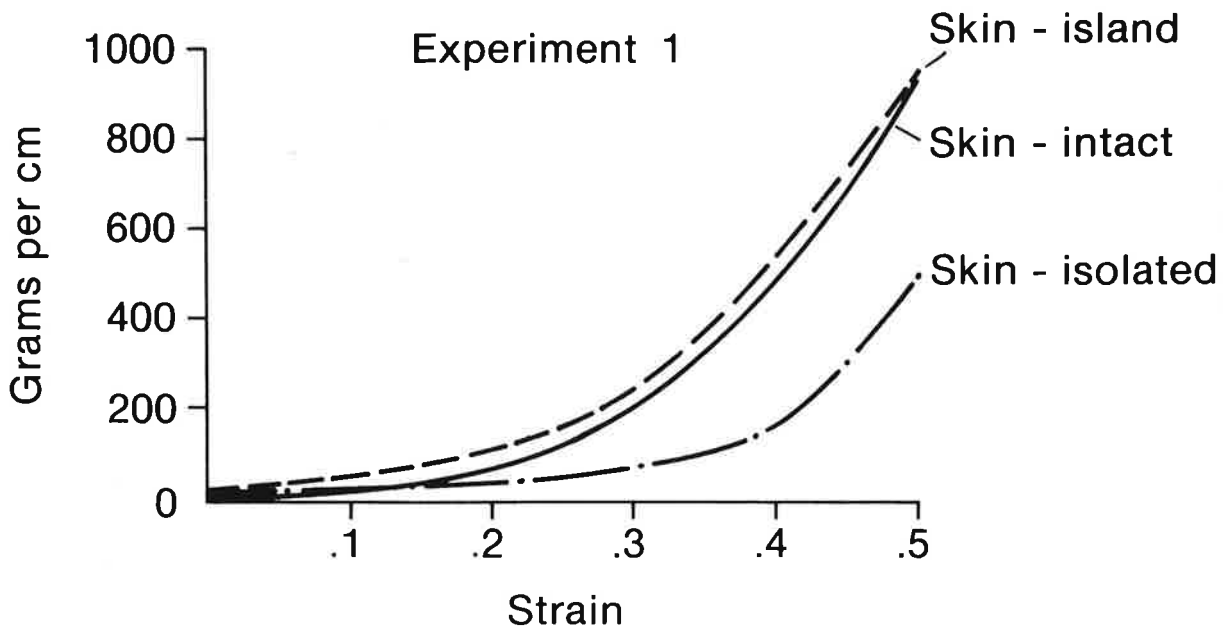

Figure 22. Experiment 1: successive force elongation curves for intact skin, skin island, and isolated skin.

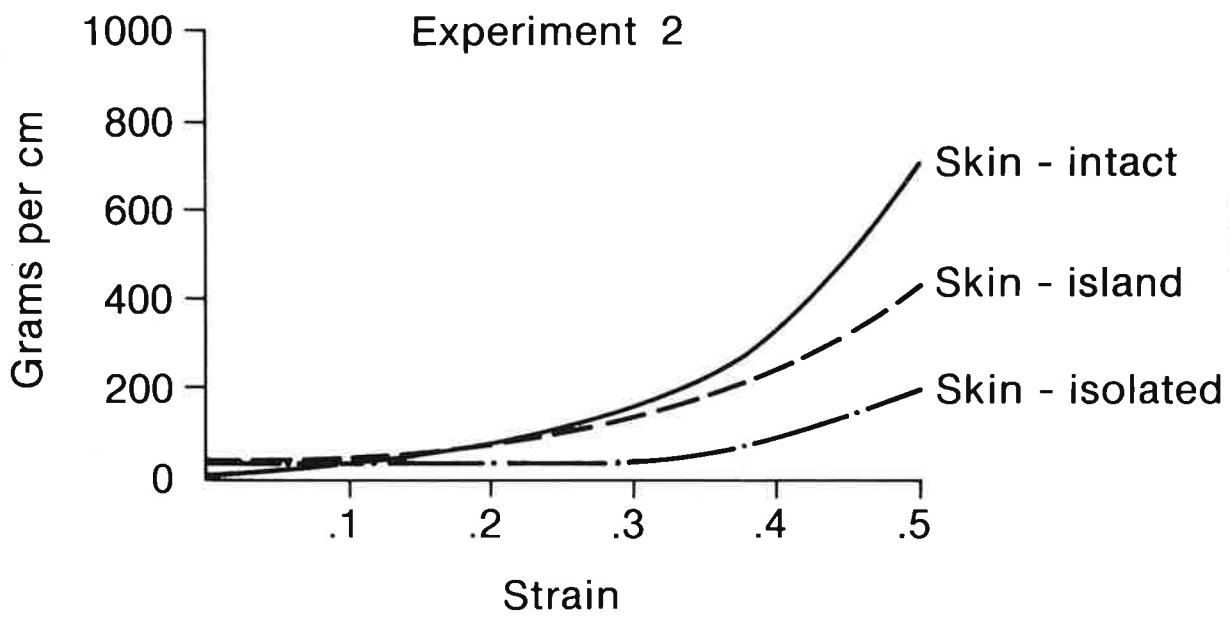

Figure 23. Experiment 2: successive force elongation curves for intact skin, skin island, and isolated skin.

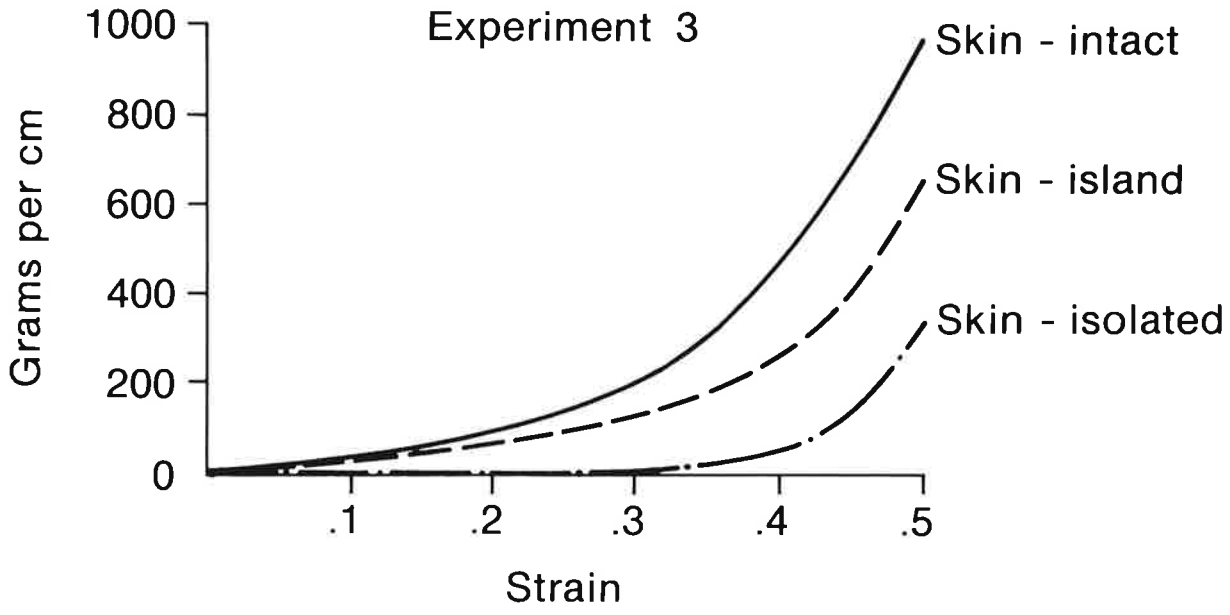

Figure 24. Experiment 3: successive force elongation curves for intact skin, skin island, and isolated skin.

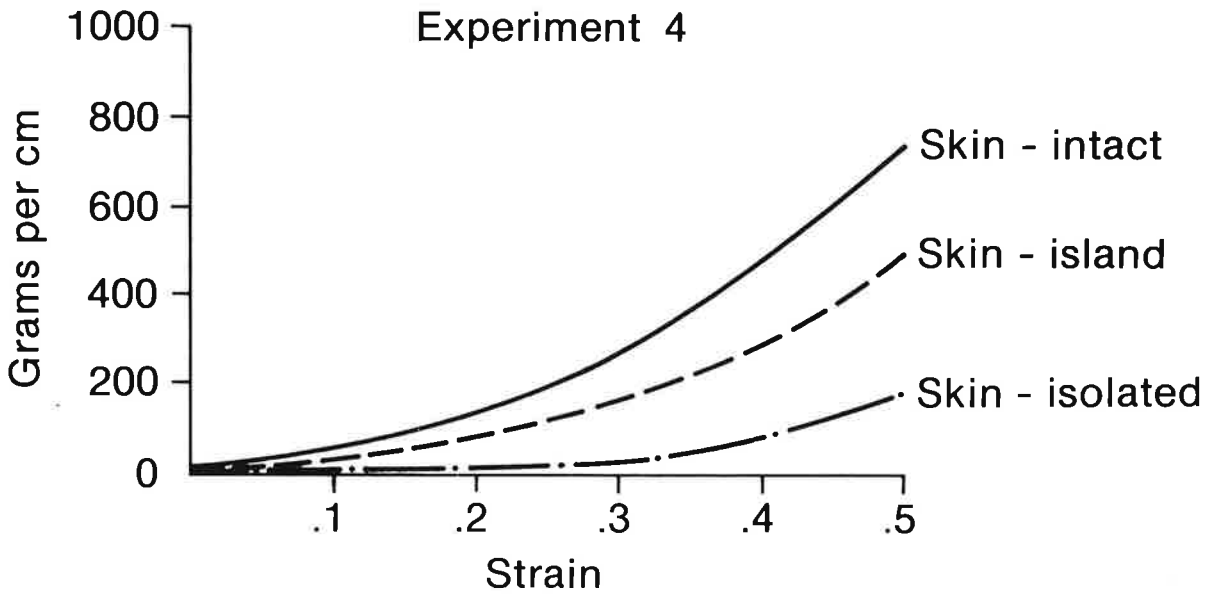

Figure 25. Experiment 4: successive force elongation curves for intact skin, skin island, and isolated skin.

Figure 26. Experiment 5: successive force elongation curves for intact skin, skin island, and isolated skin.

consistent, with successively less force being required at each stage of the experiment.

The difference between the force required to advance the skin island a given distance, and the force required to advance the isolated skin a given distance represents the contribution of the subcutaneous tissue attachments or the spring force. For the five sets of experiments, this difference was then graphed as a function of strain, and these five curves are represented in Figure 27.

Based on the shape of the curves in Figures 22 to 26, and on the determination of the stress-strain range for clinical wound closure, it was elected to analyze these curves as a linear function from strain = 0 to strain = 0.25. A linear regression was performed on the digital data for the three curves (skin intact, skin island, and isolated skin) in each of the five experiments. The slope of the linear regression line for these curves is listed in Table II. As expected, there was a large variation in the actual slope of these lines, dependent upon the local tissue properties. The ratio of the slope of the linear regression line for the skin intact versus the skin island was evaluated to see if the adhesive tab technic could predict the other results. This ratio varied from 1.4 to 2.2. One could thus approximate the slope of the skin island curve as half that of the skin intact curve. The ratio of the slope of the skin intact to the skin isolated curve varied from 15 to 41, and although the slope of the isolated

TABLE II.

Slope of Linear Regression Line From Strain = 0 to Strain = 0.25

Experiment	Skin Intact	Skin Island	Skin Isolated
1	4.1	2.2	0.9
2	4.2	1.9	0.1
3	5.5	3.4	0.2
4	6.1	4.5	0.4
5	2.8	1.7	0.1

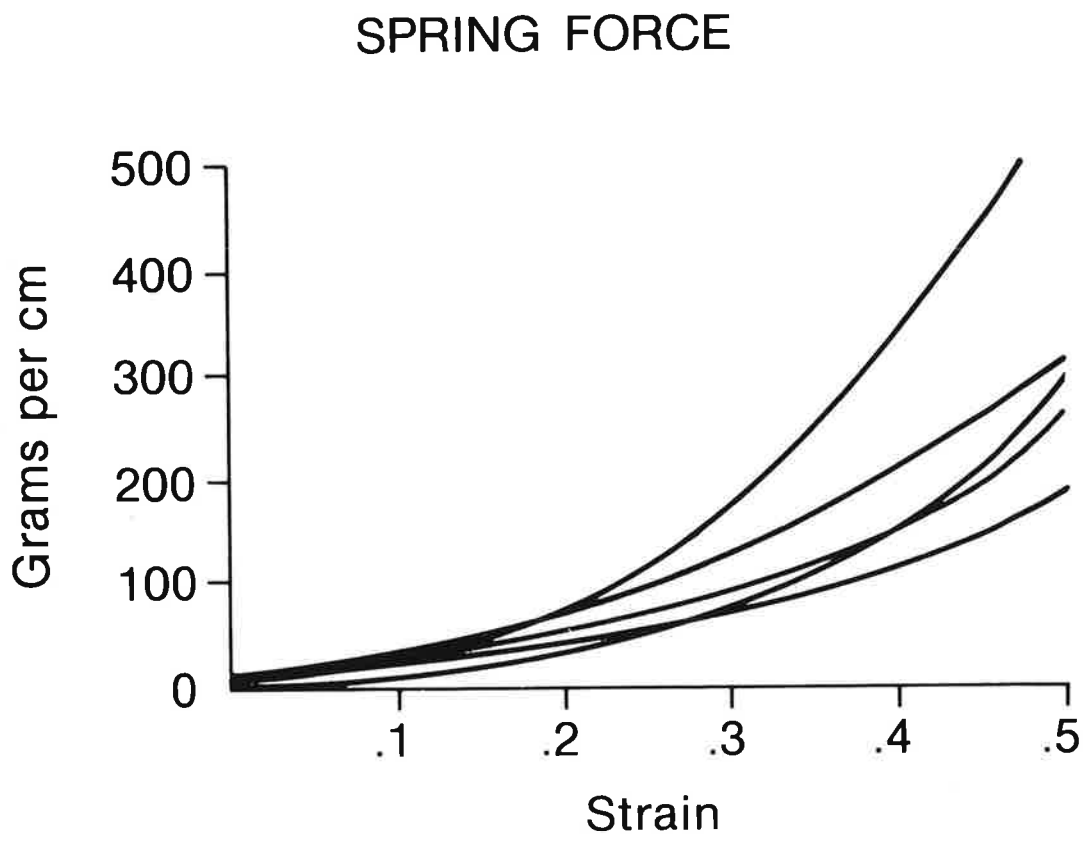

Figure 27. Force elongation curves for the spring force obtained by subtracting the skin island and isolated skin curves in experiments 1 through 5.

skin could be considered approximately 1/28 that of the intact skin slope, there was too large a range of variation for useful approximation.

Poisson's ratio was evaluated on both the skin island and the isolated skin. The 5 x 1 cm skin island was stretched in 0.5 cm increments to a maximum deformation of 2.5 cm (50% strain). The strain was performed at a rate of 1 mm/sec with a 30-second delay between each successive step of the deformation. A photograph was taken of the deformed skin and its grid between each step in the deformation. After photographing the skin island deformation, the same piece of skin was excised and analyzed in a 37° bath of Ringer's lactate. Three such experiments were performed. The photographs were developed and printed life size. The length of the strip and width of the strip at the midportion were measured with the previously described digitalizing pad. Poisson's ratio was calculated as the ratio of the strain in the length versus that in the width for each step in the three experiments. There was a wide variation in Poisson's ratio as measured with this technique. The skin island demonstrated a consistently lower Poisson's ratio than the isolated skin. The measurements ranged from 0.37 to 0.85, with a mean of 0.61.

Another set of experiments was performed to predict wound closing tension in vivo. 2 x 6 cm fusiform defects were outlined on the sides of five piglets. The strain gauges were then attached with

adhesive tabs 0.5 cm from the proposed defect at the midline. The gauges were then advanced towards each other in 0.5 cm increments at 1 mm/sec, with 30 seconds between each step. The force reading was taken at the end of this 30-second period just prior to initiation of the next step. The gauges were advanced to within 1 cm of each other (which represented closure because the tabs were placed 0.5 cm from each edge). The 2 x 6 cm defect was then excised. and the same basic experiment performed, again measuring closing tensions at each 0.5 cm increment to wound closure. A summary of that data is contained in Table III, and the same data represented graphically in Figure 28. Again there was significant variation, but with this in vivo technique the closing tensions could be fairly accurately approximated.

V. Modeling of skin deformation

A. Linear deformation of a rectangular skin island

The finite element model was utilized to investigate the mechanical properties of a rectangular island of skin. A boundary was fixed along one end of the rectangle, and the opposite end was then advanced. The sides were allowed to contract according to the mechanics of the situation. The actual boundary conditions state that the stress along the sides was 0. This relatively simple mathematical experiment allows one to investigate the relationship

TABLE III.

Prediction of Wound Closing Tension with Adhesive Plates
- 2 x 6 Fusiform Defect

Form in Grams to Advance Wound Edges: Predicted/Actual

Pig	2 cm Separation	1.5 cm Separation	1 cm Separation	0.5 cm Separation	Closure
1	0/0	21/15.4	42/49	56/70	112/172
2	0/0	0/14	7/35	28/43	56/113
3	0/0	14/21	42/56	84/84	112/112
4	0/0	21/7	43/42	63/70	137/140
5	0/0	0/14	14/26	28/42	60/109
Mean	0/0	11./14	30/42	52/62	96/120

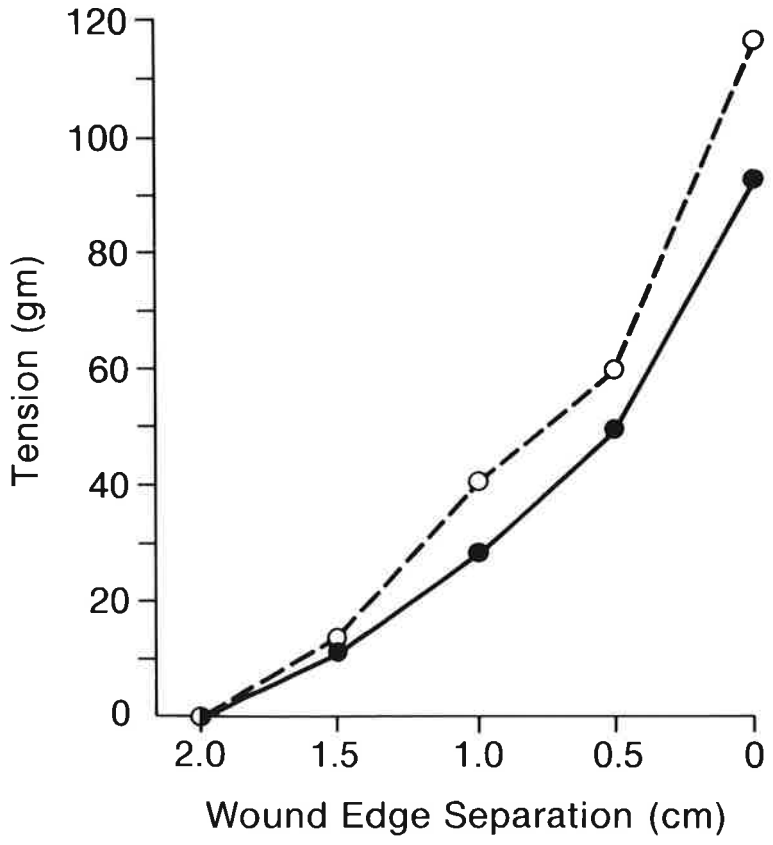

Figure 28. Predicted (dotted line) versus actual (solid line) wound closing tensions.

between the various elastic constants. Poisson's ratio was kept at 0.5 (which is the ratio for an incompressible solid) for this and subsequent experiments. From the experimental data a Young's modulus of 7.5 was chosen as representative. A typical set of skin deformations is seen in Figure 29. For this series, the skin was advanced 1 cm and the spring constant (k) was varied from 0 (isolated skin with no subcutaneous attachments) to 1.5 (extremely tight attachment of the skin to subcutaneous tissue). As can be seen in Figure 29, as k increases, the deformation becomes more and more localized.

A set of experiments was performed on the piglets to obtain actual deformation grids which could be correlated with the model. A 4 x 9 cm grid was outlined on the piglet's side. This was excised around the edges to create the skin island. The skin island was deformed by fixing one end and progressively advancing the opposite end in 0.5 cm increments at 1 mm/sec with 30 seconds between advancements. Photographic documentation was obtained as for the previous experiments. These photographs were analyzed by digitalizing the 1 cm deformation grid. Three sets of experiments were performed, first on the skin island and then on the same skin excised and deformed in a 37° Ringer's lactate bath. When skin deformation was analyzed, there was significant variation between the three sets of experiments. Two typical experimental examples were chosen and a simulation run with the mathematical model using average figures for Young's modulus and the spring constant. A

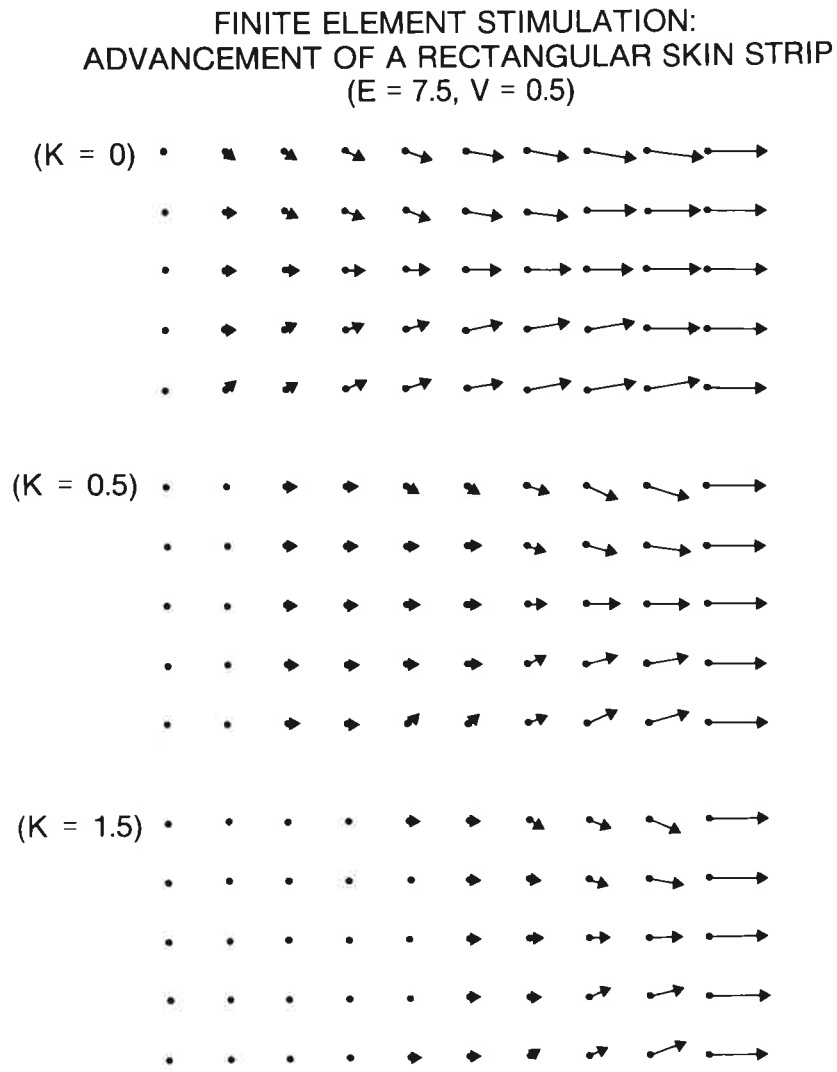

Figure 29. Deformation of a rectangular strip with variations in the spring constant k .

comparison of the resulting deformations is seen in Figure 30. The basic shapes of the deformed skin were similar to those of the simulation. The actual skin showed more irregularity than the simulation. For the skin island, with its subcutaneous attachments, in both the model and the actual experiment the narrowest part of the strip is closer to the deformed end. In the isolated skin and its simulation, the narrowest part of the skin strip is more toward the midportion of the strip. The major variance between the model simulation and the actual experiment is the absolute width of the skin strip. The current model makes no allowance for the preexisting skin tension, and therefore the contraction which takes place in the width after incising the flap makes the experimental skin strip narrower than the model simulation.

V. B. Modeling of wound closures

The finite element model was next utilized to model some actual wound closures. A defect or hole was created in the center of the skin, and closed by defining which of its vertices should be approximated. Undermining is performed by selecting the triangular elements for which the spring constant is set to 0. The simplest example is a fusiform closure such as that depicted in Figure 31. The final deformation (Figure 31C) is a fairly realistic approximation of a clinical wound closure. A more complex closure

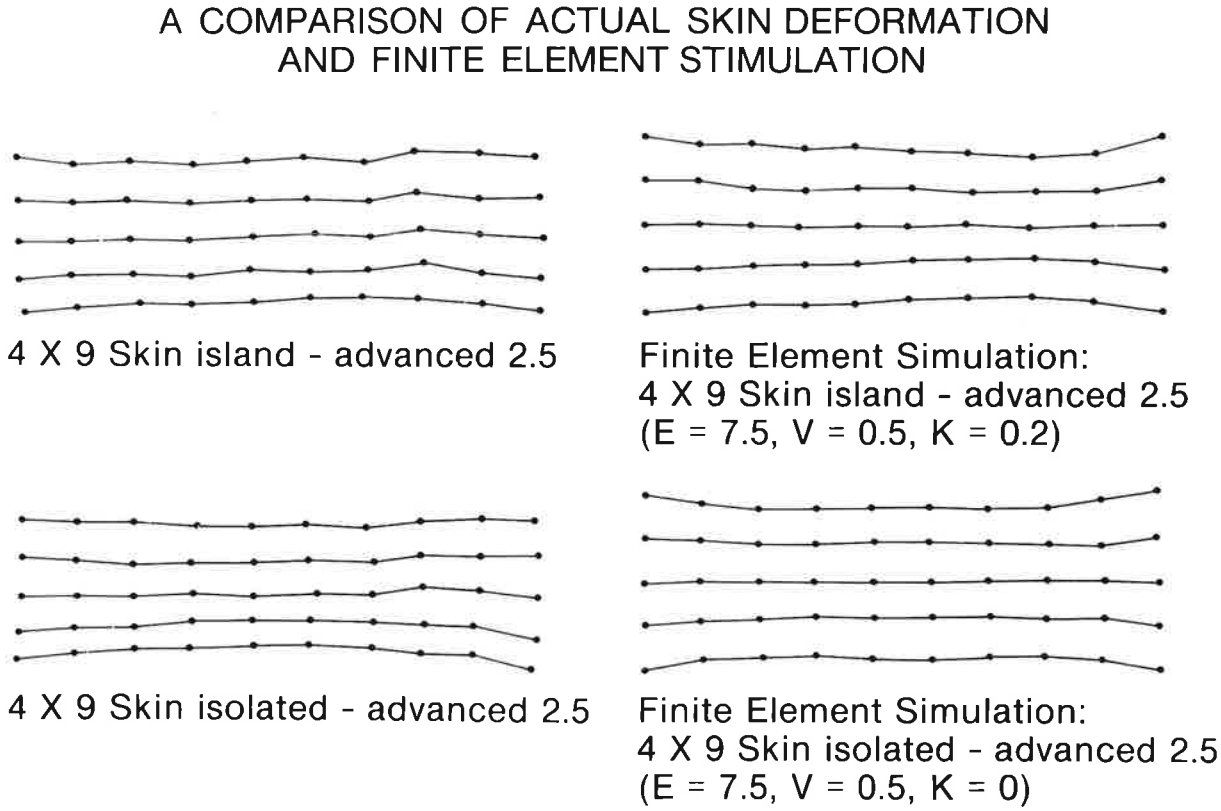

Figure 30. Comparison of rectangular skin deformation to simulated deformation by the finite element model.

was then simulated -- the rectangular advancement flap. A square defect was designed, the flap edges outlined, and the suture pairs identified to close the defect. This closure is depicted in Figure 32. For this particular example, the closure was performed by identifying those vertices along the edge of the flap which should be approximated. An alternative and somewhat more realistic technique is to perform the closure in two steps. First, the tips of the rectangular advancement flap are closed to the appropriate corners; when this step is analyzed, the sides of the flap do not approximate those of the defect. For the second step the experiment is run again, approximating the appropriate suture pairs along the sides where they tend to lie naturally. For this simple experiment there was no difference between those two approaches. Finally, a Z-plasty was performed (Figure 33). In this example, only the flaps themselves were undermined, and a relatively high spring constant was utilized so that one was simply transposing the flaps and not distorting the surrounding tissue significantly. If the spring constant is allowed to become small, and wide undermining is performed, the surrounding tissue deforms much more markedly.

VI. Discussion

The finite element model as currently developed provides a reasonable approximation of wound closures, including fairly complex ones. This is particularly encouraging given the large number of assumptions and the

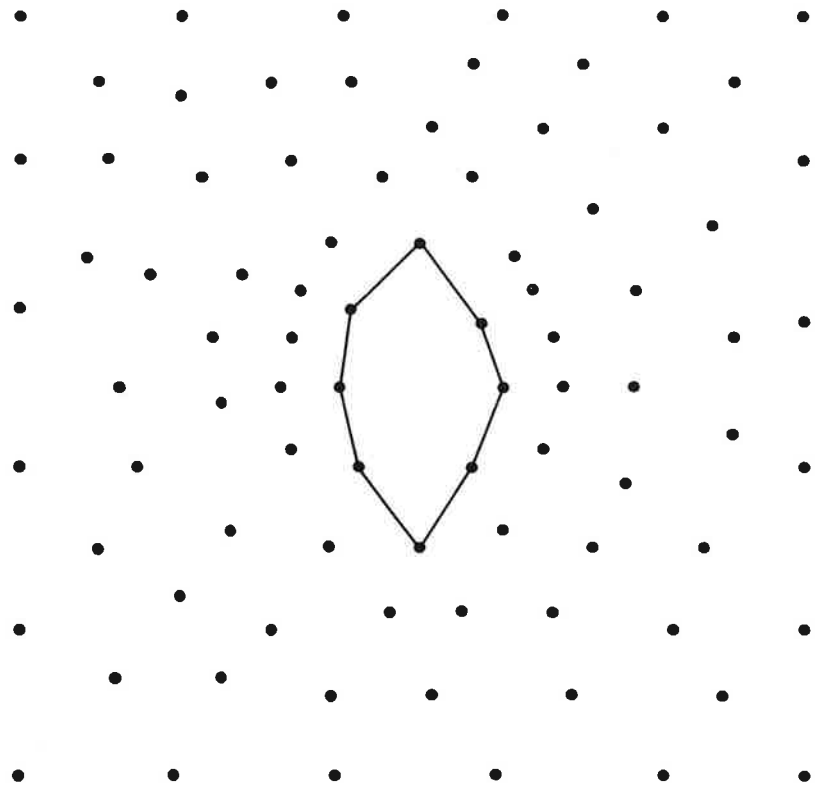

Figure 31A. Finite element model simulation of the fusiform wound closure -- set vertices and boundaries.

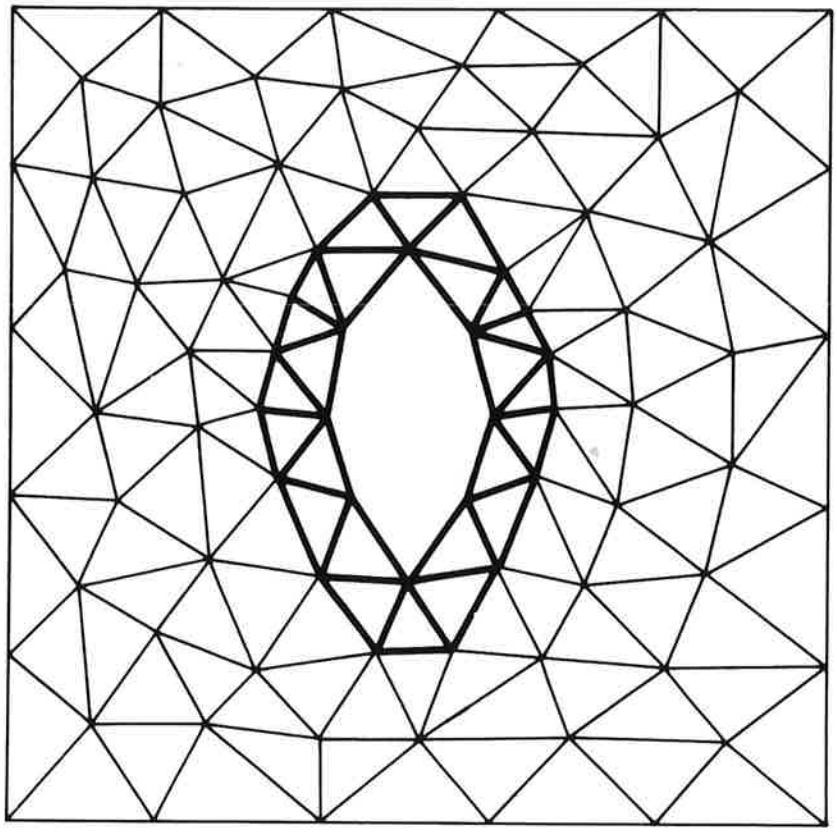

Figure 31B. Finite element model simulation of the fusiform wound closure -- define triangular elements; darker triangles are undermined.

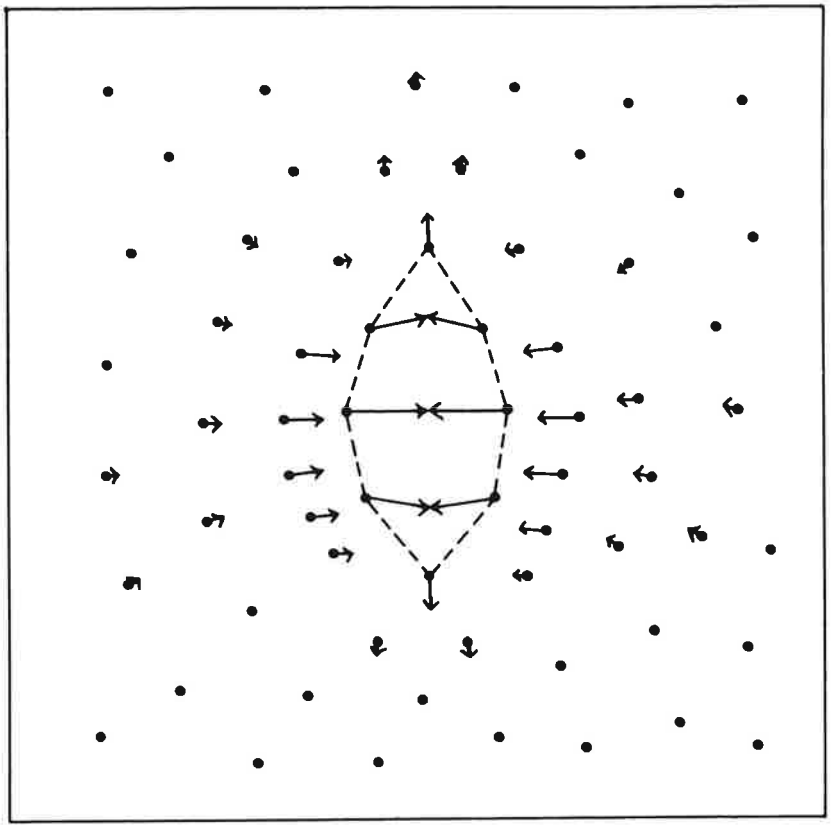

Figure 31C. Finite element model simulation of the fusiform wound closure -- final deformation.

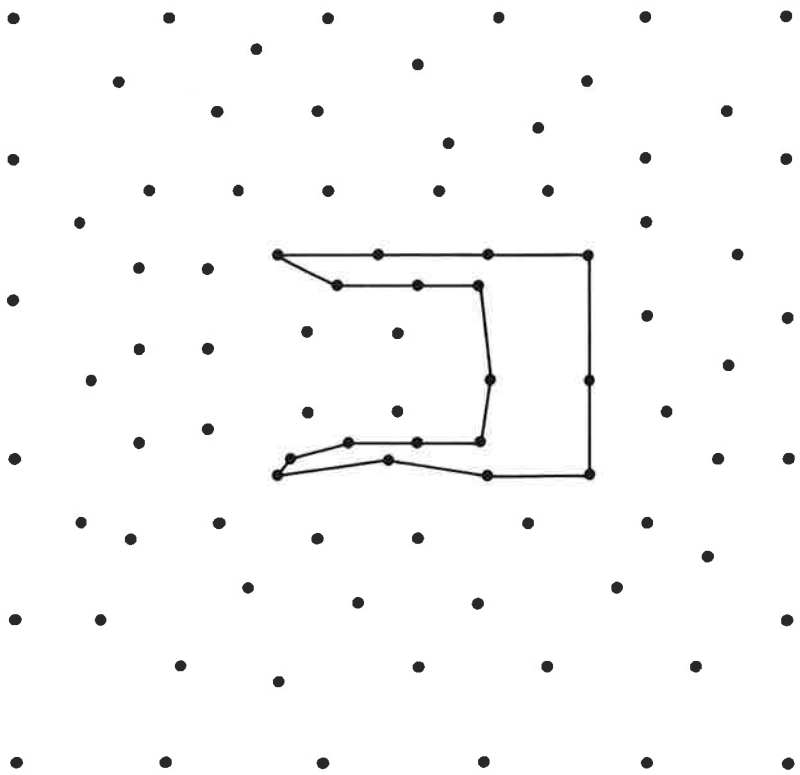

Figure 32A. The modeling of the rectangular advancement flap -- set vertices and boundaries.

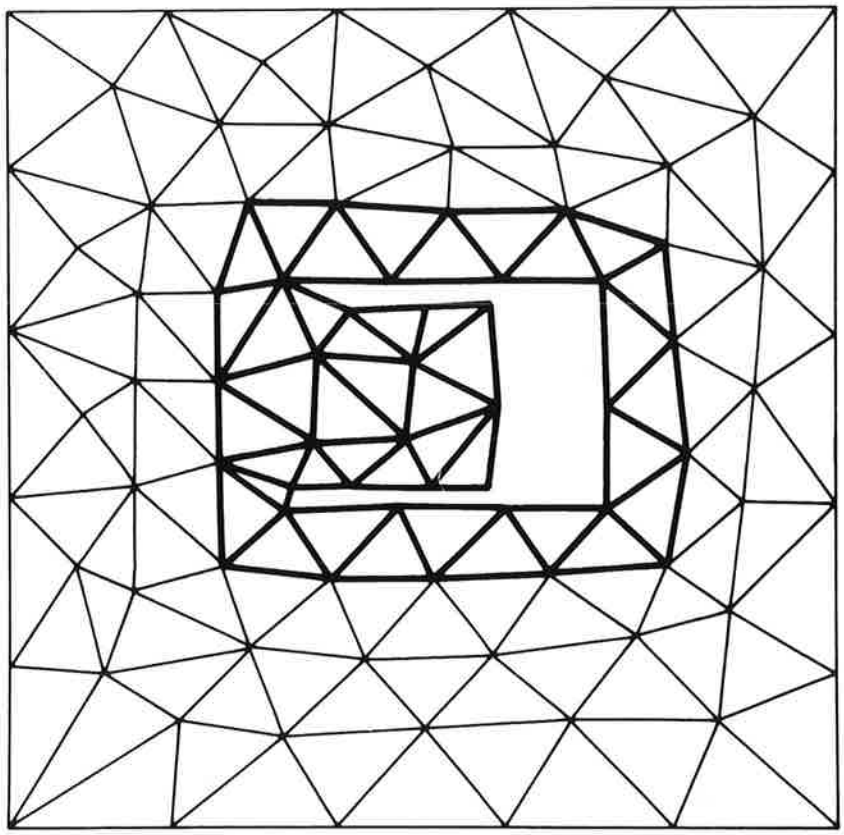

Figure 32B. The modeling of the rectangular advancement flap -- define triangular elements; darker triangles are undermined.

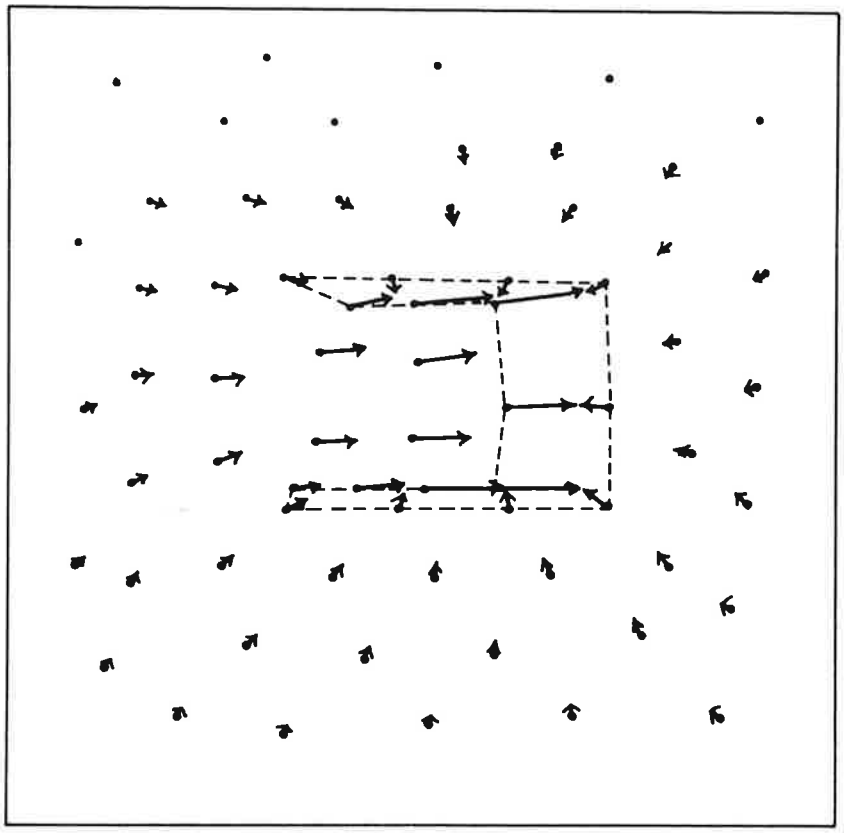

Figure 32C. The modeling of the rectangular advancement flap -- final deformation.

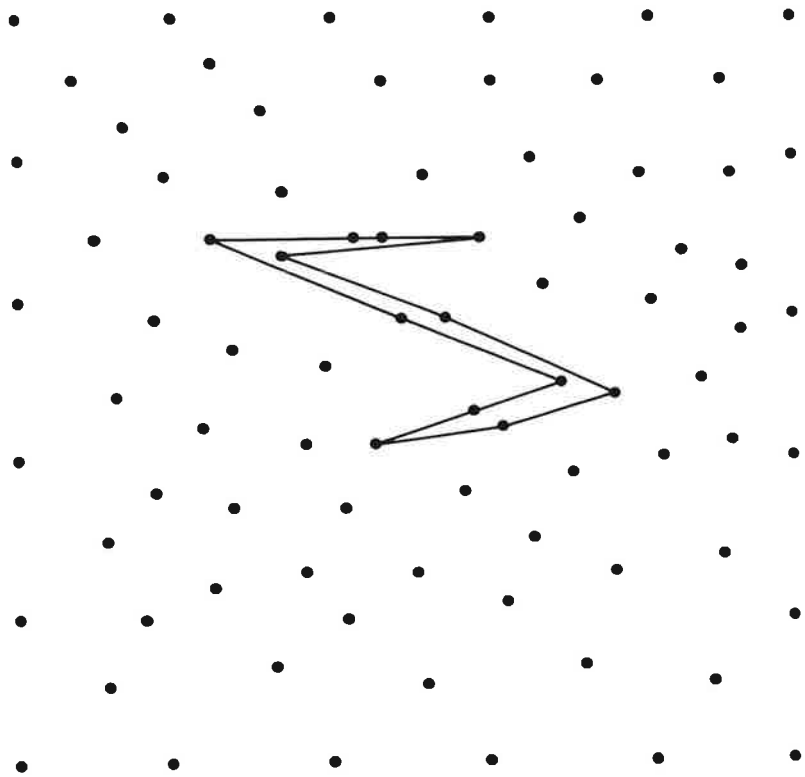

Figure 33A. Modeling of the Z-plasty -- set vertices and boundaries.

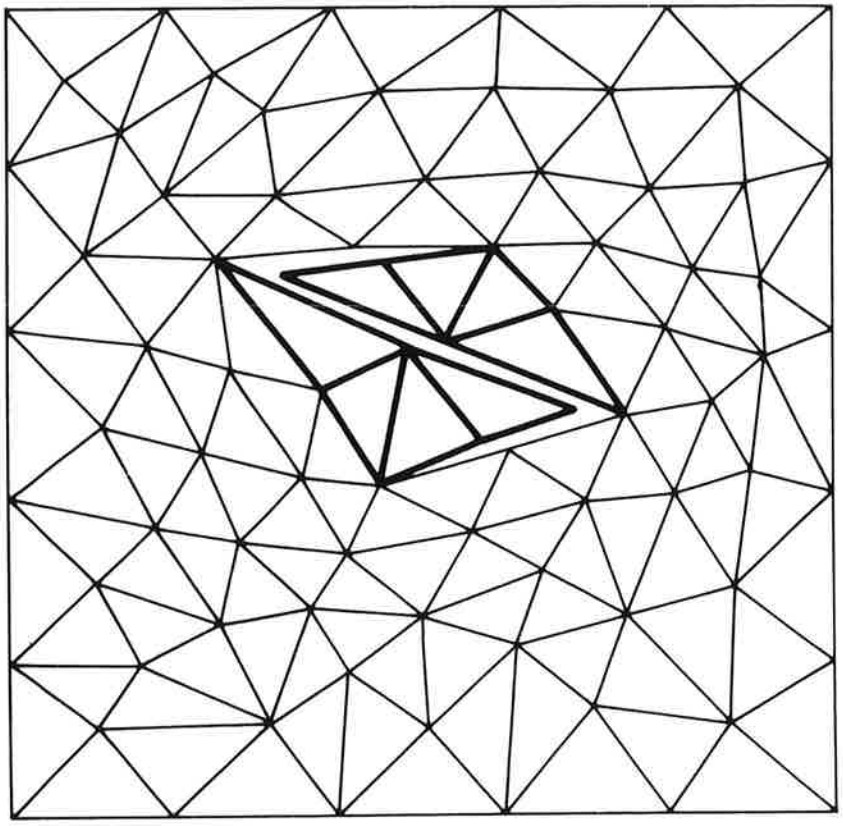

Figure 33B. Modeling of the Z-plasty -- define triangular elements; darker triangles are undermined.

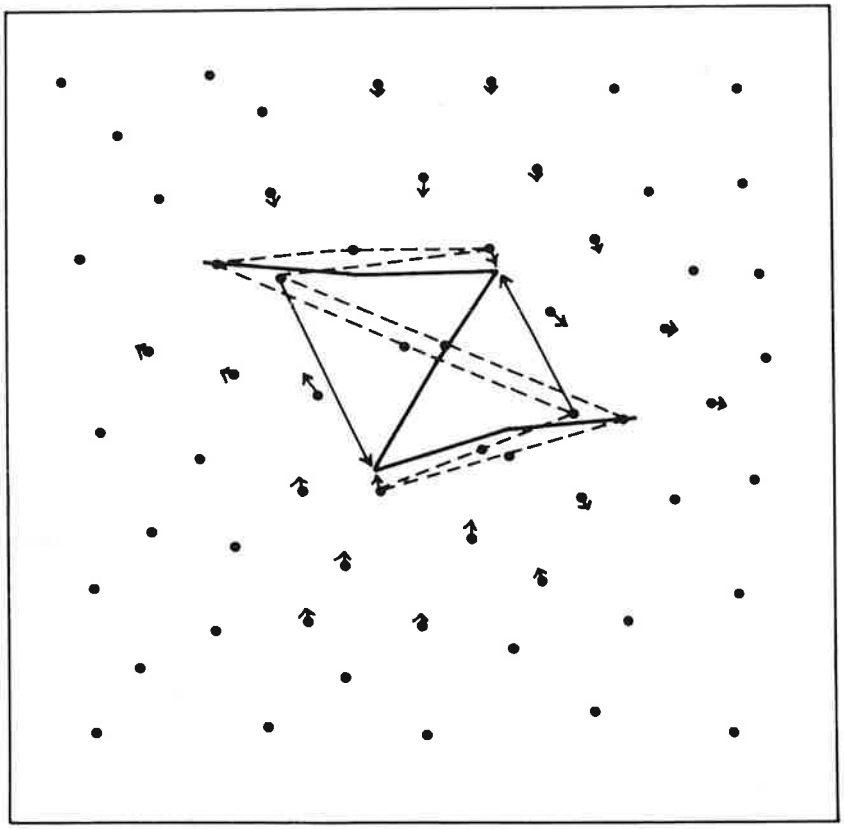

Figure 33C. Modeling of the Z-plasty -- final deformation.

relative simplicity of the model itself. The major limitations of the current model include:

1. The stress-strain relationships are represented by a simple linear function.
2. The underlying stresses in skin are not included.
3. The model is strictly two-dimensional.
4. The viscoelastic (time-dependent) properties of the skin are ignored.

There are standard engineering approaches to each of these limitations that could be implemented without too much difficulty. Obviously, however, as the model is made more and more complex, more computer memory and time is required and it becomes less practical to use. As currently formulated, the IBM 9000 requires about three minutes to solve each of the problems. The vast majority of this time is spent solving the matrices. Future steps which will be taken to make the model more realistic include:

1. placing the underlying structural stresses into the initial model;
2. using piecewise linear equations (two or three) to better approximate the true stress-strain properties of the skin and subcutaneous tissue; and
3. changing from a simple two-dimensional to a shell model of the skin surface.

The piglet model developed for this study provides a useful way to systematically study soft tissue biomechanics in vivo. The data

obtained from the piglet showed it to be a good mechanical model with results comparable to those in other animal models and in man. The subcutaneous forces measured with the skin extensometer were large and therefore should be considered in any future attempt to realistically model soft tissues. As with any animal model, there are limitations, and results cannot be applied directly to the human patient.[69] The most obvious difference between the piglet and the human is the difference in the anatomy of the skin tension lines. The piglet skin is also slightly thicker, has more hair follicles, and in all but the very youngest piglets has more subcutaneous fat than the human. Further sophisticated in vitro testing on the piglet, including biaxial testing, would be helpful to determine exactly how similar human and pig skin are mechanically; this data would also be helpful to transform a model based on the piglet to one useful for clinical problems.

The skin extensometer developed for this study is simple, reliable, and because of its software control very flexible. It might be possible to predict elastic tensions in an individual patient's skin by using a more sophisticated version of the adhesive tab method. In the piglet, wound closing tensions were fairly accurately predicted using the adhesive tabs with the skin extensometer. On the other hand, the attempt to correlate the slope of the strain force curve obtained from the intact skin with that obtained from isolated skin was not particularly successful. The major variable here was probably the need to transist from in vivo (skin island) to in vitro (skin isolated) measurement. As long as measurements were confined to the intact animal in a somewhat

physiologic condition, the results were predictable. Once the skin was isolated from the animal, its mechanical properties seemed to change significantly. In addition, the force applied to the intact skin and island prior to stretching the isolated skin probably caused some stress relaxation and altered the ultimate stress-strain curve determined for the isolated skin. In spite of these limitations, the use of the skin extensometer with adhesive tabs in clinical patients provides an approach to quantitating the skin elasticity noninvasively. Some technique such as this is essential if a mathematical model is to be applied to an individual patient.

As discussed above, the analysis of deformation curves is the ideal way to study the mechanics of wound closure in both experimental animals and man. When wound closure is performed on a relatively flat surface, the software developed in this study (Appendix C) allows standardization and comparison of pre- and postoperative grids. In addition, multiple deformation grids for a given closure can be averaged. It is possible by analyzing skin deformation to obtain a stress analysis of the entire deformation field. A technique to analyze skin deformation in three dimensions would be preferable to the current two-dimensional system. Such a three-dimensional approach is not inherently difficult but does require an accurate, reliable, three-dimensional digitalizer. These instruments are now becoming available and will almost certainly be useful in future studies of computer-aided design in soft tissue surgery. In the meantime, analysis of clinical cases on level areas such as the cheek or forehead, with two-dimensional photographs, can provide useful information.

VII. Summary

The finite element method is a flexible and practical technique for the modeling of skin deformation. In spite of its many limitations, the model developed provides a more accurate description of skin deformation during wound closure than any current technic. The model can be improved by using technics available from other fields of engineering to:

1. Represent underlying and directional stress.
2. Improve the governing equations so they better approximate the nonlinear stress-strain properties of soft tissue.
3. Create a shell (three-dimensional) model.

A more sophisticated model should provide an excellent tool for research and training in the design of local skin flaps. Although it is possible that the finite element method could eventually be applied to actual computer-aided design of skin flaps for an individual patient, this is probably impractical. This application would require the ability to accurately estimate elastic constants in the individual patient's skin, including their directionality over a very small area, and to then precisely design a flap in three dimensions. It seems unlikely that the experienced head and neck surgeon will be replaced by a computer model.

The piglet model developed in this study is a useful one for the analysis of skin and soft tissue mechanics in vivo. Further and more technically sophisticated measurements of soft tissue mechanics in vivo

are indicated and would help close the gap between the accurate in vitro data available and the relatively crude data available on in vivo systems. The ability to quantitate two-dimensional deformation fields with the digitalizing pad can be applied directly to patients at this time and for a flat area could provide useful mechanical data on human skin and soft tissue.

Because of the limitations of current animal models and the complexity of the experimental systems, an analytic approach (such as the finite element model) is the best way to investigate practical problems. With a conceptually sound model, based on a reasonable estimate of the mechanical variables, mathematical experiments in skin flap design can be quickly and easily performed. New designs and variations of classic designs can be investigated for specific geometric defects. The finite element approach, because of its ability to deal with very complex geometries, has potential applications in many areas of head and neck surgery.

REFERENCES

1. Zeis E: The Zeis index. In: History of Plastic Surgery 900 BC to 1863 AD. Baltimore: Williams & Wilkins Company, pp 78-83, 1977.

2. Thacker JG, Iachetta FA, Allaire PE, Edgerton MT, Rodeheaver GT, Edlich RF: Biomechanical properties of skin: their influence on planning surgical excisions. In: Symposium on Basic Science and Plastic Surgery. Vol 15:9:105-107. St. Louis: CB Mosby Co, 1976.

3. Dupuytren JF: Traite theorique et practique des blessure par armes de guerre, vol 1. Paris: JB Bailleu, 1834.

4. Langer AK: Zur Anatomie und Physiologie der Haut: uber die Spaltbarkeit der Cortis. SB Akad Wiss Wien 44:19, 1861.

5. Kocher T: Chirurgische Operationlehre. Jena: Gustav Fisher, 1907.

6. Cox HT: The cleavage lines of the skin. Br J Surg 29:234-240, 1941.

7. Borges AF: Elective incisions and scar revision. Boston: Little Brown & Co, 1973.

8. Limberg AA: Mathematical principles of local plastic procedures on the surface of the human body. Leningrad: Medgig, 1946.

9. Limberg AA: Design of local skin flaps. In: Gibson T, ed. Modern Trends in Plastic Surgery. London: Butterworths & Co Ltd, pp 38-61, 1966.

10. McGregor IA: The theoretical basis of the Z-plasty. Br J Plastic Surg 9:256-259, 1957.

11. Koss N, Bullock JD: A mathematical analysis of the rhomboid flap. Surg Gynecol Obstet 141:439-442, 1975.

12. Koss N: The mathematics of flaps. In: Symposium on Basic Science and Plastic Surgery. Krizek TJ, ed. CV Mosby Co, pp 274-283, 1976.

13. Fung YC: Biomechanics: Mechanical Properties of Living Tissue. New York: Springer Verlag, pp 22-61, 1981.

14. Zienkiewicz OC: The Finite Element Method in Engineering Science. New York: McGraw-Hill, 1977.

15. Jamison CE, Marangoni RD, Glaser AA: Viscoelastic properties of soft tissues by discrete model characteristics. J Eng Ind 67:239-245, 1968.

16. Tregear RT: Physical Functions of Skin. London: Academic Press, p 87, 1966.

17. Marangoni RD, Glaser AA, Must JS, Bordy GS, Beckwith TG, Walker GR, White WL: Effect of storage and handling techniques on skin tissue properties. Ann NY Acad Sci 136:439-454, 1966.

18. Craik JE, McNeil IRR: Histological studies of stressed skin. In: Kenedi RM, ed. Biomechanics and Related Bio-engineering Topics. Oxford: Pergaman Press, pp 159-164, 1967.

19. Abrahams M: The mechanical behavior of tendon collagen fibres under tension in vitro. 7th Int Conf Med Electr, Stockholm: Biol Eng, 1967.

20. Finlay B: Scanning EM of human dermis under uniaxial strain. Biomed Eng 4:322-327, 1969.

21. Wilkes GL, Brown IA, Wildnauer RH: The biomechanical properties of skin. CRC Crit Rev Bio-eng 1:453-495, 1973.

22. Morgan FR: The mechanical properties of collagen fibers. J Soc Leather Trades Chem 44:171-182, 1960.

23. Elden HR: Physical properties of collagen fibers. Int Rev Conn Tiss Res 7:283-328, 1976.

24. Gotte L: Recent observations on the structure and composition of elastin. Adv Exp Med Biol 27:105-117, 1977.

25. Carton RW, Dainauskas J, Clark JW: Elastic properties of single elastic fibers. J Appl Physiol 17:547-551, 1962.

26. Daly CH: The role of elastin in the mechanical behavior of human skin. Proc of the 8th Int Conf Med Biol Engr, Chicago, pp 18-27, 1969.

27. Wood GC: Some tensile properties of elastic tissue. Biochem Biophys Acta 15:311-314, 1954.

28. Dick JC: The tension and resistance to stretching of human skin and other membranes. J Physiol 112:102-113, 1951.

29. King AL, Lawton RW: Elasticity of body tissues. In: Glasser O, ed. Medical Physics, vol 3. Chicago: Year Book Publishers, pp 234-247, 1960.

30. Harkness MLR, Harkness RD: Effect of enzymes on mechanical properties of tissues. Nature, London 183:1821-1822, 1959.

31. Minns RJ, Soden PD, Jackson DS: The role of the fibrous components and the ground substance in the mechanical properties of biologic tissues. J Biomech 6:153-165, 1973.

32. Gibson T, Kenedi RM, Craik JE: The mobile micro-architecture of dermal collagen. Br J Surg 52:764, 1965.

33. Daly CH, Odlund GE: Age-related changes in the mechanical properties of human skin. J Invest Dermatol 73: 84-87, 1979.

34. Barbenel JC, Evans JH, Jordan MM: Tissue mechanics. Engineering in Medicine 7:5-9, 1978.

35. Wohlisch E: Untersuchengen ueber die elastichen eigen schaftern tierischer gewebe. J Z Biol 85:325-341, 1926.

36. Ridge MD, Wright V: The description of skin stiffness. J Biorheology 10: 139-155, 1964.

37. Ridge MD, Wright V: A rheological study of skin. Proc Symp on Biomechanics and related bioengineering topics. Kenedi RM, ed. Oxford: Pergaman Press, pp 165-175, 1964.

38. Ridge MD, Wright V: Mechanical properties of skin: a bioengineering study of skin structure. J Appl Physiol 21:1602-1606, 1966.

39. Kenedi RM, Gibson T, Daly CH: Bioengineering studies of the human skin. In: Proc Symposium on Biomechanics and Related Bioengineering Topics. Kenedi RM, ed. Oxford: Pergamon Press, pp 147-158, 1965.

40. Daly CH: The biomechanical characteristics of human skin. PhD thesis, University of Strathcylde, Glascow, Scotland, 1966.

41. Ridge MD, Wright V: The directional effects of skin. J Invest Dermatol 64:341-346, 1966.

42. Gibson T, Stark H, Evans JH: Directional variation in the extensibility of human skin in vivo. J Biomech 2:201-204, 1969.

43. Barbenel JC, Evans JH, Finlay JB: Stress-strain-time relations for soft connective tissues. In: Perspectives in Biomedical Engineering, Kenedi RM (ed). New York: MacMillan, pp 165-172, 1973.

44. Ohura T, Singihara T, Honda K: Postoperative evaluation in plastic surgery using the bio-skin tension meter. Ann Plast Surg 5:74-82, 1980.

45. Wijn PF, Brakkee JM, Stienen GJM, Vendrik AJH: Mechanical properties of human skin in vivo for small deformations: a comparison of uniaxial strain and torsion measurements. In: Bedsore Mechanics, Kenedi RM (ed). Baltimore: University Park Press, 1976, pp 103-108.

46. Thacker JG, Iachetta FA, Allaire PE, Edgerton MT, Rodeheaver GJ, Edlich RF: Rev Sci Instrum, 47:224-228, 1976.

47. Alexander H, Cook TH: Accounting for the natural tension in the mechanical tension of human skin. J Invest Dermatol 69:310-314, 1977.

48. Lanir Y, Fung YC: Two-dimensional mechanical properties of rabbit skin. I. Experimental system. II. Experimental results. J Biomech 7:29-34 and 171-182, 1974.

49. Schneider DC, Davidson TM, Nahum NA: In vitro biaxial stress strain response of human skin. Arch Otolaryngol 110:329-333, 1984.

50. Fung YC: Elasticity of soft tissues in simple elongation. Am J Physiol 213:1532-1544, 1967.

51. Fung YC: Biorheology of soft tissue. Biorheology 10:139-155, 1973.

52. Veronda DR, Westmann RA: Mechanical characteristics of skin--finite deformations. J Biomech 3:111, 1970.

53. Blatz PJ, Chu BM, Wayland H: On the mechanical behavior of elastic animal tissue. Trans Soc Rheol 13:83-102, 1969.

54. Crisp DC: Properties of tendon and skin. In: Fung YC, Perone N, Anliker M, eds. Biomechanics: its Foundations and Objectives. Englewood: Prentice Hall Cliffs, pp 141-179, 1972.

55. Demiray H: A note on the elasticity of soft tissues. J Biomech 5:309-331, 1972.

56. Demiray H, Vito RP: Large deformation analysis of soft biomaterials. Int J Eng Sci 14:789-793, 1976.

57. Allaire PE, Thacker JG, Edlich RF, Rodeheaver GJ, Edgerton MT: Finite deformation theory for in vivo human skin. J Bioeng 1:239-249, 1977.

58. Tong P, Fung YC: The stress-strain relationships for the skin. J Biomech 9:649, 1976.

59. Danielson DA: Human skin as an elastic membrane. J Biomech 6:539-546, 1973.

60. Danielson DA, Natarajan S: Tension field theory and the stress in stretched skin. J Biomech 8:135-142, 1975.

61. Furnas DW, Fischer GW: The Z-plasty: Biomechanics and mathematics. Br J Plast Surg 24:144-160, 1971.

62. Lanir Y: A structural theory for the homogeneous biaxial stress-strain relationships in flat collagenous tissues. J Biomech 12:423, 1979.

63. Zienkiewicz OC: From intuition to generality. App Mechs Review March:249-256, 1970.

64. Courant R: Variational methods for the solution of problems of equil and vibration. Bull Am Math Soc 49:1-23, 1943.

65. Becker EB, Carey GF, Oden JT: Finite Elements: an Introduction. San Bernadino: Hall Press Incorporated, 1981.

66. Strang G, Fix GH: An Analysis of the Finite Element Method. Englewood Cliffs: Prentice-Hall, 1973.

67. Gallagher RH, Simon BR, Johnson PC: Finite Elements in Biomechanics. New York: J Wiley & Sons, 1982.

68. Hauck J. Personal Communication, October 1984.

69. Kenedi RM, Gibson T, Evans JH, Barberel JC. Tissue mechanics. Phys Med Biol 20:699-717, 1975.

APPENDIX A.

The finite element model

```
      PROGRAM PLTMOD
C
C  THIS PROGRAM MODELS A 2 DIMENSIONAL SURFACE DEFORMATION.
C  THE METHOD OF FINITE ELEMENTS IS USED TO SOLVE THE RESULTING
C  EQUATIONS.
C  SUBROUTINES CALLED:
C    GETDAT   -  GETS THE TOPOLOGICAL TRIANGLE DATA
C    BUILDMAT -  ASSEMBLES THE MATRIX OBTAINED BY FINITE ELEMENTS
C    STRBDY   -  SETS THE DISPLACEMENT OF GIVEN VERTEX POINTS TO
C                GIVEN VALUES
C    FIXBDY   -  FIXES THE OUTER BOUNDARY DISPLACEMENTS TO ZERO
C    SETPAIRS -  TIES GIVEN PAIRS OF VERTICES TOGETHER ("CLOSES
C                THE HOLE")
C    DECOMP   -  STANDARD LU DECOMPOSITION OF THE MATRIX USING PARTIAL
C                PIVOTING
C    SOLVE    -  SOLVES THE DECOMPOSED MATRIX OUTPUT BY DECOMP
C    HEADER   -  READS IN HEADING NAME FOR THE CURRENT OUTPUT
C    NEWFIL1  -  READS A FILENAME AND OPENS THE FILE ON UNIT 1
C
C  VARIABLES:
C    TOP    -  ARRAY CONTAINING TOPOLOGICAL TRIANGLE DATA
C    SEG    -  ARRAY CONTAINING HIGHEST NUMBERED VERTEX OF EACH BOUNDARY
C    NV     -  NUMBER OF VERTICES
C    NSEG   -  NUMBER OF BOUNDARIES
C    ARSIZE -  DIMENSION OF MATRIX (TWICE THE NUMBER OF VERTICES)
C    A      -  MATRIX OF COEFFICIENTS
C    VX(I),VY(I) - X,Y POSITIONS OF VERTEX I
C    VDX(I),VDY(I) - X,Y DISPLACEMENTS OF VERTEX I
C    B      -  RIGHT HAND SIDE OF EQUATION
C    PS     -  ARRAY USED IN DECOMP AND SOLVE TO KEEP TRACK OF THE
C              PIVOTING
C    SCALES -  ARRAY USED IN DECOMP AND SOLVE FOR SCALING
C    TX     -  SOLUTION ARRAY
C    YMOD   -  YOUNG'S MODULUS
C    NU     -  POISSON'S RATIO
C    HOOKE  -  HOOKE'S LAW TYPE SPRING CONSTANT
C
      PARAMETER (IA=200)
      INTEGER TOP(2412), SEG(20), ARSIZE
      INTEGER PS(IA)
      DIMENSION A(IA,IA), VX(204), VY(204), VDX(204), VDY(204), B(IA)
      DIMENSION SCALES(IA), TX(IA)
      REAL NU
      COMMON YMOD,NU,HOOKE
C
      CALL GETDAT(TOP,SEG,VX,VY,NV,NSEG,NTRI)
      CALL BUILDMAT(NV,IA,ARSIZE,VX,VY,NTRI,TOP,SEG,A)
      PRINT*,'GIVE OUTPUT FILE NAME'
      CALL NEWFIL1
      IF ( NSEG .EQ. 1 ) THEN
         CALL STRBDY(A,B,IA,ARSIZE,SEG,VX)
      ELSE IF ( NSEG .EQ.2 ) THEN
         CALL FIXBDY(A,B,IA,ARSIZE,SEG,VX)
         CALL SETPAIRS(VX,VY,A,B,IA,ARSIZE,SEG)
      ELSE
         PRINT*,'ERROR-MORE THAN ONE HOLE IN REGION'
         STOP
      ENDIF
      CALL DECOMP(IA, ARSIZE, A, A, PS, SCALES)
      CALL SOLVE( IA, ARSIZE, A, B, TX, PS)
      CALL HEADER
      WRITE(1,14)YMOD,NU,HOOKE
14    FORMAT(//,1X,'YMOD = ',F4.1,'  NU = ',F4.1,'  K = ',F4.1)
```

```
      WRITE(1,16)
16    FORMAT(1X,/,' SOLUTION',//,1X,'VERTEX        DX          DY',//)
      DO 40 I = 1,ARSIZE/2
         WRITE(1,7)I,TX(2*I-1),TX(2*I)
40    CONTINUE
7     FORMAT(1X,I3,3X,2F11.3)
      CLOSE(1)
      STOP
      END
C
C
      SUBROUTINE BUILDMAT(NV,IA,ARSIZE,VX,VY,NTRI,TOP,SEG,A)
C
C   BUILDMAT BUILDS THE MATRIX A(I,J) USED FOR MODELING A 2-D
C   SURFACE DEFORMATION.
C   INPUTS :
C     YMOD    -  YOUNG'S MODULUS
C     NU      -  POISSON'S RATIO
C     HOOKE   -  HOOKE'S LAW TYPE OF SPRING CONSTANT
C     VERTEX AND TRIANGLE INFORMATION FROM EXTERNAL FILES :
C        VX(I),VY(I)  -  INITIAL X,Y POSITION OF VERTEX I
C        TOP          -  ARRAY CONTAINING THE TOPOLOGICAL TRIANGLE DATA
C        SEG          -  ARRAY CONTAINING HIGHEST NUMBERED VERTEX OF
C                        EACH BOUNDARY
C        NV           -  NUMBER OF VERTICES
C        NTRI         -  NUMBER OF TRIANGLES
C        IA           -  MAXIMUM ALLOWED DIMENSION OF MATRIX
C        ARSIZE       -  ACTUAL DIMENSION OF MATRIX (TWICE NV)
C   LOCAL  VARIABLES :
C     J         -  TEMPORARY STORAGE ARRAY
C     V1,V2,V3 -  TEMPORARY STORAGE VARIABLES - DENOTES VERTEX NUMBERS
C     X1,Y1,X2,Y2,X3,Y3  -  INITIAL POSITION OF VERTICES
C     DX,DY    -  TEMPORARY STORAGE ARRAYS OF BASIS FUNCTION CONSTANTS
C     AREA     -  AREA OF CURRENT TRIANGLE ELEMENT
C     ALPHA,C1,C2,C3  -  CONSTANTS APPEARING IN EQUATIONS
C
      INTEGER TOP(1), J(3), V1, V2, V3, ARSIZE, SEG(1)
      REAL NU, DX(3), DY(3), VX(1), VY(1)
      DIMENSION A(IA,IA)
      COMMON YMOD,NU,HOOKE
C
      PRINT*,'GIVE YOUNG''S MODULUS'
      READ*,YMOD
      PRINT*,'GIVE POISSON''S RATIO'
      READ*,NU
      PRINT*,'GIVE SPRING CONSTANT'
      READ*,HOOKE
      ALPHA = YMOD/(1 - NU**2)
      C1 = ALPHA / 3
      C2 = C1 * (1 + NU) / 2
      C3 = C1 * (1 - NU) / 2
C
C   CONSTRUCT MATRIX:
C
      ARSIZE = 2 * NV
      K = 2 * NV + 2
      DO 210 I1 = 1,ARSIZE
         DO 200 J1 = 1,ARSIZE
            A(I1,J1) = 0.0
200      CONTINUE
210   CONTINUE
      DO 240 II = 1, NTRI
         J(1) = TOP(II)
```

```
         J(2) = TOP(II + K)
         J(3) = TOP(II + 2 * K)
         V1 = J(1)
         V2 = J(2)
         V3 = J(3)
         X1 = VX(V1)
         Y1 = VY(V1)
         X2 = VX(V2)
         Y2 = VY(V2)
         X3 = VX(V3)
         Y3 = VY(V3)
         CALL TRIBASE(X1,Y1,X2,Y2,X3,Y3,DX1,DY1,D1,DX2,DY2,D2,
     &                DX3,DY3,D3,AREA)
         DX(1) = DX1
         DX(2) = DX2
         DX(3) = DX3
         DY(1) = DY1
         DY(2) = DY2
         DY(3) = DY3
         DO 230 J1 = 1,3
            DO 220 J2 = 1, 3
               V1 = J(J1)
               V2 = J(J2)
               AI = DX(J1)
               BI = DY(J1)
               AJ = DX(J2)
               BJ = DY(J2)
               SUM11 =  AREA *
     &                (C1*AI*AJ + C3*BI*BJ + HOOKE * DELTA(I,J))
               SUM12 =  AREA * ( C1*NU*AI*BJ + C3*BI*AJ )
               SUM21 =  AREA * ( C1*NU*BI*AJ + C3*AI*BJ )
               SUM22 =  AREA *
     &                (C1*BI*BJ + C3*AI*AJ + HOOKE * DELTA(I,J))
               IN1 = 2 * V1
               IN2 = 2 * V2
               A(IN1-1,IN2-1) = A(IN1-1,IN2-1) + SUM11
               A(IN1-1,IN2) = A(IN1-1,IN2) + SUM12
               A(IN1,IN2-1) = A(IN1,IN2-1) + SUM21
               A(IN1,IN2) = A(IN1,IN2) + SUM22
220         CONTINUE
230      CONTINUE
240   CONTINUE
C
      RETURN
      END
C
C
      FUNCTION DELTA(I,J)
      IF (I.EQ.J) THEN
         DELTA = 1.0/6.0
      ELSE
         DELTA = 1.0/12.0
      ENDIF
      RETURN
      END
C
C
      SUBROUTINE STRBDY(A,B,IA,ARSIZE,SEG)
C
C  THIS ROUTINE SETS THE DISPLACEMENTS OF GIVEN VERTICES TO GIVEN VALUES
C
C  LOCAL VARIABLES :
C    VERTEX  - ARRAY CONTAINING VERTICES OF SAME DISPLACEMENT
```

```
C
      INTEGER ARSIZE,SEG(1),VERTEX(25)
      DIMENSION A(IA,IA), B(1)
      DO 800 I = 1, ARSIZE
         B(I) = 0.0
800   CONTINUE
810   PRINT*,'GIVE VERTEX TO BE SET'
      PRINT*,'IF MORE THAN ONE VERTEX IS TO HAVE THE SAME DISPLACEMENT'
      PRINT*,'TYPE 0.  TYPE -1 TO STOP'
      READ*,N
      IF (N.EQ.-1) GOTO 850
      IF (N.EQ.0) THEN
         PRINT*,'GIVE NUMBER OF VERTICES OF ONE DISPLACEMENT'
         READ*,NN
         PRINT*,'GIVE VERTICES TO BE SET'
         READ*,(VERTEX(I),I=1,NN)
         PRINT*,'GIVE THE X,Y DISPLACEMENT'
         READ*,DX,DY
         DO 830 I = 1, NN
            II = VERTEX(I)
            DO 820 J = 1, ARSIZE
               A(2*II-1,J) = 0.0
               A(2*II,J) = 0.0
820         CONTINUE
            A(2*II-1,2*II-1) = 1
            A(2*II,2*II) = 1
            B(2*II-1) = DX
            B(2*II) = DY
830      CONTINUE
      ELSE
         PRINT*,'GIVE THE DX,DY DISPLACEMENT'
         READ*,DX,DY
         DO 840 J = 1,ARSIZE
            A(2*N-1,J) = 0.0
            A(2*N,J) = 0.0
840      CONTINUE
         A(2*N-1,2*N-1) = 1
         A(2*N,2*N) = 1
         B(2*N-1) = DX
         B(2*N) = DY
      ENDIF
      GOTO 810
850   RETURN
      END
C
C
      SUBROUTINE SETPAIRS(VX,VY,A,B,IA,ARSIZE,SEG)
C
C  SETPAIRS READS IN THE PAIRS OF VERTICES THAT WILL BE TIED
C  TOGETHER (CLOSES A HOLE).  THE MATRIX A AND THE VECTOR B WILL BE
C  CHANGED TO FIT THE NEW REQUIREMENTS.
C
C   LOCAL VARIABLES :
C      V1,V2  -  VERTICES TO BE TIED TOGETHER
C
      DIMENSION VX(1),VY(1),A(IA,IA),B(1)
      INTEGER V1,V2, ARSIZE, SEG(1)
C
C  INTITIALIZE VECTOR B
C
      DO 250 I = 1,ARSIZE
         B(J) = 0.0
250   CONTINUE
```

```
C
C   SET PAIRS
C
      PRINT*,'GIVE NUMBER OF PAIRS'
      READ*,NPAIRS
      DO 270 I = 1,NPAIRS
         PRINT*,'GIVE VERTEX NUMBERS OF PAIR',I
         READ*,V1,V2
         DELX = VX(V2) - VX(V1)
         DELY = VY(V2) - VY(V1)
         J1Y = 2 * V1
         J1X = J1Y - 1
         J2Y = 2 * V2
         J2X = J2Y - 1
         DO 260 J = 1,ARSIZE
            A(J1X,J) = A(J1X,J) + A(J2X,J)
            A(J1Y,J) = A(J1Y,J) + A(J2Y,J)
            A(J2X,J) = 0
            A(J2Y,J) = 0
            B(J1X) = B(J1X) + B(J2X)
            B(J1Y) = B(J1Y) + B(J2Y)
260      CONTINUE
         B(J2X) = B(J2X) + DELX
         B(J2Y) = B(J2Y) + DELY
         A(J2X,J1X) = 1
         A(J2Y,J1Y) = 1
         A(J2X,J2X) = -1
         A(J2Y,J2Y) = -1
270   CONTINUE
      RETURN
      END
C
C
      SUBROUTINE FIXBDY(A,B,IA,ARSIZE,SEG)
C
C  THIS ROUTINE SETS THE BOUNDARY POINT DISPLACEMENTS TO ZERO.
C
      INTEGER ARSIZE,SEG(1)
      DIMENSION A(IA,IA), B(1)
      DO 810 I = 1, SEG(1)
         DO 800 J = 1, ARSIZE
            A(2*I-1,J) = 0.0
            A(2*I,J) = 0.0
800      CONTINUE
         A(2*I-1,2*I-1) = 1
         A(2*I,2*I) = 1
         B(2*I-1) = 0.0
         B(2*I) = 0.0
810   CONTINUE
      RETURN
      END
C
C
      SUBROUTINE HEADER
C
C  READS HEADING AND WRITES IT TO UNIT 1
C
      BYTE INAME(64)
      DO 1 I=1,64
         INAME(I) = 0
1     CONTINUE
      PRINT*,'GIVE HEADING'
      READ(5,3) NCHAR,(INAME(I),I=1,NCHAR)
```

```
3     FORMAT(Q,16A1)
      WRITE(1,4) NCHAR,(INAME(I),I=1,NCHAR)
4     FORMAT(//,15X,16A1)
      END
```

```
      PROGRAM TRIGEN
C
C THIS PROGRAM WILL GENERATE ALL OF THE TOPOLOGICAL INFORMATION
C TO PARTITION A 2-DIMENSIONAL DOMAIN INTO TRIANGLES.  THE
C ROUTINE WILL TAKE UP TO 200 VERTEX POINTS IN IT'S PRESENT
C CONFIGURATION.
C THIS PROGRAM CALLS SUBROUTINE TRISET.
C REFERENCE: J.A.GALT-MASS/OMPA/NOAA - FEB 1982
C
      DIMENSION VX(204),VY(204)
      INTEGER TOP(2412),SEG(20)
C
C THE VERTEX IS READ IN FROM VERFIL
C
C
      PRINT*,'GIVE VERTEX INPUT FILENAME'
      CALL OLDFIL1
      PRINT*,'GIVE TOPOLOGICAL TRIANGLE DATA OUTPUT FILENAME'
      CALL NEWFIL2
      READ(1,1)NV,NSEG
1     FORMAT(2I7)
      DO 2 I=1,NSEG
         READ(1,3)SEG(I)
2     CONTINUE
3     FORMAT(I11)
      DO 4 I=1,NV
         READ(1,5)N,VX(I),VY(I),D
4     CONTINUE
5     FORMAT(I7,2F10.3,F10.1)
C
C THE TRIANGLE AND TOPOLOGICAL LINKS ARE CALCULATED
C
      CALL TRISET(VX,VY,TOP,SEG,NV,NSEG,NTRI)
C
C THE TOPOLOGICAL DATA IS OUTPUT ON TOPDAT
C
      K=2*NV+2
      WRITE(2,8)NTRI
      DO 6 I=1,NTRI
6        WRITE(2,7)TOP(I),TOP(K+I),TOP(2*K+I),TOP(3*K+I),TOP(4*K+I),
     &   TOP(5*K+I),I
7     FORMAT(7I10)
8     FORMAT(I10)
      CLOSE(1)
      CLOSE(2)
      STOP
      END
C
C
      SUBROUTINE TRISET(VX,VY,TOP,SEG,NV,NSEG,NTRI)
C
C   THIS WILL PARTITION AN AREA SPANNED BY (NV) POINTS INTO (NTRI)
C TRIANGLES.  THE POINTS ARE GIVEN AS CARTESIAN COORDINATES IN THE
C VECTOR VX(I) AND VY(I) AS INPUT.  THE REGION CAN BE BOUNDED BY
C (NSEG) SEGMENTS SUBJECT TO THE CONVENTION THAT ALL BOUNDARY
C VERTICES ARE ENTERED FIRST SUCH THAT WHEN MOVING FROM POINT N
C TO N+1 THE RIGHT HAND POINTS TO THE OUTSIDE OF THE DOMAIN AND
C THAT THE LAST VERTEX OF
C VECTOR SEG(1).  ALL TOPOLOGICAL INFORMATION ON THE TRIANGLES IS
C RETURNED IN THE VECTOR TOP SUCH THAT FOR TRIANGLE N
C       VERTEX 1 = TOP(N)          NEIGHBOR 1 = TOP(3K+N)
C       VERTEX 2 = TOP(K+N)        NEIGHBOR 2 = TOP(4K+N)
C       VERTEX 3 = TOP(2K+N)       NEIGHBOR 3 = TOP(5K+N)
```

```
C WHERE K = 2*NV+2
C VECTORS SHOULD BE DIMENSIONED TO
C       VX(NV+4)
C       VY(NV+4)
C       SEG(NSEG) - INTEGER ARRAY
C       TOP(6*K) - INTEGER ARRAY
C THIS SUBROUTINE CALLS SUBROUTINES ISOS,LCROSS, AND FIXTRI AS WELL
C AS THE FUNCTION GOODTRI
C REFERENCE: J.A.GALT-MASS/OMPA/NOAA - FEB 1982
C
      DIMENSION VX(1),VY(1)
      INTEGER FAC1,FAC2,FAC3,VER1,VER2,VER3,TOP(1),SEG(1),STRI(20)
      K=2*NV+2
      NTRI=K
      K1=0
      K2=K
      K3=2*K
      K4=3*K
      K5=4*K
      K6=5*K
C
C THE HYPERBOX IS SET UP
C
      XMAX=VX(1)
      XMIN=XMAX
      YMAX=VY(1)
      YMIN=YMAX
      DO 1 I=1,NV
         IF(VX(I).GT.XMAX) XMAX=VX(I)
         IF(VX(I).LT.XMIN) XMIN=VX(I)
         IF(VY(I).GT.YMAX) YMAX=VY(I)
         IF(VY(I).LT.YMIN) YMIN=VY(I)
1     CONTINUE
      DX= (XMAX-XMIN)*.5
      DY= (YMAX-YMIN)*.5
      VX(NV+1)=XMIN-DX
      VY(NV+1)=YMIN-DY
      VX(NV+2)=XMAX+DX
      VY(NV+2)=YMIN-DY
      VX(NV+3)=XMAX+DX
      VY(NV+3)=YMAX+DY
      VX(NV+4)=XMIN-DX
      VY(NV+4)=YMAX+DY
C
C ORIGINAL FOUR TRIANGLES ARE SET UP
C
      NEXTRI=5
      TOP(K1+1)=NV+1
      TOP(K2+1)=NV+2
      TOP(K3+1)=1
      TOP(K4+1)=2
      TOP(K5+1)=4
      TOP(K6+1)=-1
      TOP(K1+2)=NV+2
      TOP(K2+2)=NV+3
      TOP(K3+2)=1
      TOP(K4+2)=3
      TOP(K5+2)=1
      TOP(K6+2)=-1
      TOP(K1+3)=NV+3
      TOP(K2+3)=NV+4
      TOP(K3+3)=1
      TOP(K4+3)=4
```

```
      TOP(K5+3)=2
      TOP(K6+3)=-1
      TOP(K1+4)=NV+4
      TOP(K2+4)=NV+1
      TOP(K3+4)=1
      TOP(K4+4)=1
      TOP(K5+4)=3
      TOP(K6+4)=-1
C
C THE NEXT VERTEX IS ADDED UNTIL ALL ARE INCLUDED
C
      DO 6 I=2,NV
         X=VX(I)
         Y=VY(I)
C
C FIRST THE TRIANGLE CONTAINING THE NEW VERTEX IS IDENTIFIED
C
         J1=NEXTRI-1
         DO 2 J=1,J1
            X1=VX(TOP(K1+J))
            Y1=VY(TOP(K1+J))
            X2=VX(TOP(K2+J))
            Y2=VY(TOP(K2+J))
            X3=VX(TOP(K3+J))
            Y3=VY(TOP(K3+J))
            CALL ISOS(X1,Y1,X2,Y2,X3,Y3,X,Y,IFLAG)
            IF(IFLAG.EQ.1)GOTO 3
2        CONTINUE
C
C THE FIRST OF THE NEW TRIANGLES IS ADDED
C
3        TOP(K1+NEXTRI)=TOP(K1+J)
         TOP(K2+NEXTRI)=TOP(K2+J)
         TOP(K3+NEXTRI)=I
         TOP(K4+NEXTRI)=NEXTRI+1
         TOP(K5+NEXTRI)=J
         TOP(K6+NEXTRI)=TOP(K6+J)
C
C THE SECOND OF THE NEW TRIANGLES IS ADDED
C
         TOP(K1+NEXTRI+1)=TOP(K2+J)
         TOP(K2+NEXTRI+1)=TOP(K3+J)
         TOP(K3+NEXTRI+1)=I
         TOP(K4+NEXTRI+1)=J
         TOP(K5+NEXTRI+1)=NEXTRI
         TOP(K6+NEXTRI+1)=TOP(K4+J)
C
C THE TRIANGLE J IS REBUILT
C
         TOP(K2+J)=I
         TOP(K4+J)=NEXTRI+1
         TOP(K6+J)=NEXTRI
C
C THE SURROUNDING TRIANGLES ARE CORRECTED FOR THE NEW TRIANGLES
C
         JTR1=TOP(K6+NEXTRI)
         JTR2=TOP(K6+NEXTRI+1)
         DO 5 J1=1,3
            J2=K*J1+K3
            IF(JTR1.EQ.-1)GOTO 4
            IF(TOP(J2+JTR1).EQ.J)TOP(J2+JTR1)=NEXTRI
4           IF(JTR2.EQ.-1)GOTO 5
            IF(TOP(J2+JTR2).EQ.J)TOP(J2+JTR2)=NEXTRI+1
```

```
5         CONTINUE
C
C THE THREE NEW TRIANGLES ARE CHECKED FOR SHAPE
C
          ICHG=0
          J1=NEXTRI
          J2=TOP(K6+NEXTRI)
          CALL FIXTRI(ICHG,J1,J2,DX,DY,NV,TOP,VX,VY)
          ICHG=0
          J1=NEXTRI+1
          J2=TOP(K6+NEXTRI+1)
          CALL FIXTRI(ICHG,J1,J2,DX,DY,NV,TOP,VX,VY)
          ICHG=0
          J1=J
          J2=TOP(K5+J)
          CALL FIXTRI(ICHG,J1,J2,DX,DY,NV,TOP,VX,VY)
6         NEXTRI=NEXTRI+2
C
C THIS SECTION MAKES SURE THE BOUNDARY SEGMENTS ARE ACTUAL TRIANGLE SIDES
C
      DO 15 I=1,NSEG
          IF(I.EQ.1)N1=1
          IF(I.NE.1)N1=SEG(I-1)+1
7         N2=N1+1
          IF(N1.EQ.SEG(I).AND.I.EQ.1)N2=1
          IF(N1.EQ.SEG(I).AND.I.NE.1)N2=SEG(I-1)+1
C
C THIS CHECKS TRIANGLES FOR N1 AND N2
C
8         DO 9 J=1,K
             VER1=TOP(K1+J)
             VER2=TOP(K2+J)
             VER3=TOP(K3+J)
             IF(VER1.NE.N1.AND.VER2.NE.N1.AND.VER3.NE.N1)GOTO 9
             IF(VER1.NE.N2.AND.VER2.NE.N2.AND.VER3.NE.N2)GOTO 9
             GOTO 14
9         CONTINUE
C
C THE EDGE SEGMENT HAS NOT BEEN FOUND, REORIENT: START BY
C FINDING THE TRIANGLES CROSSED BY THE MISSING EDGE SEGMENT
C
          III=0
          DO 10 J=1,K
             JA=TOP(K1+J)
             JB=TOP(K2+J)
             JC=TOP(K3+J)
             X1=VX(JA)
             Y1=VY(JA)
             X2=VX(JB)
             Y2=VY(JB)
             X3=VX(JC)
             Y3=VY(JC)
             X4=VX(N1)
             Y4=VY(N1)
             X5=VX(N2)
             Y5=VY(N2)
             CALL LCROSS(X1,Y1,X2,Y2,X3,Y3,X4,Y4,X5,Y5,IFLAG)
             IF(IFLAG.EQ.0)GOTO 10
             III=III+1
             STRI(III)=J
10        CONTINUE
C
C THE TRIANGLES CROSSED BY THE MISSING EDGE ARE REORIENTED
```

```
C
          DX=VX(N1)-VX(N2)
          DY=VY(N1)-VY(N2)
          DO 11 JA=1,III
             DO 11 JB=JA,III
                J1=STRI(JA)
                J2=STRI(JB)
                IF(J1.EQ.J2)GOTO 11
                ICHG=2
                CALL FIXTRI(ICHG,J1,J2,DX,DY,NV,TOP,VX,VY)
11        CONTINUE
          GOTO 8
C
C THE EDGE HAS BEEN FOUND, SET UP THE NEXT EDGE
C
14        CONTINUE
          N1=N1+1
          IF(N2.EQ.1)GOTO 15
          M=1
          IF(I.NE.1)M=SEG(I-1)+1
          IF(I.NE.1.AND.N2.EQ.M)GOTO 15
          GOTO 7
15     CONTINUE
C
C CONVEX BOUNDARY TRIANGLES ARE MARKED FOR REMOVAL
C
       DO 17 I=1,K
          J3=MAX0(TOP(K1+I),TOP(K2+I),TOP(K3+I))
           J1=MIN0(TOP(K1+I),TOP(K2+I),TOP(K3+I))
           DO 16 I2=1,NSEG
              IF(I2.EQ.1)N1=1
              IF(I2.NE.1)N1=SEG(I2-1)+1
              N2=SEG(I2)
              IF(J3.GT.N2.OR.J1.LT.N1)GOTO 16
              IF(TOP(K1+I).NE.J3.AND.TOP(K1+I).NE.J1)J2=TOP(K1+I)
              IF(TOP(K2+I).NE.J3.AND.TOP(K2+I).NE.J1)J2=TOP(K2+I)
              IF(TOP(K3+I).NE.J3.AND.TOP(K3+I).NE.J1)J2=TOP(K3+I)
C
C J1,J2,J3 ARE THE VERTICES (IN ASCENDING ORDER) OF A TRIANGLE
C ALL OF WHOSE VERTICES ARE ON A SINGLE BOUNDARY SEGMENT
C
             X1=VX(J1)
             Y1=VY(J1)
             X2=VX(J2)
             Y2=VY(J2)
             X3=VX(J3)
             Y3=VY(J3)
C
C CONVEX TRIANGLES ARE IDENTIFIED AND MARKED
C
             X=X2*Y3-X3*Y2-X1*Y3+X3*Y1+X1*Y2-X2*Y1
             IF(X.LT.0.)TOP(K1+I)=-1
16        CONTINUE
17     CONTINUE
C
C TRIANGLES THAT HAVE A VERTEX ON THE HYPERSQUARE ARE MARKED
C
       DO 18 I=1,K
          DO 18 J1=1,3
             J=(J1-1)*K2
             IF(TOP(J+I).GT.NV)TOP(K1+I)=-1
18     CONTINUE
C
```

```
C ALL TRIANGLES WITH CORRECT NEIGHBORS CORRECT THE RECORDS
C
      DO 19 I=1,K
         DO 19 J1=1,3
            J=K3+J1*K2
            N1=TOP(J+I)
            IF(TOP(K1+N1).EQ.-1)TOP(J+I)=-1
19    CONTINUE
C
C MARKED TRIANGLES ARE ELIMINATED
C
      NTRI=K
      KK=K-1
      IF(TOP(K).EQ.-1)TOP(K2+K)=-1
      DO 23 I=1,K
20       IF(TOP(K1+I).NE.-1)GOTO 23
         NTRI=NTRI-1
         IF(TOP(K2+I).EQ.-1)GOTO 24
         DO 21 J=I,KK
            DO 21 J1=1,6
               M=(J1-1)*K
21       TOP(M+J)=TOP(M+J+1)
         DO 22 I1=1,NTRI
            DO 22 I2=3,5
               IF(TOP(I2*K+I1).GT.I)TOP(I2*K+I1)=TOP(I2*K+I1)-1
22       CONTINUE
         GOTO 20
23    CONTINUE
24    CONTINUE
C
C THE FINAL IMPROVEMENT IN TRIANGLE SHAPE IS MADE
C
      DO 25 M=1,10
         DO 25 J1=1,NTRI
            DO 25 I=1,3
               J=K3+I*K2
               J2=TOP(J+J1)
               ICHG=0
               J1T=J1
               CALL FIXTRI(ICHG,J1T,J2,DX,DY,NV,TOP,VX,VY)
25    CONTINUE
      RETURN
      END
C
C
      FUNCTION GOODTRI(X1,Y1,X2,Y2,X3,Y3)
C
C THIS RETURNS THE RATIO OF THE SQUARE ROOT OF THE TRI AREA TO THE
C PERIMETER
C REFERENCE: J.A.GALT-MASS/OMPA/NOAA - FEB 1982
C
      S = SQRT((X2-X1)**2+(Y2-Y1)**2)+SQRT((X3-X2)**2+(Y3-Y2)**2)
     &    +SQRT((X1-X3)**2+(Y1-Y3)**2)
      A = ABS(X2*Y3-X3*Y2-X1*Y3+X3*Y1+X1*Y2-X2*Y1)/2
      GOODTRI = SQRT(A)/S
      RETURN
      END
C
C
      SUBROUTINE ISOS(X1,Y1,X2,Y2,X3,Y3,X,Y,IFLAG)
C
C THIS TAKES A TRIANGLE WITH VERTICES LISTED IN COUNTER
C CLOCKWISE ORDER AND RETURNS IFLAG=1 IF THE POINT IS IN THE
```

```
C
C REFERENCE: J.A. GALT-MASS/OMPA/NOAA - FEB 1982
C
      IFLAG = 1
      FAC = X*Y2-X2*Y-X*Y3+X3*Y+X2*Y3-X3*Y2
      IF(ABS(FAC).LT..0000001) FAC = .0
      IF(FAC.LT.0.)GOTO 1
      FAC = X1*Y-X*Y1-X1*Y3+X3*Y1+X*Y3-X3*Y
      IF(ABS(FAC).LT..0000001) FAC = .0
      IF(FAC.LT.0.)GOTO 1
      FAC = X1*Y2-X2*Y1-X1*Y+X*Y1+X2*Y-X*Y2
      IF(ABS(FAC).LT..0000001) FAC = .0
      IF(FAC.LT.0.)GOTO 1
      RETURN
1     IFLAG = -1
      RETURN
      END
C
C
      SUBROUTINE FIXTRI(ICHG,J1,J2,DX,DY,NV,TOP,VX,VY)
C
C THIS SUBROUTINE CHECKS TO SEE IF TWO TRIANGLES ARE ADJACENT TO
C EACH OTHER AND IF THEY ARE NOT THEN ICHG IS RETURNED AS (-1).  IF
C ICHG IS INITIALLY (0) THEN THE ADJACENT TRIANGLES ARE REORIENTED IF
C DOING SO MAKES THE NEW PAIR BETTER SHAPED.  IF ICHG IS INITIALLY
C (+1) THE PAIR OF TRIANGLES IS AUTOMATICALLY REORIENTED UNLESS THEY
C ARE CONVEX IN WHICH CASE ICHG IS RETURNED (-2).  IF ICHANGE IS
C INITIALLY (+2) THE ADJACENT TRIANGLES ARE REORIENTED IF THE NEWLY
C CREATED SIDE WILL BE MORE CLEARLY PARALLEL TO THE LINE SEGMENT
C SPECIFIED BY (DX,DY) THEN THE SIDE THAT WILL BE REPLACED.
C REFERENCE: J.A.GALT-MASS/OMPA/NOAA - FEB 1982
C
      DIMENSION VX(1),VY(1)
      INTEGER VER1,VER2,VER3,VER4,TOP(1)
      IF(J1.LE.0.OR.J2.LE.0)GOTO 10
      K=2*NV+2
      KMOD=3*K
      IF(J1.EQ.TOP(3*K+J2))GOTO 11
      IF(J1.EQ.TOP(4*K+J2))GOTO 11
      IF(J1.EQ.TOP(5*K+J2))GOTO 11
10    ICHG=-1
      RETURN
11    CONTINUE
C
C THE TWO NON-COMMON VERTICES ARE IDENTIFIED
C
      DO 1 I=1,3
         J = (I-1)*K
         IF(TOP(J+KMOD+J1).EQ.J2) J1V = J
         IF(TOP(J+KMOD+J2).EQ.J1) J2V = J
1     CONTINUE
C
C THE COMMON RECTANGLE IS LABELED
C
      VER1 = TOP(J1V+J1)
      I = J1V+K
      I = MOD(I,KMOD)
      VER2 = TOP(I+J1)
      J3 = TOP(I+KMOD+J1)
      I = I+K
      I =  MOD(I,KMOD)
      VER3 = TOP(I+J1)
      J4 = TOP(I+KMOD+J1)
```

```
      VER4 = TOP(J2V+J2)
      I = J2V+K
      I = MOD(I,KMOD)
      J5 = TOP(I+KMOD+J2)
      I = I+K
      I = MOD(I,KMOD)
      J6 = TOP(I+KMOD+J2)
C
C HERE A CHECK IS MADE TO SEE IF THE RECTANGULAR DOMAIN IS CONCAVE
C AND THE GOODNESS OF THE ALTERNATE TRIANGLES IS CALCULATED
C
      X1 = VX(VER1)
      Y1 = VY(VER1)
      X2 = VX(VER2)
      Y2 = VY(VER2)
      X3 = VX(VER4)
      Y3 = VY(VER4)
      X = VX(VER3)
      Y = VY(VER3)
      CALL ISOS(X1,Y1,X2,Y2,X3,Y3,X,Y,IFLAG)
      IF(IFLAG.EQ.1)ICHG=-2
      IF(IFLAG.EQ.1)GOTO 3
      T1 = GOODTRI(X1,Y1,X2,Y2,X3,Y3)
      X2 = VX(VER4)
      Y2 = VY(VER4)
      X3 = VX(VER3)
      Y3 = VY(VER3)
      X = VX(VER2)
      Y = VY(VER2)
      CALL ISOS(X1,Y1,X2,Y2,X3,Y3,X,Y,IFLAG)
      IF(IFLAG.EQ.1)ICHG=-2
      IF(IFLAG.EQ.1)GOTO 3
      T2 = GOODTRI(X1,Y1,X2,Y2,X3,Y3)
      IF(ICHG.EQ.1)GOTO 2
      IF(ICHG.EQ.2)GOTO 4
C
C THE GOODNESS OF THE PRESENT TRIANGLES ARE CHECKED
C
      X2 = VX(VER2)
      Y2 = VY(VER2)
      T3 = GOODTRI(X1,Y1,X2,Y2,X3,Y3)
      X1 = VX(VER2)
      Y1 = VY(VER2)
      X2 = VX(VER4)
      Y2 = VY(VER4)
      T4 = GOODTRI(X1,Y1,X2,Y2,X3,Y3)
      T = AMIN1(T1,T2,T3,T4)
      IF(T.EQ.T1.OR.T.EQ.T2)GOTO 3
C
C THE ALTERNATE TRIANGLES REPLACE THE ORIGINAL TRIANGLES
C
2     TOP(J1) = VER1
      TOP(K+J1) = VER2
      TOP(2*K+J1) = VER4
      TOP(3*K+J1) = J5
      TOP(4*K+J1) = J2
      TOP(5*K+J1) = J4
      TOP(J2) = VER4
      TOP(K+J2) = VER3
      TOP(2*K+J2) = VER1
      TOP(3*K+J2) = J3
      TOP(4*K+J2) = J1
      TOP(5*K+J2) = J6
```

```
C
C NEIGHBORING TRIANGLES ARE CORRECTED
C
      DO 33 KK=1,3
         KK2 = (KK+2)*K
         IF(J5.EQ.-1)GOTO 32
         IF(TOP(KK2+J5).EQ.J2) TOP(KK2+J5)=J1
32       IF(J3.EQ.-1)GOTO 33
         IF(TOP(KK2+J3).EQ.J1) TOP(KK2+J3)=J2
33    CONTINUE
3     CONTINUE
      RETURN
C
C IF IT IS PARALLEL TO THE DESIRED LINE SEGMENT
C
4     DX0 = VX(VER2)-VX(VER3)
      DY0 = VY(VER2)-VY(VER3)
      DXN = VX(VER1)-VX(VER4)
      DYN = VY(VER1)-VY(VER4)
      DOT1 = ABS((DX*DX0+DY*DY0)/SQRT(DX0**2+DY0**2))
      DOT2 = ABS((DX*DXN+DY*DYN)/SQRT(DXN**2+DYN**2))
      IF(DOT2.GT.DOT1)GOTO 2
      RETURN
      END
C
C
      SUBROUTINE LCROSS(X1,Y1,X2,Y2,X3,Y3,X4,Y4,X5,Y5,IFLAG)
C
C THE SUBROUTINE CHECKS TO SEE IF A LINE FROM (X4,Y4) TO (X5,Y5)
C GOES THROUGH THE TRIANGLE DEFINED BY THE (COUNTERCLOCKWISE)ORDERED
C VERTICES (X1,Y1),(X2,Y2),AND (X3,Y3). IF THE ANSWER IS YES, THEN
C IFLAG IS SET TO (+1), OTHERWISE IFLAG IS SET TO (0).
C REFERENCE: J.A.GALT-MASS/OMPA/NOAA - FEB 1982
C
      IFLAG = 0
C
C THE LINE SEGMENT IS MADE AN OPEN SET
C
      X0 = .99*X4 + .01*X5
      X5 = .99*X5 + .01*X4
      X4 = X0
      Y0 = .99*Y4 + .01*Y5
      Y5 = .99*Y5 + .01*Y4
      Y4 = Y0
C
C SHAPE FUNCTION COORDINATES ARE CALCULATED
C
      AREA = X1*Y2 + X2*Y3 + X3*Y1 - X1*Y3 -X2*Y1 - X3*Y2
      P1 = (X1*Y2 + X2*Y4 + X4*Y1 - X1*Y4 - X2*Y1 - X4*Y2)/AREA
      P2 = (X1*Y2 + X2*Y5 + X5*Y1 - X1*Y5 - X2*Y1 - X5*Y2)/AREA
      Q1 = (X2*Y3 + X3*Y4 + X4*Y2 - X2*Y4 - X3*Y2 - X4*Y3)/AREA
      Q2 = (X2*Y3 + X3*Y5 + X5*Y2 - X2*Y5 - X3*Y2 - X5*Y3)/AREA
      DP = P2 - P1
      DQ = Q2 - Q1
C
C THE CHARACTERISTICS OF THE LINE ARE CALCULATED
C
      IF(ABS(DQ).GT..00001)GOTO 1
      XI = 10000
      YI = Q1
      GOTO 3
1     IF(ABS(DP).GT..00001)GOTO 2
      XI = P1
```

```
      YI = 10000
      GOTO 3
2     XI = (P1*DQ - Q1*DP)/DQ
      YI = Q1 - (DQ/DP)*P1
3     CONTINUE
C
      IF(0.0.LT.XI.AND.1.0.GT.XI)GOTO 4
      IF(XI.EQ.0.0.AND.(P1*Q1).GT.0.0)GOTO 4
      IF(0.0.LT.YI.AND.1.0.GT.YI)GOTO 5
      IF(YI.EQ.0.0.AND.(P1*Q1).GT.0.0)GOTO 5
      RETURN
4     IF(P1.LT.XI.AND.P2.GT.XI)GOTO 7
      IF(P2.LT.XI.AND.P1.GT.XI)GOTO 7
      GOTO 6
5     IF(Q1.LT.YI.AND.Q2.GT.YI)GOTO 7
      IF(Q2.LT.YI.AND.Q1.GT.YI)GOTO 7
6     IF(P1.GT.0.0.AND.Q1.GT.0.0.AND.(P1÷Q1).LT.1.0)GOTO 7
      IF(P2.GT.0.0.AND.Q2.GT.0.0.AND.(P2÷Q2).LT.1.0)GOTO7
      RETURN
7     IFLAG = 1
      RETURN
      END
```

```
      SUBROUTINE DECOMP(IA ,N, A, LU, PS, SCALES)
C  ARGUMENTS:
      INTEGER N
      REAL A(IA,IA), LU(IA,IA), SCALES(1)
      INTEGER PS(1)
C  LOCAL DECLARATIONS:
      REAL NRMROW, BIG, SIZE, MULT, PIVOT
      INTEGER I,J,K,PVTIDX, IP, KP
C
C  DECOMP COMPUTES TRIANGULAR MATRICES L AND U AND PERMUTATION MATRIX
C  P SO THAT LU = PA.  STORE L-I AND U IN LU.  ARRAY PS CONTAINS
C  PERMUTED ROW INDICES.
C
C  DECOMP(IA, N, A, A, PS, SCALES) OVERWRITES A WITH LU
C
C  INITIALIZE PS, LU, SCALES:
      DO 105 I = 1,N
         PS(I) = I
         NRMROW = 0.0
         DO 100 J = 1,N
            LU(I,J) = A(I,J)
              IF(NRMROW .LT. ABS(LU(I,J))) NRMROW = ABS(LU(I,J))
100      CONTINUE
         IF (NRMROW .NE. 0.0) THEN
            SCALES(I) = 1.0/NRMROW
         ELSE
C          ERROR CONDITION - CALL SINGLR
            SCALES(I) = 0.0
            CALL SINGLR(0)
            STOP
         ENDIF
105   CONTINUE
C
C  GAUSSIAN ELIMINATION WITH PARTIAL PIVOTING
      DO 140 K = 1,N-1
         BIG = 0
         DO 110 I = K,N
            IP = PS(I)
            SIZE = ABS(LU(IP,K)) * SCALES(IP)
            IF ( BIG .LT. SIZE) THEN
               BIG = SIZE
               PVTIDX = I
            ENDIF
110      CONTINUE
         IF (BIG .EQ. 0) THEN
C         ERROR CONDITION - CALL SINGLR AND ABORT THIS LOOP
            CALL SINGLR(1)
            STOP
         ENDIF
         IF (PVTIDX .NE. K) THEN
            KP = PS(K)
            PS(K) = PS(PVTIDX)
            PS(PVTIDX) = KP
         ENDIF
         KP = PS(K)
         PIVOT = LU(KP,K)
         DO 130 I = K+1,N
            IP = PS(I)
            MULT = LU(IP,K) / PIVOT
            LU(IP,K) = MULT
            IF (MULT .NE. 0.0) THEN
               DO 120 J = K+1,N
                  LU(IP,J) = LU(IP,J) - MULT * LU(KP,J)
```

```
120            CONTINUE
             ENDIF
130        CONTINUE
140     CONTINUE
        IP = PS(N)
        IF (LU(IP,N) .EQ. 0.0) THEN
C        ERROR CONDITION
           CALL SINGLR(1)
           STOP
        ENDIF
        RETURN
        END
```

```
      SUBROUTINE SOLVE(IA, N, LU, B, X, PS)
C   ARGUMENTS:
      INTEGER N
        REAL LU(IA,IA), B(1), X(1)
      INTEGER PS(1)
C   LOCAL DECLARATIONS:
      INTEGER I, J, IP, IBACK
      REAL DOT
C
C   SOLVES AX = B USING LU FROM DECOMP
C
      DO 210 I = 1,N
         DOT = 0.0
         IP = PS(I)
         DO 200 J =1,I-1
            DOT = DOT + LU(IP,J) * X(J)
200      CONTINUE
         X(I) = B(IP) - DOT
210   CONTINUE
      DO 230 IBACK = 1,N
         I = N + 1 - IBACK
C     (FOR I = N DOWNTO 1 DO)
         DOT = 0.0
         IP = PS(I)
         DO 220 J = I+1,N
            DOT = DOT + LU(IP,J) * X(J)
220      CONTINUE
         X(I) = (X(I) - DOT) / LU(IP,I)
230   CONTINUE
      RETURN
      END
```

```
      SUBROUTINE GETDAT(TOP,SEG,VX,VY,NV,NSEG,NTRI)
      INTEGER TOP(1), SEG(1)
      DIMENSION VX(1), VY(1)
C
C  GET VERTEX AND TRIANGLE INFO
C
      PRINT*,'GIVE NAME OF VERTEX DATA FILE'
      CALL OLDFIL1
      READ(1,1)NV,NSEG
1     FORMAT(2I7)
      DO 5 I = 1, NSEG
         READ(1,2)SEG(I)
5     CONTINUE
2     FORMAT(I11)
      DO 10 I = 1,NV
         READ(1,3)N,VX(I),VY(I),D
10    CONTINUE
3     FORMAT(I7,2F10.3,F10.1)
      CLOSE(1)
      K = 2 * NV + 2
      PRINT*,'GIVE NAME OF TOPOLOGICAL TRIANGLE DATA FILE'
      CALL OLDFIL1
      READ(1,4)NTRI
4     FORMAT(I10)
      DO 15 I = 1,NTRI
         READ(1,6)TOP(I),TOP(K+I),TOP(2*K+I),TOP(3*K+I),TOP(4*K+I),
     &   TOP(5*K+I)
15    CONTINUE
6     FORMAT(7I10)
      CLOSE(1)
C
      RETURN
      END
```

```
      SUBROUTINE NEWFIL1
C
C  READS A FILENAME AND OPENS THE FILE ON UNIT 1
C
      BYTE FNAME(16)
      DO 900 I = 1,16
         FNAME(I) = 0
900   CONTINUE
      READ(5,910) NCHAR,(FNAME(I), I = 1, NCHAR)
910   FORMAT(Q,16A1)
      OPEN(UNIT=1,FILE=FNAME,STATUS='NEW')
      RETURN
      END
```

```
      SUBROUTINE OLDFIL1
C
C  READS AN EXISTING FILENAME AND OPENS THE FILE ON UNIT 1
C
      BYTE FNAME(16)
      DO 900 I = 1,16
         FNAME(I) = 0
900   CONTINUE
      READ(5,910) NCHAR,(FNAME(I), I = 1, NCHAR)
910   FORMAT(Q,16A1)
      OPEN(UNIT=1,FILE=FNAME,STATUS='OLD')
      RETURN
      END
```

```
      SUBROUTINE TRIBASE(X1,Y1,X2,Y2,X3,Y3,DX1,DY1,D1,DX2,DY2,D2,
     &                   DX3,DY3,D3,AREA)
      AREA = X1*Y2 + X3*Y1 + X2*Y3 - X3*Y2 - X1*Y3 - X2*Y1
      DX1 = (Y2 - Y3)/AREA
      DY1 = (X3 - X2)/AREA
      D1 = (X2*Y3 - X3*Y2)/AREA
      DX2 = (Y3 - Y1)/AREA
      DY2 = (X1 - X3)/AREA
      D2 = (X3*Y1 - X1*Y3)/AREA
      DX3 = (Y1 - Y2)/AREA
      DY3 = (X2 - X1)/AREA
      D3 = (X1*Y2 - X2*Y1)/AREA
      AREA = ABS(AREA)/2.
      RETURN
      END
```

APPENDIX B.

Software developed to control the skin extensometer

```
0  LOMEM: 24576:D% = 0: HIMEM: 34816
1  REM **********************
2  REM * SKIN STRETCHER 1.0  *
3  REM *                    *
4  REM *                    *
5  REM **********************
6  REM *  LINE  #0   MUST BE *
7  REM *  FIRST LINE IN      *
8  REM *  PROGRAM!!!         *
9  REM **********************
20  TEXT : HOME
100  GOSUB 10000
110  REM **********************
111  REM *   MAIN  MENU       *
112  REM **********************
120  PRINT "THIS PROGRAM WILL ALLOW YOU TO SET THE  MOTORS IN A DESIRED POSITION
AND THEN MOVE THEM A SPECIFIED DISTANCE"
122  PRINT : PRINT "NOTE: The only value that works for     speed is one (1)
mm/sec"
125  INVERSE : PRINT "    NOTE: YOU MUST CHOOSE OPTION 4 FIRSTEACH TIME YOU
RUN THE PROGRAM    ": NORMAL
130  PRINT
140  PRINT : PRINT "<1> SET MOTORS                          <2> MOVE MOTORS
OR PROCESS DATA"
141  PRINT "<3> PRINT A/D VALUES"
142  PRINT "<4> CALIBRATE A/D CONVERTER"
143  PRINT "<ESC> TO END"
145  PRINT "CHOOSE ONE:";: GOSUB 1000
147  IF A =  - 1 THEN  END
148  IF A < 1 OR A > 4 THEN 140
150  ON A GOSUB 8000,2000,9000,12000
170  GOTO 140
999  END
1000  REM *********************
1001  REM * GENERAL LINE INPUT*
1002  REM *ROUTINE, A$=INPUT  *
1003  REM *  A=-1 IF <ESC>    *
1009  REM *********************
1050 A$ = "":A = 0:C$ = ""
1060  GET C$
1070  IF C$ <  > BAK$ AND C$ <  > DL$ AND C$ <  > RET$ AND C$ <  > ESC$ THEN
1140
1080  IF  NOT (C$ = BAK$ OR C$ = DL$) THEN 1120 AND  LEN (A$) > 0 THEN A$ =
 LEFT$ (A$, LEN (A$) - 1): PRINT BAK$" "BAK$;: GOTO 1060
1090  IF  LEN (A$) > 1 THEN A$ =  LEFT$ (A$, LEN (A$) - 1): GOTO 1110
1100  IF  LEN (A$) = 1 THEN A$ = ""
1110  PRINT BAK$" "BAK$;: GOTO 1060
1120  IF C$ = ESC$ THEN A$ = "":A =  - 1: RETURN
1130  IF C$ = RET$ THEN  PRINT RET$:A =  VAL (A$): RETURN
1140 A$ = A$ + C$: PRINT C$;: GOTO 1060
1170  RETURN
2000  REM *********************
2001  REM * SECONDARY MENU    *
```

```
2002  REM *                    *
2003  REM *********************
2020  HOME
2030  PRINT : PRINT "<1> MOVE MOTOR WITH NEW PARAMATERS"
2040  PRINT "<2> REPEAT LAST PARAMATERS"
2043  PRINT "<3> HOLD AT CONSTANT TENSION"
2045  PRINT "<4> HOLD AT CONSTANT DISTANCE"
2050  PRINT "<5> PROCESS DATA"
2060  PRINT "<ESC> EXIT TO MENU"
2070  PRINT "CHOOSE ONE:";: GOSUB 1000
2080  IF A =  - 1 THEN  RETURN
2090  IF A < 1 OR A > 5 THEN 2030
2100  ON A GOSUB 3000,3180,15000,16000,6000
2110  GOTO 2030
3000  REM *********************
3001  REM *MOVE IN MOTOR 'A'  *
3002  REM *A CERTAIN DISTANCE *
3003  REM *********************
3020  PRINT
3030  PRINT "MOTOR A SHOULD BE MOSTLY OUT, AND MOTOR B SHOULD BE MOSTLY IN"
3040  PRINT "(MOTOR A DOES THE MOVING)"
3050  PRINT
3060  INPUT "DISTANCE (MM)=";MM
3070  INPUT "SPEED (MM/SEC)=";SP
3080  INPUT "TENSION (G)=";G
3090  INPUT "HAVE MOTOR RETURN TO START (Y/N):";RT$:RT = (RT$ = "Y")
3100 DIR% = 0
3110 PULSES =  FN PULSES(MM)
3115 LN(0) = PULSES
3120 TN =  FN TN(G)
3130  REM *********************
3140  REM * ENTRY POINT FOR   *
3150  REM * REPEATING LAST    *
3160  REM * STRETCH           *
3170  REM *********************
3180  PRINT "HIT <ESC> TO ABORT, ANY OTHER KEY TO START.";: GOSUB 1000: IF A
=  - 1 THEN  RETURN
3190  GOSUB 4020
3200  IF RT THEN  GOSUB 5000
3210  RETURN
4000  REM *********************
4001  REM * MOVE MOTOR A AT A *
4002  REM *CERTAIN SPEED WHILE*
4003  REM * CHECKING TENSION  *
4004  REM * AND RECORDING DATA*
4009  REM *********************
4020 MODE% = 0
4030 P = 1
4040  FOR I = 1 TO PULSES
4050  FOR W = 1 TO WT: NEXT W
4060  & MOTA,P,DIR%,MODE%
4070 D% = 5: CALL 800: PRINT "Distance=" FN MM(I)"   GRAMS  =" FN G(D%)"   "
4080  IF  NOT DIR% THEN MM(0,I) =  FN MM(I):G(0,I) =  FN G(D%)
4090  IF DIR% THEN MM(1,I) =  FN MM(PULSES - I):G(1,I) =  FN G(D%)
4100  IF  NOT DIR% AND D% > TN THEN LN(0) = I:I = PULSES + 1:PULSES = LN(0):
```

```
PRINT "*** STOPPED AT " FN MM(LN(0))" MM AND " FN G(D%)" GRAMS."
4110  NEXT
4120  RETURN
5000  REM ********************
5001  REM *MOVE BACK MOTOR 'A'*
5002  REM *@CERTAIN SPEED WITH*
5003  REM *NO TENSION CHECK   *
5004  REM ********************
5020  PRINT "HIT RETURN TO MOVE MOTOR BACK,          OR HIT <ESC> TO ABORT"
5030  GOSUB 1000: IF A =  - 1 THEN  PRINT "ABORTED": RETURN
5040  PRINT : PRINT "NOW MOVING MOTOR BACK"
5045 LN(1) = PULSES
5050 DIR% =  NOT DIR%
5060  GOSUB 4000
5070 DIR% =  NOT DIR%
5080  RETURN
6000  REM ********************
6001  REM * OUTPUT DATA TO    *
6002  REM * PRINTER OR DISK   *
6003  REM * OR SCREEN         *
6004  REM ********************
6020  PRINT
6030  GOSUB 7200: IF A =  - 1 THEN  RETURN
6040  PRINT : PRINT "<1> SAVE DATA TO DISK"
6050  PRINT "<2> OUTPUT DATA TO PRINTER"
6060  PRINT "<3> OUTPUT DATA TO SCREEN"
6070  PRINT "<ESC> EXIT TO MENU"
6080  PRINT "CHOOSE ONE:";: GOSUB 1000
6090  IF A =  - 1 THEN  RETURN
6100  IF A < 1 OR A > 3 THEN 6040
6110  ON A GOSUB 6500,6700,7000
6120  GOTO 6020
6500  REM ********************
6501  REM * OUTPUT DATA TO    *
6502  REM * DISK. FORMAT IS:  *
6503  REM *# OF DATA ITEMS    *
6504  REM *ZERO               *
6505  REM *----FOLLOWED BY THE*
6506  REM *----DATA, ORDERED: *
6507  REM *DISTANACE          *
6508  REM *TENSION            *
6509  REM *(THIS IS APPLEPLOT *
6510  REM * FORMAT  )         *
6515  REM ********************
6520  PRINT "<<SAVE DATA TO DISK>>"
6530  PRINT "DISK DRIVE <1> OR <2> ";: GOSUB 1000: IF A <  > 1 AND A <  > 2
AND A <  >  - 1 THEN 6530
6540 DD = A: IF A =  - 1 THEN  RETURN
6550  PRINT "FILENAME TO SAVE OR <RETURN> FOR CATALOGOR <ESC> TO EXIT": GOSUB
1000:F$ = A$
6560  IF A =  - 1 THEN  RETURN
6570  IF F$ = "" THEN  PRINT D$"CATALOG,D"DD: GOTO 6550
6580  PRINT D$"MONICO"
6590  PRINT D$"OPEN "F$",D"DD
6600  PRINT D$"WRITE "F$
```

```
6610  PRINT LN(DT - 1): PRINT 0
6620  FOR I = 1 TO LN(DT - 1)
6630  PRINT MM(DT - 1,I): PRINT G(DT - 1,I)
6640  NEXT I
6650  PRINT D$"CLOSE "F$
6660  RETURN
6700  REM *********************
6701  REM * OUTPUT DATA TO    *
6702  REM * PRINTER           *
6704  REM *********************
6720  PRINT "<<OUTPUT DATA TO PRINTER>>"
6730  PRINT "READY PRINTER AND HIT <RETURN> OR HIT   <ESC> TO QUIT"
6740  GOSUB 1000: IF A =  - 1 THEN  RETURN
6750  PRINT
6760  PRINT D$"PR#1"
6770  GOSUB 7000
6780  PRINT D$"PR#0"
6790  RETURN
7000  REM *********************
7001  REM * PRINT DATA        *
7002  REM * IN MM(X) AND G(X) *
7004  REM *********************
7020  FOR I = 1 TO LN(DT - 1)
7030  PRINT I; TAB( 10);MM(DT - 1,I); TAB( 20);G(DT - 1,I)
7040  NEXT
7090  RETURN
7200  REM *********************
7201  REM * GET CHOICE OF DATA*
7202  REM * TYPE TO WORK WITH *
7209  REM *********************
7250  PRINT : PRINT "What data type to use?"
7260  PRINT "<1> Stretch data"
7270  PRINT "<2> Relax (motor return) data"
7280  PRINT "<3> Constant tension data"
7290  PRINT "<4> Constant distance data"
7300  PRINT "<ESC> to Abort"
7310  PRINT "CHOOSE ONE:";: GOSUB 1000: IF A =  - 1 THEN  RETURN
7320  IF A < 1 OR A > 4 THEN 7250
7340 DT = A
7390  RETURN
8000  REM *********************
8001  REM * SET MOTORS BY     *
8002  REM * KEYBOARD CONTROL  *
8003  REM * & PRINT TENSION   *
8004  REM *********************
8020  HOME
8030  PRINT : PRINT "MOTOR A          MOTOR B"
8040  PRINT "IN    OUT        IN    OUT"
8050  PRINT "<Q>   <W>        <Z>   <X>"
8060  PRINT : PRINT "MOVE MOTORS BY USING KEYS SHOWN ABOVE"
8070  PRINT "WHEN DONE, HIT ESC"
8080 PULSES = 5:MODE% = 0
8090  GET A$
8100 DIR% = 1
8110  IF A$ = "Q" OR A$ = "Z" THEN DIR% = 0
```

```
8120  IF A$ = "Q" OR A$ = "W" THEN  & MOTA,PULSES,DIR%,MODE%
8130  IF A$ = "Z" OR A$ = "X" THEN  & MOTB,PULSES,DIR%,MODE%
8140  IF A$ = ESC$ THEN  RETURN
8150 D% = 5: CALL 800: FOR W = 1 TO 150: NEXT
8160  VTAB 10: PRINT "TENSION="D%"    "
8170  PRINT "GRAMS  =" FN G(D%)"    "
8180  GOTO 8090
9000  REM ********************
9001  REM * PRINT A/D VALUES  *
9002  REM * FROM CARD IN SLOT *
9003  REM * NUMBER FIVE       *
9004  REM ********************
9020  PRINT : PRINT "VALUES OF A/D CONVERTER WILL BE PRINTED ON THE SCREEN.
 HIT ANY KEY TO START AND<ESC> TO EXIT."
9030  GOSUB 1000: IF A =  - 1 THEN  RETURN
9040 D% = 5: CALL 800:D% = 5: CALL 800: REM  CLEAR A/D CONVERTER
9050 D% = 5
9060  CALL 800
9070  PRINT D%" COUNTS, " FN G(D%)" GRAMS"
9080  FOR I = 1 TO 200: NEXT I
9090  IF  PEEK (KBD) <  > 155 THEN 9050
9100  RETURN
10000  REM ********************
10001  REM * INITALIZE VARS   *
10002  REM * AND LOAD DATA AND*
10003  REM * PROGRAMS         *
10004  REM ********************
10020 D$ =  CHR$ (4)
10040  INVERSE : PRINT "LOADING DATA": NORMAL
10050  PRINT D$"BLOAD RMPDATA"
10060  PRINT D$"BLOAD RMPDATB"
10070  PRINT D$"BRUN AMPRAMP"
10080  PRINT D$"BLOAD ADOBJ"
10090  CALL 36864
10110 D$ =  CHR$ (4):ESC$ =  CHR$ (27):RET$ =  CHR$ (13)
10120 BAK$ =  CHR$ (8):DL$ =  CHR$ (127)
10130 KBD =  - 16368
10135  REM ********************
10136  REM * ARRAY 0-3 ARE :  *
10137  REM *0=STRETCH 1=RELAX *
10138  REM *2=CONSTANT TENSION*
10139  REM *3=CONSTANT DISTNCE*
10140  REM ********************
10145  DIM MM(3,200),G(3,200)
10155  REM ********************
10180  REM *>TCAL IS # OF A/D *
10190  REM *STEPS PER GRAM    *
10195  REM *OF TENSION        *
10200  REM *>DCAL IS # OF MM  *
10210  REM *PER MOTOR STEP    *
10212  REM *>THE 4 FUNCTIONS  *
10214  REM *CONVERT TO & FROM *
10216  REM *GRAMS,MM,A/D STEPS*
10218  REM ********************
10219 TCAL = 3.3:DCAL = .15
```

```
10220  DEF  FN G(X) = (X - ZCAL) / TCAL: DEF  FN TN(X) = ZCAL + (X * TCAL)
10223  DEF  FN PULSES(X) = MM / DCAL: DEF  FN MM(X) = X * DCAL
10230  RETURN
12000  REM *********************
12001  REM * CALIBRATE A/D     *
12002  REM * CONVERTER         *
12004  REM *********************
12020  PRINT : PRINT "CALIBRATE--SET ZERO LEVEL"
12030  PRINT : PRINT "PLEASE SET ARMS AT ZERO TENSION AND HIT RETURN TO CALCULATE
ZCAL, OR HIT <ESC>  TO EXIT."
12040  GOSUB 1000: IF A =  - 1 THEN  RETURN
12050 D% = 5: CALL 800:D% = 5: CALL 800
12060 T = 0
12070  FOR I = 1 TO 10
12080 D% = 5: CALL 800
12090  FOR W = 1 TO 100: NEXT
12100 T = T + D%
12110  NEXT
12120 ZCAL = T / 10
12130  PRINT : PRINT "ZERO GRAMS = "ZCAL" COUNTS ON THE A/D   CONVERTER"
12140  RETURN
15000  REM *********************
15001  REM * HOLD AT CONSTANT  *
15002  REM * TENSION           *
15003  REM *                   *
15004  REM *********************
15005 MODE% = 0:DIR% = 0:P = 1
15006 D$ =  CHR$ (4)
15007 D = 0
15020  PRINT : PRINT "---Hold at constant tension---"
15030  REM
15040  PRINT : PRINT "<1> Hold at tension & record length"
15045  PRINT "<2> Set motors"
15060  PRINT "<ESC> to EXIT"
15070  PRINT "CHOOSE ONE:";: GOSUB 1000: IF A =  - 1 THEN  RETURN
15080  ON A GOSUB 15200,8000
15090  GOTO 15030
15200  REM ********************
15201  REM * HOLD AND RECORD  *
15202  REM * DATA             *
15203  REM ********************
15220  INPUT "Tension in grams:";G
15230  INPUT "How many seconds per data item:";SEC
15240  INPUT "How many data items:";LN(2)
15250  PRINT "That will take "LN(2) * SEC / 60" minutes"
15255  INPUT " Return motor to start (y/n) ";A$:RT = (A$ = "Y")
15270  PRINT "Hit return to start or <ESC> to abort  ";: GOSUB 1000: IF A =
 - 1 THEN  RETURN
15275 MODE% = 0:DIR% = 0:P = 1:D$ =  CHR$ (4)
15280  PRINT : PRINT
15290  GOSUB 15700
15295  PRINT D
15300  FOR I = 1 TO LN(2)
15310  FOR W = 1 TO SEC
15320  PRINT D$"PR#4": PRINT D$"IN#4": INPUT "#";ZZ,ZZ,ZZ,ZZ,MN,SC: PRINT D$"PR#0":
```

```
PRINT D$"IN#0"
15322 D% = 5: CALL 800: IF  FN G(D%) <  = G THEN  GOSUB 15700
15325  IF SC = OSC THEN 15320
15330 OSC = SC
15340  NEXT W
15360 MM(2,I) =  FN MM(D):G(2,I) = I * SEC
15370  PRINT I * SEC" SEC, " FN MM(D)" MM, " FN G(D%)" GRAMS."
15380  IF  PEEK (KBD) = 128 + 27 THEN  RETURN
15390  NEXT I
15395  IF RT THEN PULSES = D: GOSUB 5000
15400  RETURN
15700  REM   *ADJUST TENSION   *
15720 D% = 5: CALL 800
15730  IF  FN G(D%) <  = G THEN D = D + 1: & MOTA,P,DIR%,MODE%: GOTO 15720
15790  RETURN
16000  REM ********************
16001  REM * HOLD AT CONSTANT  *
16002  REM * DISTANCE & RECORD *
16003  REM *                   *
16004  REM ********************
16005 D$ =  CHR$ (4)
16020  PRINT : PRINT "---- Hold at constant distance ----"
16040  PRINT : PRINT "<1> Hold at distance and record data"
16050  PRINT "<2> Set motors"
16070  PRINT "<ESC> to Exit
16080  PRINT "CHOOSE ONE:";: GOSUB 1000: IF A =  - 1 THEN  RETURN
16100  IF A < 1 OR A > 2 THEN 16040
16110  ON A GOSUB 16500,8000
16120  GOTO 16040
16500  REM
16520  INPUT "Distance to move (in MM):";MM
16530  INPUT " Seconds per data item:";SEC
16540  INPUT " # of data items:";LN(3)
16550  INPUT "Have motor return to start(Y/N):";A$:RT = (A$ = "Y")
16560  PRINT "HIT RETURN TO START OR <ESC> TO EXIT": GOSUB 1000: IF A =  - 1
THEN  RETURN
16580 PULSES =  FN PULSES(MM):DIR% = 0:MODE% = 0:TN = 1E10:WT = 0: GOSUB 4000
16590 D$ =  CHR$ (4)
16600  FOR I = 1 TO LN(3)
16630  FOR W = 1 TO SEC
16640  PRINT D$"PR#4": PRINT D$"IN#4": INPUT "#";ZZ,ZZ,ZZ,ZZ,MN,SC: PRINT D$"PR#0":
PRINT D$"IN#0"
16650  IF SC = OSC THEN 16640
16660 OSC = SC
16670  NEXT W
16680 D% = 5: CALL 800
16690 MM(3,I) = I * SEC:G(3,I) =  FN G(D%)
16700  PRINT I * SEC" SEC, "MM" MM, " FN G(D%)" GRAMS."
16720  IF  PEEK (KBD) = 27 + 128 THEN  RETURN
16750  NEXT I
16770  IF RT THEN PULSES =  FN PULSES(MM): GOSUB 5000
16790  RETURN

]
```

APPENDIX C.

Software developed to measure skin deformation

LIST

```
10  GOTO 1000
20  ONERR  GOTO 900
100  PR# 1
110  PRINT  CHR$ (27); CHR$ (69)
120  FOR I = 1 TO 29
130  PRINT I;".  ";PN$(I)
140  NEXT I
150  PRINT  CHR$ (12)
160  FOR I = 1 TO 40
170  PRINT I;".  ";CAL$(I)
180  NEXT I
190  PRINT  CHR$ (12)
200  END
900  HOME
920  PRINT D$;"CLOSE ";GX$
940  VTAB 10: PRINT " AN ERROR HAS OCCURED,"
950  PRINT "  PLEASE RESTART PROGRAM"
970  END
1000  REM  ********************
1010  REM  * GRID ANALYSIS    *
1015  REM  * VERSION     1.0  *
1020  REM  *                  *
1030  REM  *                  *
1040  REM  *                  *
1050  REM  ********************
1800  GOSUB 23000
1810  GOSUB 16000
1820  GOSUB 20000
1840  ON CC GOSUB 3000,5000,10000,13000,15000,9000,9000,9100,1900
1880  GOTO 1820
1900  HOME
1905  REM  (GOTO 100)
1920  END
3000  REM  *******************
3001  REM  * CAPTURE GRID ID *
3003  REM  *******************
3020  GOSUB 19900
3030  PRINT "ENTER GRID IDENTIFICATION"
3040  PRINT "   (MAX 12 CHARACTERS)"
3045  PRINT "    -            -"
3050  VTAB 6: HTAB 6: INPUT GN$
3060 GX$ = GN$ + ".GRID"
3070  PRINT " ": INPUT "HOW MANY POINTS ON 'X' AXIS? ";XA
3080  PRINT " ": INPUT "HOW MANY POINTS ON 'Y' AXIS? ";YA
3090 TN = XA * YA
3100  PRINT D$;"OPEN ";GX$
3110  PRINT D$;"WRITE ";GX$
3120  PRINT GN$;",";TN
3125  PRINT D$
3130  GOSUB 4200
3140  RETURN
4200  REM  *******************
```

```
4210  REM  * CAPTURE CONTROL *
4220  REM  * POINTS, SCALE   *
4230  REM  ******************
4240  GOSUB 19900
4250  FOR I = 10 TO 14
4260  VTAB 6: HTAB 1: PRINT MN$(I)
4280  IF DP < > 0 THEN  GOSUB 9880
4290  IF DB = 0 THEN  GOSUB 9820
4300 J = I - 9
4320  GOSUB 18000:PX(J) = XP:PY(J) = YP
4330  VTAB 6: HTAB 1: PRINT  SPC( 28)
4340  NEXT I
4420  GOSUB 21700
4440  IF X$ < > "Y" GOTO 4240
4450 J = 4:K = 5:L = 3: GOSUB 17000
4455 CM = LLN(L)
4460  VTAB 10: HTAB 1: INPUT "HOW LONG IS THE SCALE (CM) ";CX
4470 CM = CM / CX
4480 J = 1:K = 2:L = 1: GOSUB 17000
4490 J = 2:K = 3:L = 2: GOSUB 17000
4525  REM  * CALCULATE ANGLE *
4526  GOSUB 7000
4528  PRINT "SIN ="; SIN (NGL);"  COS ="; COS (NGL)
4529  INPUT Z$
4533  REM  ****************
4534  REM  * CAPTURE GRID *
4535  REM  * POINTS       *
4536  REM  ****************
4540  GOSUB 19900
4545  IF DP < > 0 THEN  GOSUB 9880
4550  IF DP = 0 THEN  GOSUB 9820
4555  PRINT "FOR POINT NUMBER"
4570  FOR I = 1 TO TN
4580  VTAB 5: HTAB 18: PRINT I
4600  GOSUB 18000
4603 XP = XP - PX(2):YP = YP - PY(2)
4605  VTAB 6: HTAB 1: PRINT  SPC( 40)
4610 NX = (XP *  COS (NGL) + YP *  SIN (NGL)) / CM
4615 NY = ( - XP *  SIN (NGL) + YP *  COS (NGL)) / CM
4620 NX =  INT (NX * P + .5) / P:NY =  INT (NY * P + .5) / P
4625  GOSUB 7600
4630  NEXT I
4700  PRINT D$;"CLOSE ";GX$
4710  PRINT D$
4720  RETURN
4900  RETURN
5000  REM  ********************
5001  REM  * DISPLAY ABSOLUTE *
5002  REM  * COORDINATES      *
5003  REM  ********************
5010  GOSUB 19900
5020  PRINT "ENTER GRID-ID TO DISPLAY"
5030  PRINT "    -            -"
5040  VTAB 5: HTAB 6: INPUT GN$
5050 GX$ = GN$ + ".GRID"
```

```
5060  PRINT D$;"OPEN ";GX$
5070  PRINT D$;"READ ";GX$
5080  INPUT G1$,TN
5085  PRINT D$
5090  GOSUB 21800
5100  IF YN$ = "Y" THEN  PRINT  CHR$ (12); CHR$ (27); CHR$ (69)
5105  HOME
5110  PRINT "GRID NUMBER ";G1$: PRINT " ": PRINT " "
5115  PRINT D$
5120  FOR I = 1 TO TN
5130  GOSUB 7800
5140  PRINT PN;".",MX,MY
5150  NEXT I
5153  PRINT D$;"CLOSE ";GX$: PRINT D$
5155  PRINT " ": PRINT " ": HTAB 5: PRINT "PRESS ANY KEY": GET Z$
5157  IF YN$ <  > "Y" GOTO 5170
5159  PRINT D$
5160  PRINT D$;"PR#0"
5170  RETURN
7000  REM  **********************
7001  REM  * CALCULATE ANGLE OF *
7002  REM  * GRID RELATIVE TO   *
7003  REM  * BASE               *
7005  REM  **********************
7010 SL(1) = 0
7020 L1 = 2:L2 = 3:N = 2: GOSUB 17600
7030 NGL = SL(N)
7035 N1 = 1:N2 = 2
7040 M = 1: GOSUB 17700
7050  RETURN
7300  REM  ***********************
7301  REM  * CALCULATE CONSTANTS *
7302  REM  *  (NOT USED)     *
7305  REM  ***********************
7310 J = 2:K = 1:L = 4: GOSUB 17000
7320 J = 2:K = 3:L = 5: GOSUB 17000
7330 RV = LLN(4) / CM:RH = LLN(5) / CM
7340 G = LLN(1):H = LLN(2)
7350 XU = (G / RV) * ( COS (NGL) +  SIN (NGL) - PX(2) *  COS (NGL) - PY(2)
*  SIN (NGL))
7360 YU = ( - H / RH) * ( SIN (NGL) +  COS (NGL) + PX(2) *  SIN (NGL) -
 PY(2) *  COS (NGL))
7370  RETURN
7600  REM  *********************
7601  REM  * WRITE OUT PART OF *
7602  REM  * GRID TO DISK      *
7610  REM  *********************
7612  PRINT D$
7615  PRINT D$;"WRITE ";GX$
7650  PRINT I;",";NX;",";NY
7660  PRINT D$
7670  RETURN
7800  REM  *********************
7801  REM  * READ PART OF GRID *
7802  REM  * FROM DISK         *
```

```
7810  REM  *********************
7830  PRINT D$;"READ ";GX$
7840  INPUT PN,MX,MY
7850  PRINT D$
7860  RETURN
9000  REM  * UNDEFINED *
9010  RETURN
9100  REM  *****************
9110  REM  * REPLACE       *
9120  REM  * SITE OPTIONS  *
9130  REM  *****************
9140  GOSUB 19900
9150 D$ =  CHR$ (4)
9155  PRINT D$;"CLOSE"
9160  PRINT "    REPLACE CURRENT SITE OPTIONS"
9170  PRINT " ": PRINT " "
9173  PRINT "MAKE SURE PROGRAM DISKETTE": PRINT "IS IN DRIVE 1 (WRITE ENABLED)"
9175  PRINT " ": PRINT "   THEN PRESS ANY KEY": GET X$
9177  PRINT " "
9180  PRINT D$;"OPEN SITE.OPT"
9200  PRINT D$;"DELETE SITE.OPT"
9220  PRINT D$;"OPEN SITE.OPT"
9240  INPUT "ENTER SERIAL PORT SLOT #";S1
9250  PRINT " "
9260  INPUT "ENTER PRINTER PORT SLOT #";S2
9270  PRINT " "
9280  PRINT "ENTER REPORT HEADING "
9290  INPUT HD$
9340  PRINT D$;"WRITE SITE.OPT"
9360  PRINT S1;",";S2;","HD$
9370  PRINT D$;"CLOSE SITE.OPT"
9380  PRINT D$
9460  GOSUB 16000
9500  RETURN
9799  REM  *****************
9800  REM  * KEYBOARD OR   *
9810  REM  * KEYPAD MSSGS  *
9811  REM  *****************
9820  PRINT "ENTER X AND Y COORDINATES THRU KEYBOARD"
9830  RETURN
9880  PRINT "PRESS BUTTON 'O' ON KEYPAD"
9890  RETURN
10000  REM  ********************
10001  REM  * CALCULATE        *
10002  REM  * AVERAGE          *
10003  REM  * ROUTINE          *
10004  REM  ********************
10010  GOSUB 19900
10020  PRINT "CALCULATE AVERAGES "
10030  VTAB 22: PRINT "PRESS ANY KEY": GET Z$
10040  RETURN
13000  REM  ********************
13001  REM  * DISPLAY          *
13002  REM  * DISPLACEMENTS    *
13003  REM  ********************
```

```
13005  GOSUB 19900
13020  PRINT "ENTER GRID ID FOR FIRST GRID"
13040  INPUT GI$(1)
13060  PRINT " ": PRINT "ENTER GRID ID FOR SECOND GRID"
13080  INPUT GI$(2)
13100  FOR M = 1 TO 2
13110 GI$(M) = GI$(M) + ".GRID"
13120  PRINT D$;"OPEN ";GI$(M)
13140  PRINT D$;"READ ";GI$(M)
13160  INPUT GM$(M),TX(M)
13180  PRINT D$
13200  NEXT M
13210  IF TX(1) <  > TX(2) GOTO 13900
13220 TN = TX(1)
13230  GOSUB 21800
13240  IF YN$ = "Y" THEN  PRINT  CHR$ (12); CHR$ (27); CHR$ (69)
13250  PRINT "DISPLACEMENT FROM ";GM$(1)
13260  PRINT " TO ";GM$(2): PRINT " "
13270  FOR I = 1 TO TN
13280  FOR L = 1 TO 2
13290  PRINT D$;"READ ";GI$(L)
13300  INPUT J,PX(L),PY(L)
13310  PRINT D$
13320  NEXT L
13330 XD =  INT ((PX(1) - PX(2)) * P + .5) / P
13335 YD =  INT ((PY(1) - PY(2)) * P + .5) / P
13340  PRINT I;".   ";XD;",   ";YD
13350  NEXT I
13360  PRINT " ": PRINT " "
13370  IF YN$ = "Y" THEN  PRINT D$;"PR#0"
13375  PRINT D$
13380  PRINT "PRESS ANY KEY": GET Z$
13385  PRINT D$
13390  FOR L = 1 TO 2
13400  PRINT D$;"CLOSE ";GI$(L)
13410  PRINT D$
13420  NEXT L
13450  RETURN
13900  PRINT "GRIDS ARE NOT THE SAME SIZE"
13910  PRINT "-UNABLE TO CALCULATE DISPLACTMENT"
13920  PRINT " ": PRINT " "
13930  PRINT "PRESS ANY KEY"
13940  GET X$
14950  GOTO 13450
15000  REM  *******************
15005  REM  * DISPLAY CATALOG *
15008  REM  *    ROUTINE      *
15010  REM  *******************
15020  HOME
15030  GOSUB 21800
15035  IF YN$ <  > "Y" GOTO 15120
15040  VTAB 10: PRINT "MAKE SURE PRINTER IS READY, THEN"
15045  HTAB 8: INPUT "PRESS <RETURN>";X$
15050  HOME
15060  PRINT D$;"PR#";PP
```

```
15065  PRINT D$
15070  REM  * EMPHASIZED TYPE *
15080  PRINT  CHR$ (27); CHR$ (69)
15100  PRINT  CHR$ (12)
15110  PRINT D$;"CATALOG"
15115  GOTO 15400
15120  PRINT D$;"CATALOG"
15130  PRINT " ": PRINT "PRESS ANY KEY ": GET Z$
15380  IF YN$ <  > "Y" GOTO 15440
15400  PRINT  CHR$ (12)
15420  PRINT D$;"PR#0"
15440  HOME
15480  RETURN
15500  REM
15510  REM
15520  REM
15530  REM
15550  REM
16000  REM  ********************
16010  REM  * DISK I/O ROUTINES*
16020  REM  ********************
16030 D$ =  CHR$ (4)
16035  HOME
16040  PRINT D$;"OPEN SITE.OPT"
16050  PRINT D$;"READ SITE.OPT"
16060  INPUT DP,PP,HD$
16070  PRINT D$;"CLOSE SITE.OPT"
16075  PRINT D$
16080  PRINT "INSERT DATA DISKETTE IN DRIVE 1"
16083  PRINT "      (WRITE ENABLED)"
16087  PRINT "THEN PRESS ANY KEY": GET X$
16090  RETURN
17000  REM  ********************
17010  REM  * EQUATION FOR THE *
17020  REM  * LENGTH OF A LINE *
17030  REM  ********************
17060 LLN(L) =  SQR ((PX(J) - PX(K)) © 2 + (PY(J) - PY(K)) © 2)
17090 LLN(L) =  INT (LLN(L) * P + .5) / P
17095  PRINT "LEN ";L;" = ";LLN(L)
17096  INPUT Z$
17100  RETURN
17600  REM  *********************
17610  REM  * EQUATION FOR THE  *
17620  REM  * SLOPE OF A LINE   *
17630  REM  *********************
17640 SL(N) = (PY(L2) - PY(L1)) / (PX(L2) - PX(L1))
17660  RETURN
17700  REM  *********************
17710  REM  * EQUATION FOR ANGLE*
17720  REM  * BETWEEN TWO LINES *
17730  REM  *********************
17740 NGL = (SL(N2) - SL(N1)) / (1 + SL(N2) * SL(N1))
17760 RN = ( ATN (NGL)) * 57.296
17780 AN(M) =  INT (RN * P + .5) / P
17785  PRINT "ANGLE = ";AN(M)
```

```
17786  INPUT Z$
17790  RETURN
18000  REM  ********************
18010  REM  * CAPTURE DATA FROM*
18020  REM  * DIGITIZING TABLET*
18030  REM  ********************
18040  REM  * TABLET OUTPUT IS *
18050  REM  * NXXXXX YYYYYCRLF *
18060  REM  * N= PUSHBUTTON NO.*
18070  REM  * X= X COORDINATE  *
18080  REM  * Y= Y COORDINATE  *
18090  REM  ********************
18095  IF DP = 0 GOTO 18320
18120  PRINT D$;"PR#";DP: PRINT D$;"IN#";DP
18140 INVL$ = ""
18150 HP =  POS (0)
18180  INPUT INVL$
18190  HTAB HP: PRINT  SPC( 14)
18200 KV$ =  LEFT$ (INVL$,1)
18220 X1$ =  MID$ (INVL$,2,5)
18240 Y1$ =  RIGHT$ (INVL$,5)
18260 XP =  VAL (X1$):YP =  VAL (Y1$)
18280  PRINT D$;"PR#0": PRINT D$;"IN#0"
18300  RETURN
18310  REM  * DIRECT KEYBOARD INPUT *
18320  REM  * IN PLACE OF DIGITIZING*
18330  REM  * TABLET                *
18340  VTAB 8: HTAB 1: PRINT  SPC( 14)
18350  VTAB 8: HTAB 1
18360  INPUT XP,YP
18370  GOTO 18300
19000  REM  ********************
19010  REM  * STRING INPUT FROM*
19020  REM  * KEYBOARD         *
19030  REM  ********************
19060 IN$ = "":NH = SH(I):NV = SV(I):MAX = SMAX(I):CT = 1
19080  VTAB NV: HTAB NH: GET I1$
19100  IF  ASC (I1$) = 13 THEN 19220
19120 IN$ = IN$ + I1$
19140  VTAB NV: HTAB NH: PRINT I1$
19160 NH = NH + 1:CT = CT + 1
19180  IF CT <  = MAX THEN 19080
19220  RETURN
19240  REM  * BACK-UP THE CURSOR *
19260 NH = NH - 1
19900  REM  ********************
19910  REM  * CLS/PRINT TITLE  *
19920  REM  ********************
19930  HOME : HTAB 8: PRINT HD$
19940  HTAB 1: VTAB 4:
19950  RETURN
20000  REM  ********************
20010  REM  * MENU ROUTINES    *
20020  REM  ********************
20040  GOSUB 19900
```

```
20050  REM  * MAIN MENU *
20060  FOR L = 1 TO 9
20080  PRINT MN$(L): PRINT " "
20100  NEXT L
20120  GOSUB 22500
20160  RETURN
21000  REM  * COMPARE/ANALYZE *
21010  REM  *   SUB MENU      *
21020  GOSUB 19900
21040  FOR L = 11 TO 19
21060  PRINT MN$(L): PRINT " "
21080  NEXT L
21100  GOSUB 22500
21120  RETURN
21699  REM  *****************
21700  REM  * IS INPUT DATA *
21710  REM  * CORRECT?      *
21711  REM  *****************
21740  VTAB 22: HTAB 4: PRINT "IS DATA ENTERED CORRECTLY (Y/N)?"
21750  VTAB 22: HTAB 37: GET X$
21790  RETURN
21800  REM  ******************
21801  REM  * IS PRINT-OUT   *
21802  REM  * REQUIRED       *
21803  REM  ******************
21810  VTAB 22: HTAB 5: PRINT "IS PRINT-OUT REQUIRED?   (Y/N)"
21820  VTAB 22: HTAB 28: GET YN$
21830  VTAB 22: PRINT  SPC( 35)
21835  PRINT D$
21840  IF YN$ = "Y" GOTO 21860
21850  RETURN
21860  PRINT D$;"PR#";PP
21870  GOTO 21850
22500  VTAB 23: HTAB 6: PRINT "SELECT FUNCTION BY NUMBER <": VTAB 23: HTAB
34: PRINT ">"
22520  VTAB 23: HTAB 33: GET C$
22540  IF  ASC (C$) < 49 THEN 22520
22560  IF  ASC (C$) > 57 THEN 22500
22580  VTAB 23: HTAB 33: PRINT C$
22600 CC =  VAL (C$)
22620  RETURN
23000  REM  *******************
23003  REM  * DIMENSION       *
23005  REM  * STATEMENTS      *
23007  REM  *******************
23030  DIM MN$(20),PX(40),PY(40),XX(40),YY(40)
23040  DIM SL(5),AN(5),LLN(5)
23050  DIM GI$(11),TX(11),GM$(11)
23080 P = 100
23500  FOR I = 1 TO 14
23520  READ MN$(I)
23540  NEXT I
23560  DATA  "1. CAPTURE GRID","2. DISPLAY ABSOLUTE COORDINATES"
23600  DATA  "3. COMPUTE AVERAGE FOR MULTIPLE GRIDS","4. COMPUTE, DISPLAY
DISPLACEMENTS","5. DISPLAY CATALOG OF GRIDS"
```

```
23610  DATA  "6.","7."
23620  DATA  "8. MODIFY INSTALLATION OPTIONS","9. EXIT PROGRAM"
23630  DATA  "ENTER UPPER LEFT CORNER POINT","ENTER LOWER LEFT CORNER POINT","ENTER
LOWER RIGHT CORNER POINT"
23640  DATA  "ENTER FIRST POINT ON SCALE     ","ENTER SECOND POINT ON SCALE
  "
25000  RETURN

]
```